Geothermics

Course Outline:

1. Thermal conditions of the early Earth and present-day Earth's structure
2. Thermal parameters of the rocks
3. Thermal structure of the lithospheric continental areas (steady state)
4. Thermal structure of the lithospheric oceanic areas
5. Thermal structure of the lithosphere for transient conditions in various tectonic settings
6. Heat balance of the Earth
7. Thermal structure of the sedimentary basins
8. Thermal maturity of sediments
9. **Mantle convection and hot spots**
10. Magmatic processes and volcanoes
11. Heat transfer in hydrogeological settings
12. Geothermal Systems

Convection and Conduction

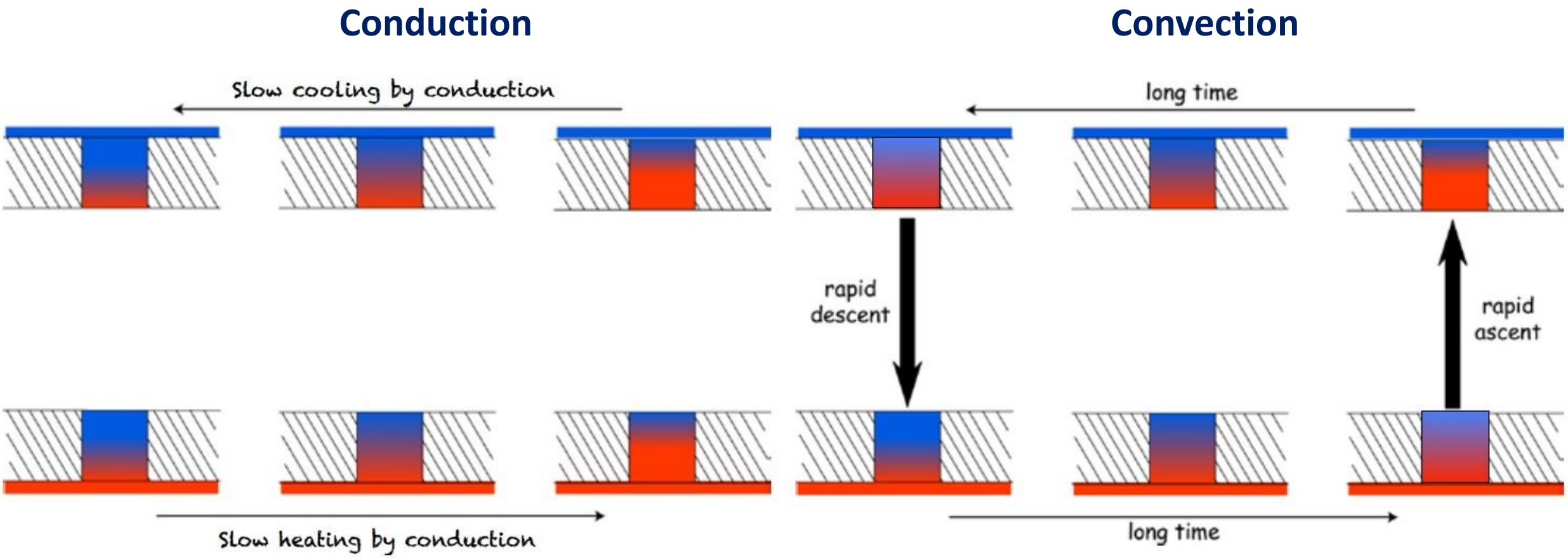

Convection and Conduction

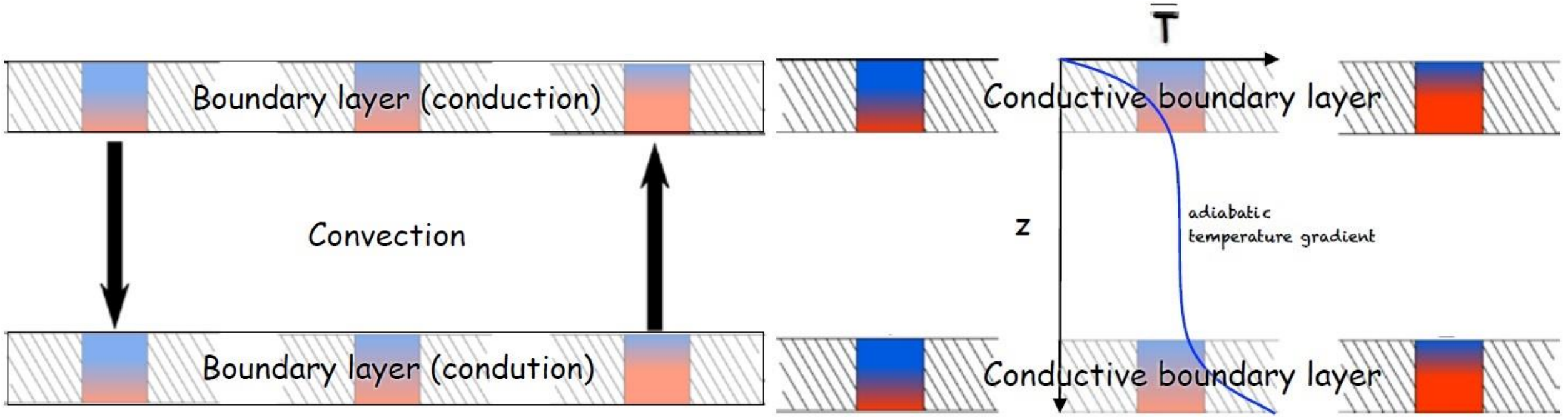

Speed of plate tectonics (~10 cm/j) is determined by the time it takes to cool and heat the boundary layers

Thermal regime of the deep interior

- The *adiabatic temperature gradient* in the mantle is the rate of increase of temperature with depth as a result of compression of the rock by the weight of the overlying material.
- During adiabatic compression the increasing pressure does work on the material as it compresses, and this increases the internal energy of the material, which is expressed as a rise in temperature.
- Mantle is sufficiently compressible to originate adiabatic temperature gradients. Olivine—spinel and spinel—post-spinel transitions provided the benchmark temperatures of ~1600°C at 410 km (13.5 GPa) and ~ 1700°C at 660 km (23 GPa).
- The adiabatic temperature gradient can be calculated from the thermodynamic relation between entropy per unit mass *s*, *T*, and *P*:

$$ds = \frac{c_p}{T} dT - \frac{\alpha_v}{\rho} dp,$$

c_p is the specific heat at constant pressure, α_v the expansion coefficient, and *ds, dT*, and *dp* are infinitesimal changes in entropy (s), *T*, and *P*. The entropy change in an adiabatic process is zero if the process is also reversible, thus if *ds*=0:

$$\left(\frac{dT}{dp}\right)_s = \left(\frac{\alpha_v T}{\rho c_p}\right) = \frac{\gamma\, T}{K_S} \qquad \gamma = \frac{\alpha\, K_S}{\rho\ c_p}; \qquad \gamma\text{=0.5-1.5}$$

Since the increase in pressure with depth is given by: $\frac{dp}{dy} = \rho g$ we obtain: $\left(\frac{dT}{dy}\right)_s = \frac{\alpha_v g T}{c_p}.$

$$(\mathrm{d}T/\mathrm{d}Z)_s = T\alpha g/C_p \sim 0.5 - 0.6\,^{\circ}\mathrm{C/km}$$ (in the upper mantle)

The definition of adiabatic gradient provides an estimate of the variation of the adiabatic temperature:

The integration of $\left(\frac{dT}{dp}\right)_s = \left(\frac{\alpha_v T}{\rho c_p}\right) = \frac{\gamma\, T}{K_S}$ gives: $\ln\left(\frac{T_2}{T_1}\right) = \gamma \int_{p_1}^{p_2} \frac{\mathrm{d}p}{K_S}$ $K_S = \rho(\partial P/\partial \rho)_S$ We get: $\frac{T_2}{T_1} = \left(\frac{\rho_2}{\rho_1}\right)^{\gamma}$

It represents the variation of adiabatic temperature through a finite interval of depth in terms of density ratio.

Thermal regime of the deep interior

- Solid melts when the thermal oscillation of atoms reaches a critical amplitude:

$$T_m = C\ m\ V^{2/3}\vartheta_D^2$$ Poirier, 1991

C=constant, *m* and *V* = mass and volume of the atoms , ϑ_D =Debye temperature

Debye temperature ϑ_D is directly related to the maximum frequency of vibration of the solid v_m:

$$\vartheta_D = \frac{h\,v_m}{k_B} \qquad \vartheta_D = 61.2\,k_l + 385$$ For silicate minerals (Horai and Simmons, 1970)

h = Planck constant (6.626 x 10^{-34} J s) and k_B = Boltzmann constant (1.381 x 10^{-23} J K^{-1})

To calculate T_m at pressure P_m:

$$\frac{p_m}{p_o} = \left(\frac{T_m}{T_{m_o}}\right)^c - 1 \qquad c = (6\gamma + 1)/(6\gamma - 2)$$ Gilvarry, 1956

T_{m0}=melting *T* at zero pressure, p_0 = (negative) melting *P* at zero *T*, γ= Grüneisen parameter

$$\gamma = \frac{\alpha\,K_S}{\rho\ c_p} = \frac{\alpha\,K_T}{\rho\ c_V} = \frac{\alpha v_b^2}{C_P} \qquad K_S = \rho(\partial P/\partial\rho)_S \qquad v_b = \sqrt{\frac{K}{\rho}}$$

c_p and c_V are the specific heats at constant pressure *P* and volume *V*, K_S and K_T are bulk moduli at constant entropy *S* and temperature *T*, and α is the thermal expansion coefficient, v_b=bulk sound speed.

- **The Grüneisen parameter (γ) expresses the ratio between thermal pressure and thermal energy per unit volume (it measures the rate at which *P* increases as heat is input or the pressure required to prevent thermal expansion).**
- **γ is weakly dependent on pressure and temperature (for most minerals it varies between ~1.0 and 1.5).**

Thermal regime of the deep interior

$\phi = K_s/\rho$

Density ρ, pressure p, seismic parameter ϕ, electrical conductivity σ_e, thermal conductivity k, Grüneisen parameter γ, specific heat c_p, expansion coefficient α, Debye temperature T_D, melting temperature T_m and temperature T in correspondence of the major discontinuities

z km	ρ kg m^{-3}	p GPa	ϕ km^2 s^{-2}	σ_e S m^{-1}	k W m^{-1} K^{-1}	γ	c_p J kg^{-1} K^{-1}	α 10^{-6} K^{-1}	T_D	T_m	T K
Upper mantle											
100	3370	3	38	0.01	5	0.5	1200	16	700	1800	1500
400	3540	13	49	0.01	5	0.6	1250	16	850	2100	1850
Transition zone											
400	3720	13	51	0.05	5	0.6	1250	15	850	2100	1850
670	3990	24	64	0.1	5	0.7	1250	15	900	2750	1950
Lower mantle											
670	4380	24	69	1.0	7	1.0	1275	19	1000	2750	1950
2741	5490	127	117	30	10	1.0	1275	9	1450	3800	3000
Layer D″[a]											
2741	5490	127	117	30	10	0.8	1250	9	1450	3850	3550
2891	5560	136	65	50	10	0.8	1250	9	1400	3850	3750
Outer core											
2891	9900	136	65	3×10^5	28	1.4	700	16	–	3450	3750
5150	12170	329	107	3×10^5	37	1.3	650	8	–	4950	4950
Inner core											
5150	12760	329	105	4×10^5	50	1.1	650	7	1300	4950	4950
6371	13090	364	109	4×10^5	50	1.1	650	6	1350	5200	5100

Electrical conductivity is linked to the motion of ions:

(in the uppermost crust) $\sigma_e = \sigma_{ef}\, \xi^n$ $\sigma_e = \sigma_{e\infty} \exp\left(-\frac{E^*}{k_B\, T}\right)$ (in the lower crust and at >> depths)

Conductivity of unconsolidated sediments = 0.1-5.0 S m^{-1} Conductivity of upper crust= 0.001–0.01 S m^{-1}

σ_{ef}= conductivity of the fluid, ξ=fraction of pores filled with the fluid, and n constant (1.3-2.5)

E*=Activation energy, k_b=Botzmann constant, $\sigma_{e\infty}$ extrapolated conductivity for T $\longrightarrow \infty$

Wiedemann–Franz law

In the core: $\frac{k}{\sigma_e} = L\, T$ L = 2.5 10^{-8} W S^{-1}K^{-2} = Lorentz number (with K =50 W m^{-1}K^{-1} and T = 5000 K, 10^5S m^{-1})

Thermal regime of the deep interior

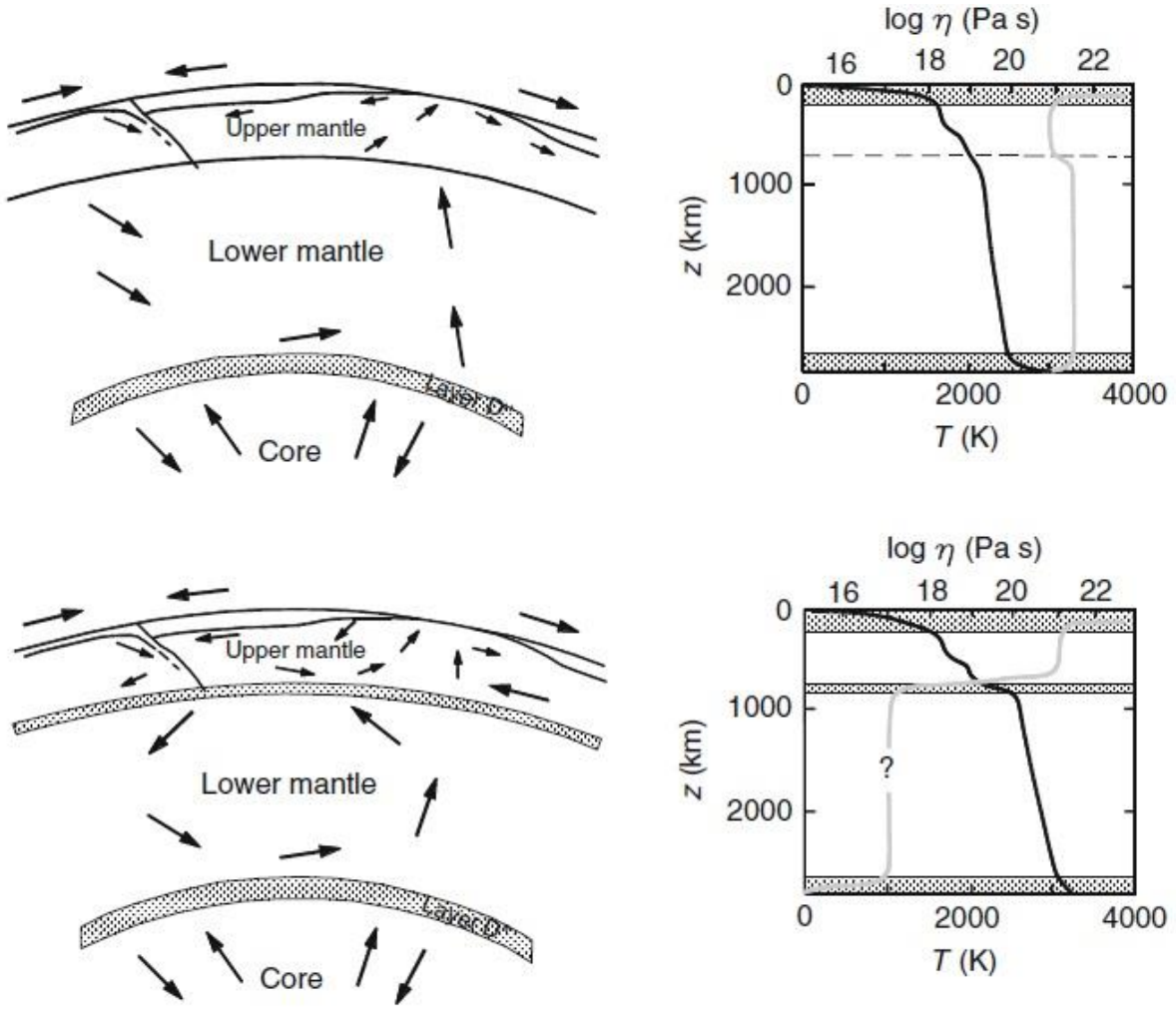

- Factors that could inhibit a mantle-wide convection are (1) a viscosity increase with depth, (2) a phase change with an inclination of the Clapeyron curve sufficiently negative and (3) the lack of mixing between chemically different layers.
- Phase changes are not an obstacle to convection, since Claperyon curve is positive for the transition olivine-spinel (dp/dt= 4MPaK^{-1}).

Convection

Convection: fluid flow driven by internal **buoyancy (B)**

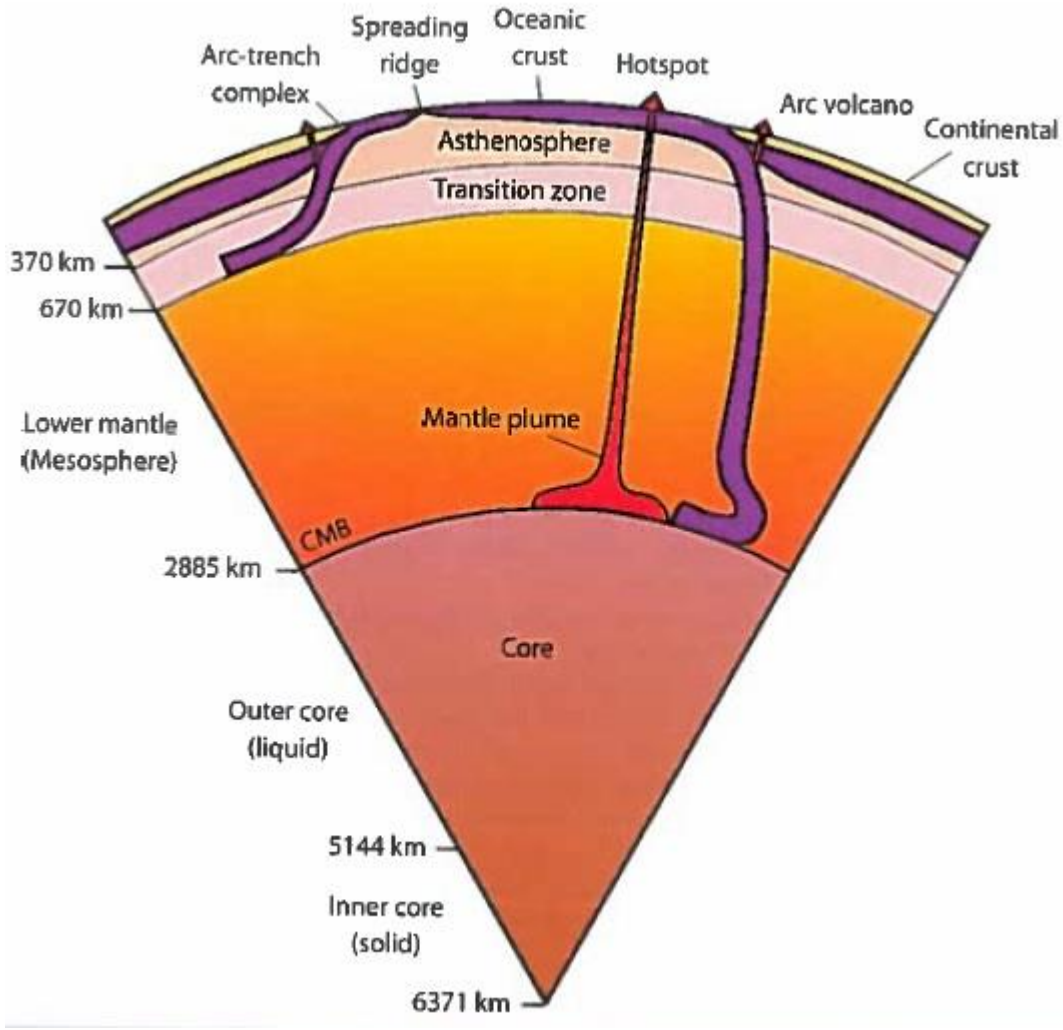

$B = -gV\rho = -g\Delta m$

Δm = mass anomaly due to a volume V with a density difference induced by temperature and/or composition

Buoyancy

Thermal buoyancy: $\rho = \rho_0[1 - \alpha(T - T_0)]$

With α about 3.0 x 10^{-5}/°C, a temperature contrast of 1000 °C gives rise to a density contrast of about 3%.

Thermal expansion coefficient

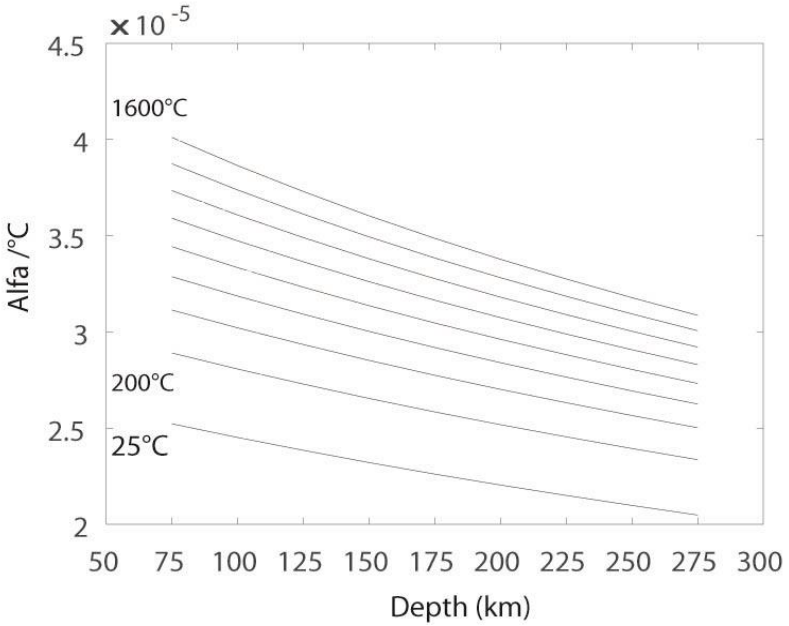

Examples:

1. A plume head 1000 km in diameter with ΔT 300 °C would have a B ~2 x 10^{20}N.
2. A Lithospheric slab subducted extended to the bottom of the mantle (3000 km), its B would be about -200 TN/m.
3. Subducting oceanic crust (7 km) gives a contribution to slab buoyancy of only ~20 TN/m.

Compositional buoyancy: induced by small variations in the upper/lower mantle composition

Larger density variations in the mantle are due to pressure-induced phase transformations of the mineral assemblage (not necessarily a source of buoyancy).

Convection model

Balance between buoyancy forces (B) and viscous resistance (R):

Motion of the plate (subducting slab) is resisted by the viscous stresses (proportional to velocity) accompanying mantle flow

Buoyancy (B) = $B = g \cdot Dd \cdot \rho\alpha\Delta T$

with ΔT the average difference in temperature between the descending lithosphere and fluid interior $\Delta T = -T/2$ and d, thickness of the subducting lithosphere (of the layer that diffused), depending on time (t) spent at the surface $t = D/v$.

$$d = \sqrt{\kappa t} = \sqrt{\kappa D/v}$$

The resisting viscous stress σ acting on the side of the descending slab: $\sigma = \mu \cdot 2v/D$

Viscous resistance R (per unit length)

$$R = D\sigma = D \cdot 2\mu v/D = 2\mu v$$

Balance between two forces: B+R=0 ⟶ $v = -g \cdot Dd\rho\alpha T/4\mu$

$$v = D\left(\frac{g\rho\alpha T\sqrt{\kappa}}{4\mu}\right)^{2/3}$$

For D= 3000 km, ρ= 4000 kg/m^3, α = *2* x 10^{-5}/°C, *T* = 1400 °C, κ=10^{-6}m^2/s and μ=10^{22}Pa s
v = 2.8 x 10^{-9}m/s = 90 mm/yr (close to velocity of plate motion).

From previous equations: $\left(\frac{D}{d}\right)^3 = \frac{g\rho\alpha TD^3}{4\kappa\mu}$

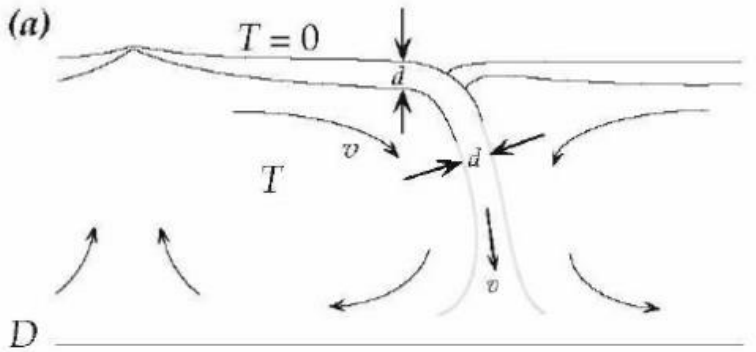

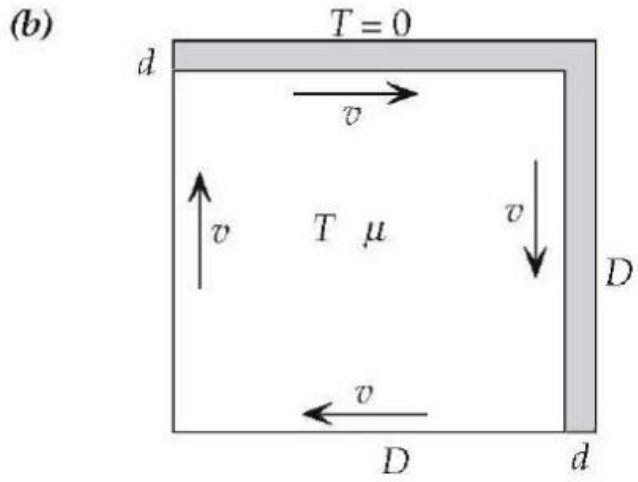

Convection model

Rayleigh Number (T): $Ra = \frac{g\rho\alpha T D^3}{\kappa\mu}$ For the mantle R_a = 3 x 10^6

Rayleigh Number (q) $R_q = \frac{g\rho\alpha D^3 \Delta T_q}{\kappa\mu} = \frac{g\rho\alpha q D^4}{K\kappa\mu}$ $Nu = q/q_K = \Delta T_q/\Delta T$ $\Delta T_q = qD/K$ $\frac{R_q}{Ra} = \frac{\Delta T_q}{\Delta T} = Nu$ $Nu \sim Ra^{1/3}$ $R_q \sim Ra^{4/3}$

Nusselt number $Nu \equiv q/q_K = qD/KT$ $d/D \sim Ra^{-1/3}$ $q = KT/d$ $q = (KT/D)Ra^{1/3}$ $Nu \sim Ra^{1/3}$ For the mantle *Nu* = 100

q=KΔT_q/d (heat flux) q_k=KΔT/D (the heat that would be conducted in the absence of convection)

Peclet number $Pe \equiv v(D/\kappa) \equiv v/V \sim Ra^{2/3}$ For the mantle *Pe* = 9000

Reynolds number $\mathrm{Re} = \frac{ud}{\nu}$ For the mantle Re = 10^{-18}

ν= μ/ρ (kinematic viscosity ~ 10^{17} m^2s^{-1}), u=velocity of the flow (30mmyr^{-1})

u=flow velocity *d*=length scale

Prandt number: $\mathrm{Pr} = \frac{\nu}{\alpha} = \frac{\text{viscous diffusion rate}}{\text{thermal diffusion rate}} = \frac{\mu/\rho}{k/(c_p\rho)} = \frac{c_p\mu}{k}$ For the mantle Pr = 10^{25}

R_a= Onset and vigor of convection.

Pe = ratio between convective and diffusive heat transport rates.

Nu= ratio between the actual heat flux (in the presence of convection) and heat flux that would be conducted with the same temperature difference across the layer. Thus, it express the efficiency of convection as a heat transport mechanism relative to conduction.

Nu can be also expressed as the ratio of the temperature difference, ΔT_q, that would be required to conduct the heat flux *q* through the layer, to the actual temperature difference in the presence of convection ΔT.

Re = turbulence of the flow : the flow is laminar if Re< 10^3.

Pr= ratio of momentum diffusivity (kinematic viscosity) to thermal diffusivity. For Pr << 1 the thermal diffusivity dominates, while for Pr >> 1, the momentum diffusivity dominates the behavior. For magma and Earth mantle convection is very effective in transferring energy in comparison to pure conduction, so momentum diffusivity is dominant.

Diffusion time scale (t_κ): estimates the time it would take the fluid layer to cool by conduction in the absence of convection $t_\kappa \equiv D/V = D^2/\kappa$

Convective time scale (t_v): time needed for a fluid to cross the depth of the fluid layer at the convective velocity *v* decreases with increase of *Ra*:

Convection is a much more efficient heat transport mechanism than conduction. $t_v = D/v = t_\kappa Ra^{-2/3}$

Convection model

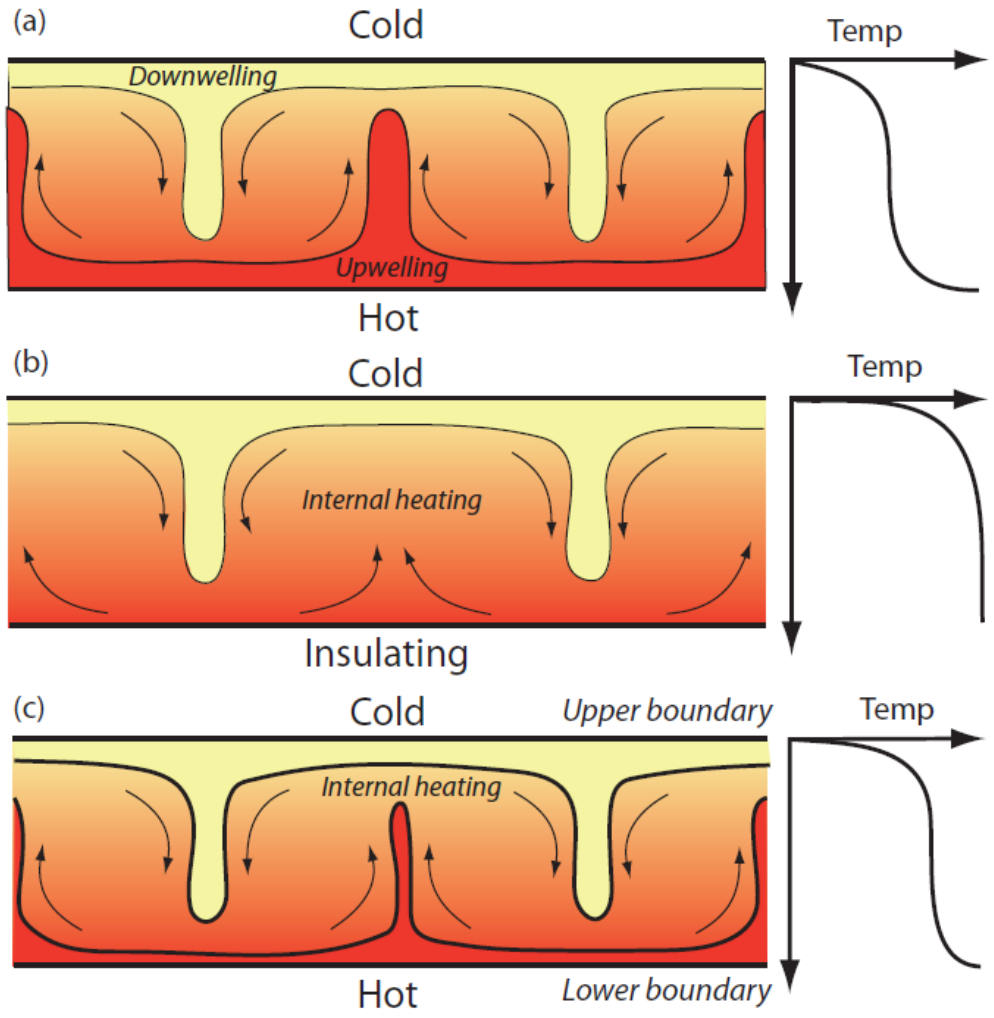

Active upwelling: heat entering from below and there is no heat generated within (Rayleigh-Bernard convection).

Passive upwelling: a fluid layer is heated from within by radioactivity and the cool fluid sinking form the top boundary layer drives circulation. In this condition, upwellings would be a passive response rather than involving positively buoyant material.

Active and passive upwelling: the heat input to the fluid layer might be a combination of heat entering from below and heat generated within.
The upper thermal boundary layer conducts outward both the basal and internal heat and thus develops a greater temperature drop than the basal boundary (no symmetry between upwellings and downwellings).

- Convection requires a super-adiabatic gradient: In order to have buoyancy that will drive convection, a deep portion of the mantle must start hotter than its surroundings, while an upper portion must be cooler, forming a negatively buoyant lithospheric material.
- If the layer covects more vigorously, the thickness of the layer having homogeneous temperature will increase, the thermal boundary layers will be thinner and the temperature gradients through them will be higher, driving larger heat fluxes.

Convection model

Marginal stability

- For a fluid layer heated uniformly on a lower horizontal boundary, there is a minimum amount of heating below which convection does not occur.
- The transition from conduction to convection, just at the point of instability, is called **marginal stability**, which occurs when *Ra* ~ 1000.

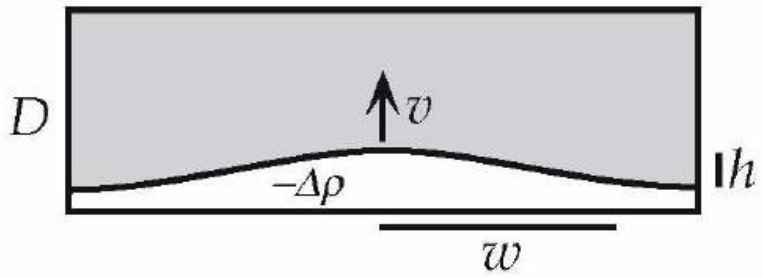

From the balance of buoyancy (B) and viscous resistance (R_s) force:

$B=g\Delta\rho wh$ if $w<<D$ $R_s = \mu(v/w)w = \mu v = \mu\partial h/\partial t$

we get: $\frac{\partial h}{\partial t} = \frac{g\Delta\rho w}{\mu}h$ and $h = h_0 \exp(t/\tau_s)$, where $\tau_s = \frac{\mu}{g\Delta\rho w}$ h_0=constant

The bulge grows exponentially with a time constant τ_s, because the interface is unstable (Rayleigh-Taylor instability).
Since τ_s gets smaller as w gets bigger, broader bulge grows more quickly.

If $w>>D$ the dominant viscous resistance comes from horizontal shear flow with velocity u along the layer.

By conservation of mass: $uD = vw$. The characteristic velocity gradient of this shear flow: $u/D = vw/D^2$

$R_1 = \mu(u/D)w = \mu v w^2/D^2$ $\frac{\partial h}{\partial t} = \frac{g\Delta\rho D^2}{\mu w}h$ $\tau_1 = \frac{\mu w}{g\Delta\rho D^2}$ τ_1 gets bigger for larger w

If w=D the time scale of the growth of the instability gets smaller (fastest growing bulge) $\tau_{RT} = \frac{\mu}{g\Delta\rho D}$

There is a competition between the buoyancy and the thermal diffusion, expressed in terms of the time scales of the two processes: τ_{RT} for the buoyant growth and τ_k or the thermal diffusion ($\tau_k = D^2/\kappa$): In order for the bulge to grow $\tau_{RT} << \tau_k$ $Ra = \frac{\tau_\kappa}{\tau_{RT}}$ $\frac{g\Delta\rho D^3}{\kappa\mu} = Ra \geq c$

There is a value of the Rayleigh number that must be exceeded before the thermal boundary layer can rise unstably in the presence of continuous heat loss by thermal diffusion (*Ra*>>1000), otherwise no thermal convection!

Convection model

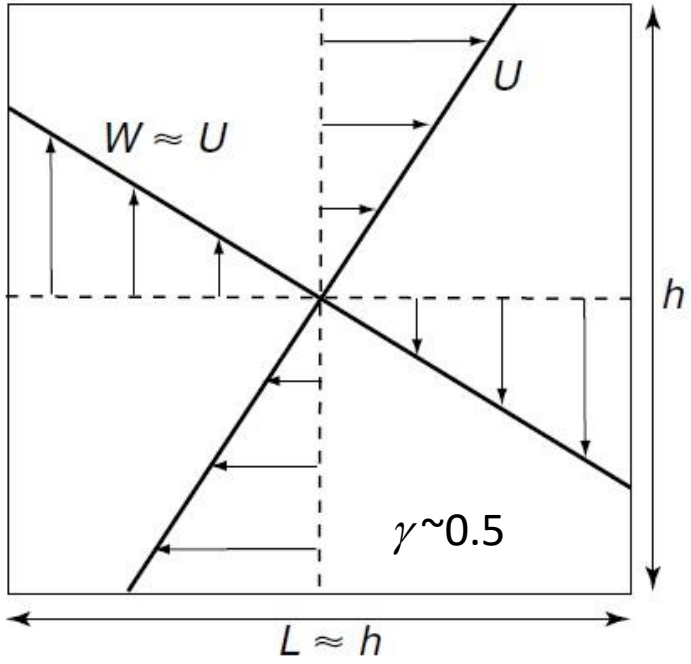

Convection cell of aspect ratio ≈ 1 (Rayleigh–Benard convection)

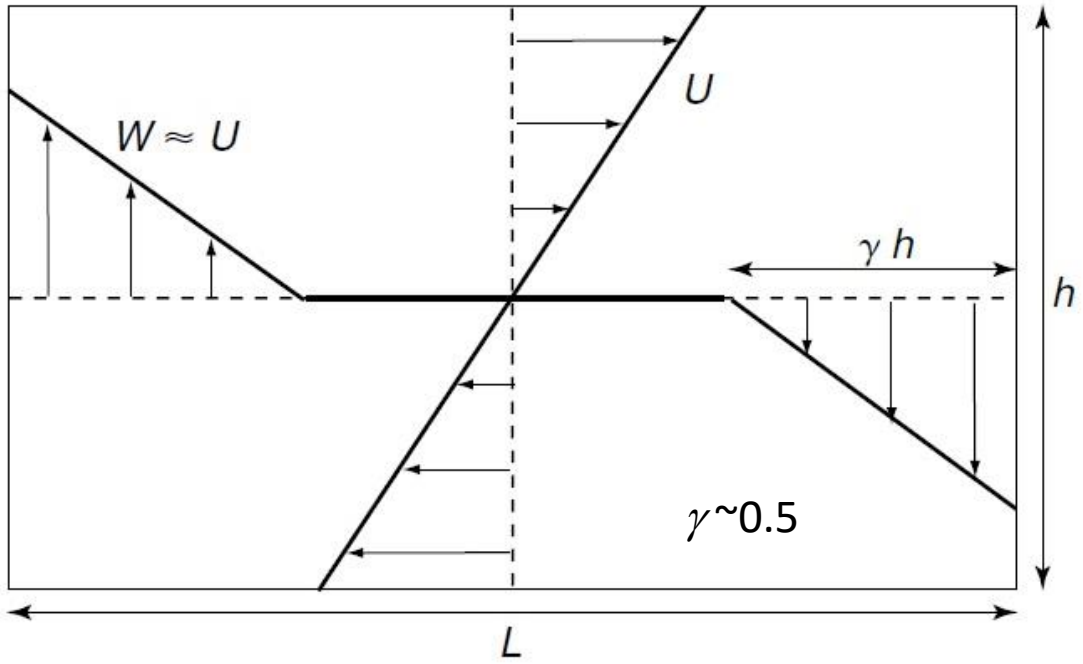

Convection cell of aspect ratio >1

- Kinetic dissipation may be split into two different components: one is generated by the horizontal shear flow with a vertical gradient of horizontal velocity ~2U/h, while the other component is associated with the vertical flow, which is such that velocity drops from the maximum value W over horizontal distance $\delta = \gamma h$.
- If the cell of aspect ratio >1 the horizontal velocity field stretches over the whole layer thickness, whereas the vertical velocity field extends over kinetic boundary layers of width γh.

Convection model

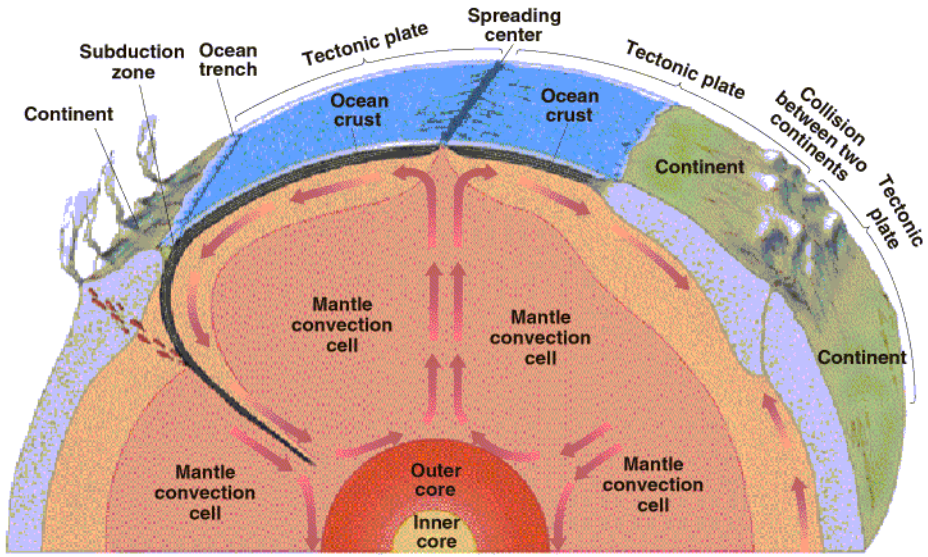

- For Rayleigh-Benard convection in a fluid layer, convection regime takes the form of cells that are about as wide as the layer thickness *h*, as long as Ra<10^5.
- Mantle convection cells change size based on continental/oceanic areas distribution: the wider is the continental plate the wider is the cell.
- The Earth today has cells of aspect ratio (L/h) ~3 (horizontal heat transport can be neglected), so that its rate of heat loss is ~half that for cells of L/h=1 (cooling of the Earth is less efficient in presence of continents).
- The main effect for an aspect ratio > 1 (wide cells) is that the Nusselt number and average heat flux across the cell decreases as *L* increases.
- Continents perturb the convective flow pattern as their lithospheric roots divert mantle flow.

Nusselt number

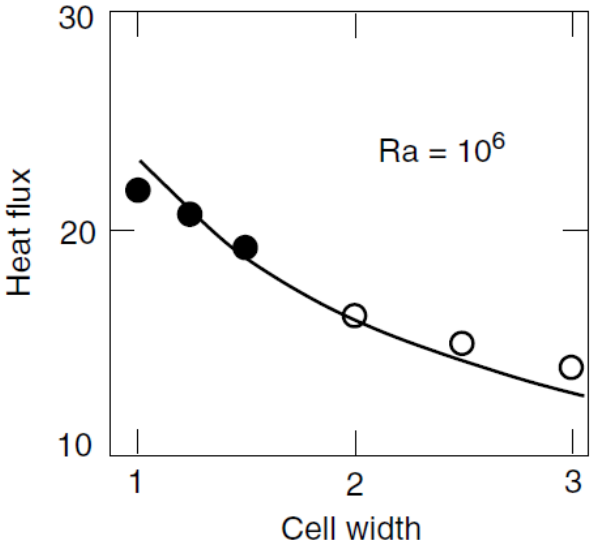

Convection model

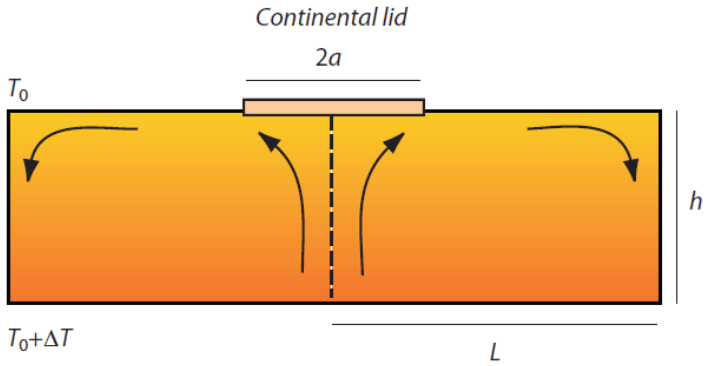

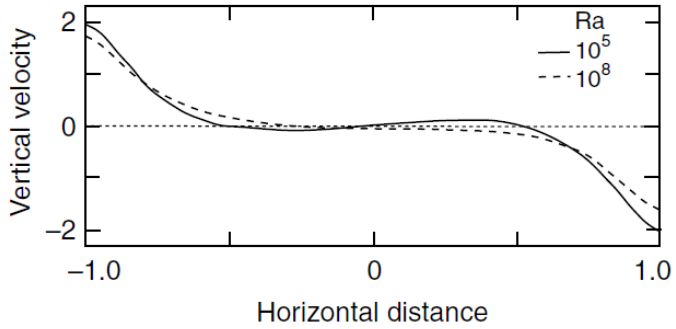

- **In presence of poorly conductive lid, the base of the lid is at higher *T* than the top of the fluid away from the lid at T_0. Then, the fluid beneath the lid is heated and becomes involved in an upwelling centered on the continent that feeds horizontal flow extending to large distances. The upper and lower horizontal surfaces of the cell move in the horizontal direction with velocity U and –U at the top and bottom, respectively, while the velocity is zero in the middle of the cell.**
- **Aspect ratio of the cells (*L*/*h*) depends on the width of the lid and *Ra*: for *Ra*> 10^6 the flow involves small-scale instabilities superimposed on a larger-scale circulation.**
- **Because of the difference in the efficiency of heat transport at the upper and lower boundaries, the average temperature of the fluid layer is larger than *To*+ΔT/2.**

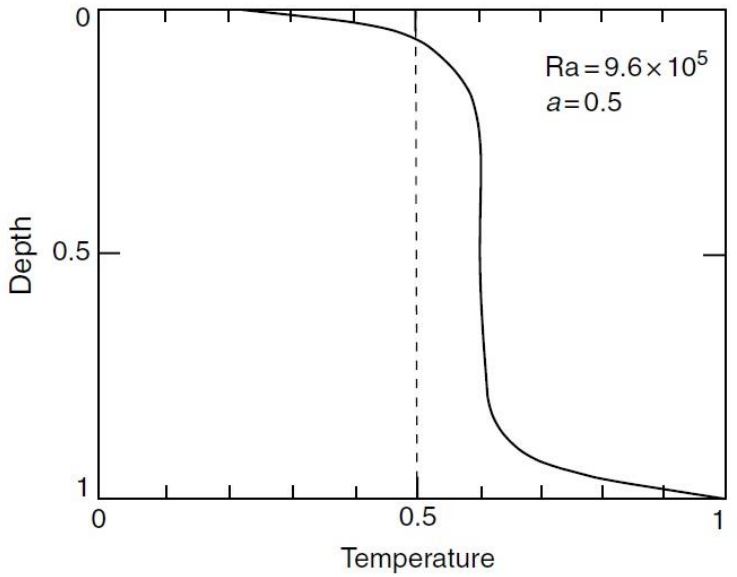

a=dimensionless lid width

Convection model

Continental insulation acts to increase the average mantle temperature and decrease its heat flux

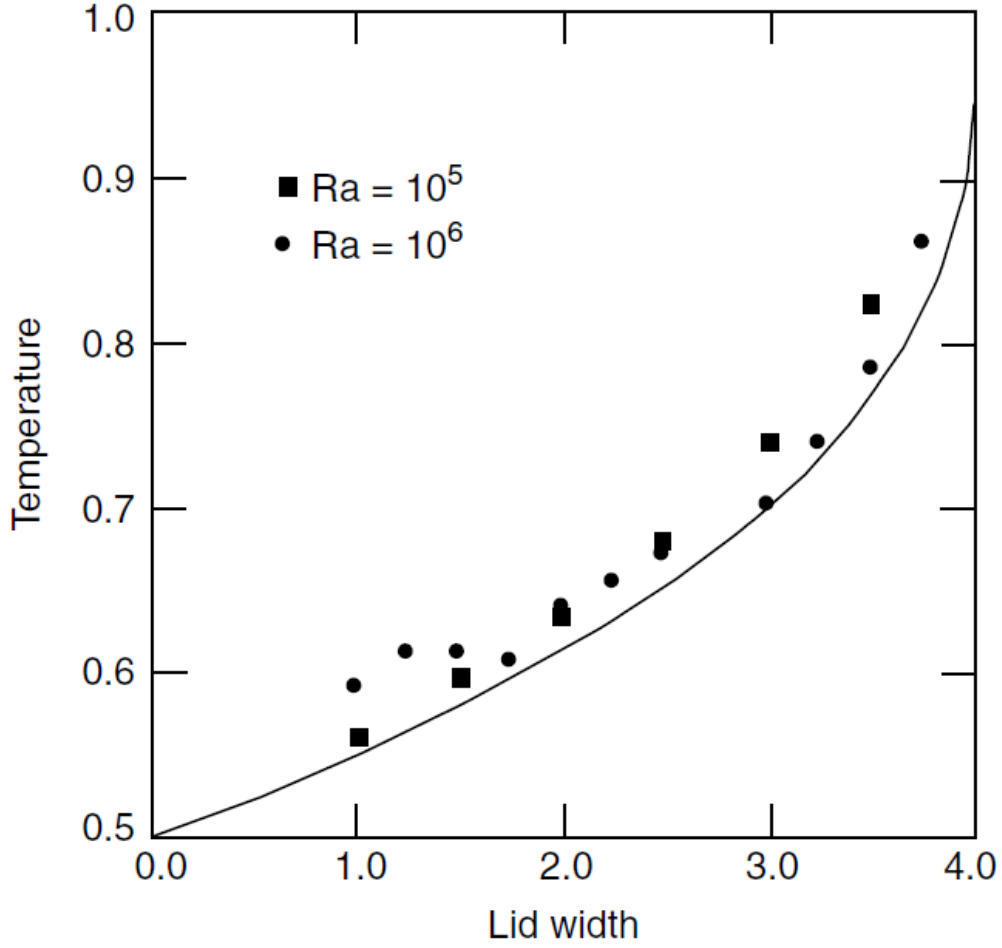

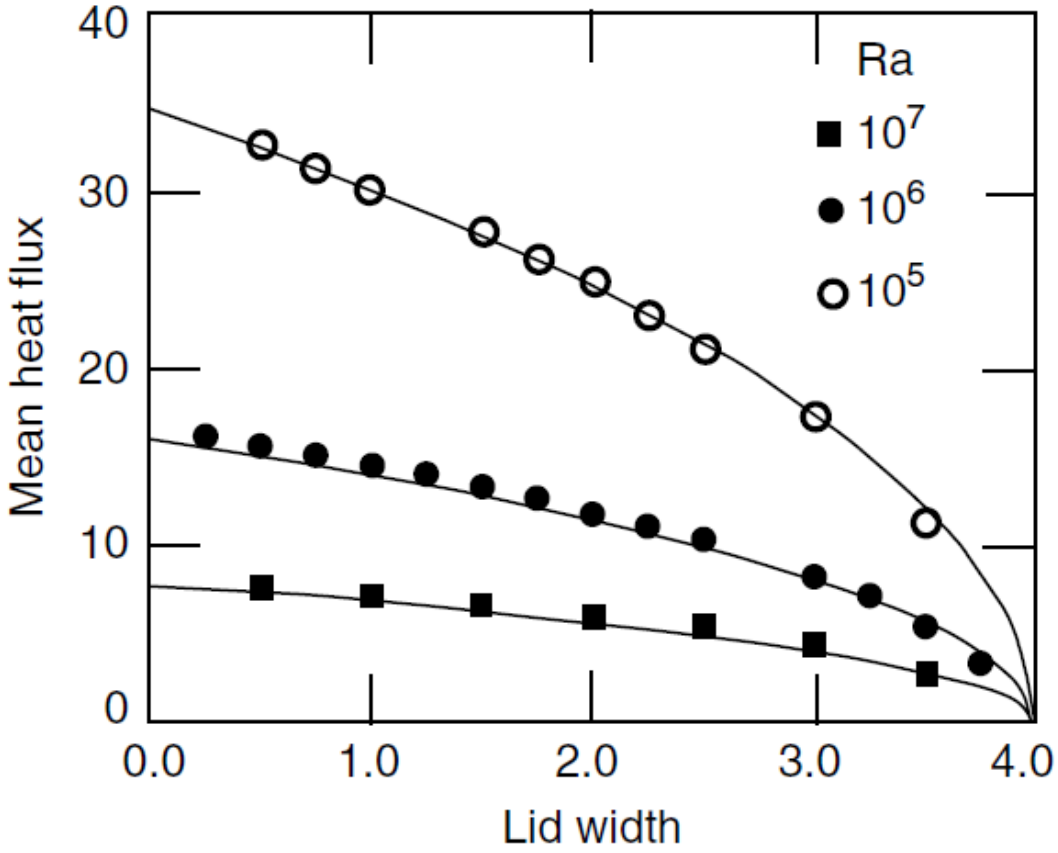

Convection model

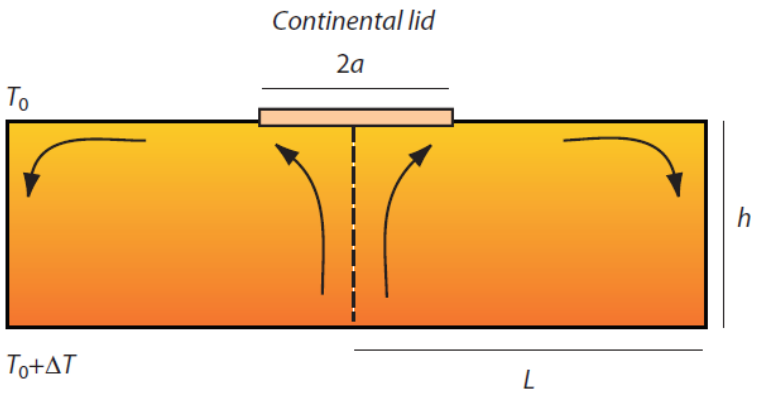

A wide insulating lid (during supercontinent assembly) warms the mantle beneath it and the entire interior of the Earth:

- it may cause plumes localization and would explain the flood basalts with supercontinental break-up.
- Presence of the lid prevents the heat from escaping to the surface (as under the oceans).
- It makes the cooling effect of subduction absent.
- It influences the formation of elongated large-scale cells with a size dependent on the width of the insulating lid (it increases the mean temperatures of the convective fluid layer).

Very large continent can cause drip-type instabilities associated to small-scale convention cells ($\lambda < 1000$ km) and thus form intracratonic basins depocenters.

Convection model

In a thin lid with large aspect ratio vertical heat transport dominates:

The heat flux through the lid is: $q = +\lambda_L \frac{T - T_o}{d}$

If we neglect the lid thickness in comparison with the fluid layer depth, the heat flux at the top of the fluid, i.e. at $z = 0$ is:

$$\left(\lambda \frac{\partial T}{\partial z}\right)_{z=0} = \lambda_L \frac{T - T_o}{d}$$

$$\left(\frac{\partial T}{\partial z}\right)_{z=0} - \mathrm{B}T = 0 \qquad \mathrm{B} = \frac{\lambda_L}{\lambda}\frac{h}{d}$$

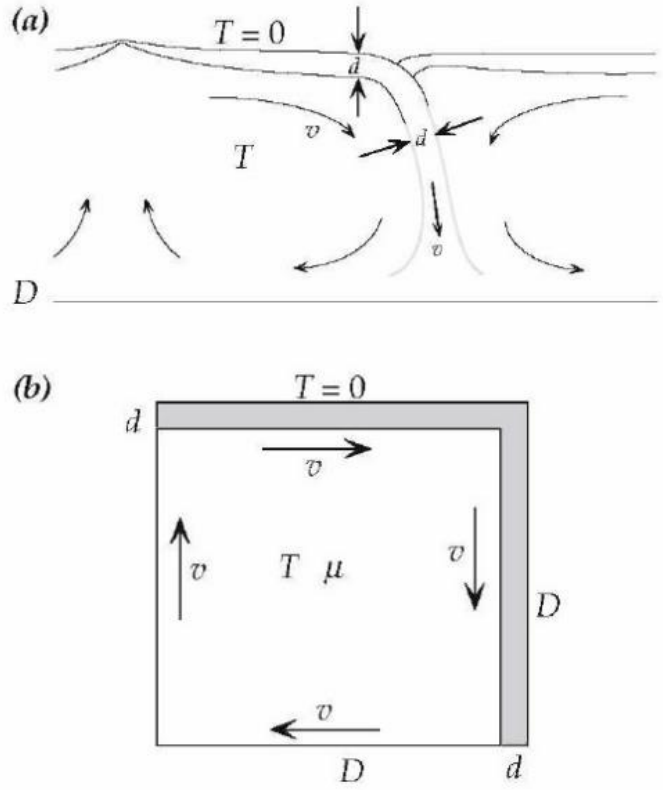

$h=D$ (thickness of the fluid layer) ~ 3000 km
d=thickness of the lid ~ 300 km
T_0=0
λ_L=thermal conductivity of the lid, λ=thermal conductivity of the fluid, λ_L/λ ~ 1
B=Biot Number (B=10, since h/d=10) is small, since it leads to heat fluxes that are small fraction of those of free convective cells (e.g., q~ 12mWm^{-2} at the base of the cratonic lithosphere, q~ 100mWm^{-2} close to the ridges).
For B <<1 (d>> or λ_L <<) heat flux approaches zero.

Hot Spot, mantle plumes, and Large Igneous Provinces (LIPs)

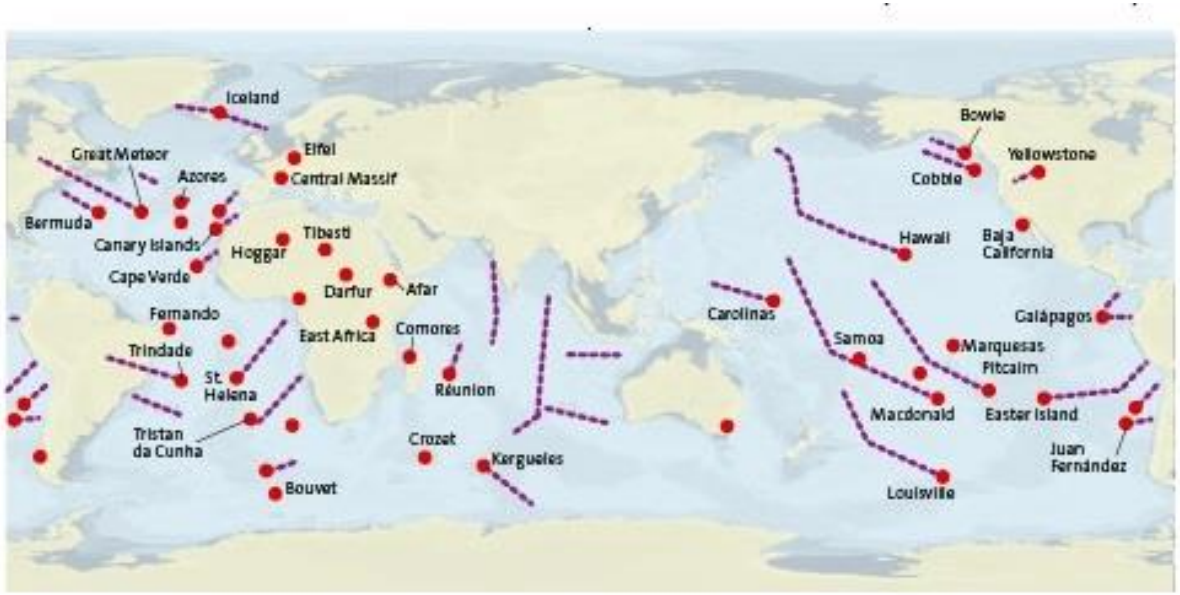

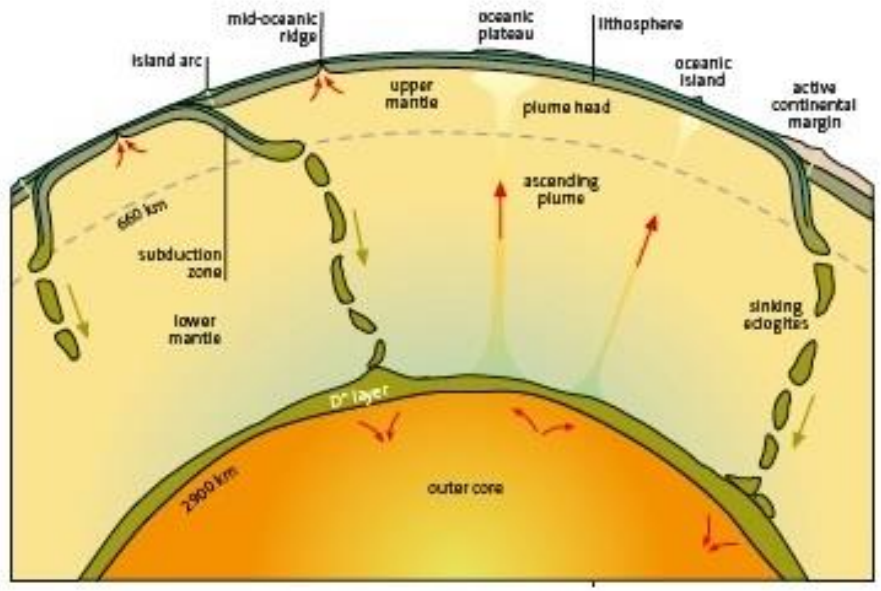

Plumes

- Hot mantle rocks (300 °C higher than surrounding mantle), not molten, because of the high pressure, arising from the lower mantle (or shallower depths).
- Depth formation of mantle plumes is imaged by the seismic tomography and reflected by the geochemistry.
- Hot spot lifetime is about 100 Myr.
- The influence on the Earth energy budget of the heat flux carried by mantle plumes is of ≈ 2–4 TW < 10% of the global heat flow.

Hot Spot and geoid anomalies

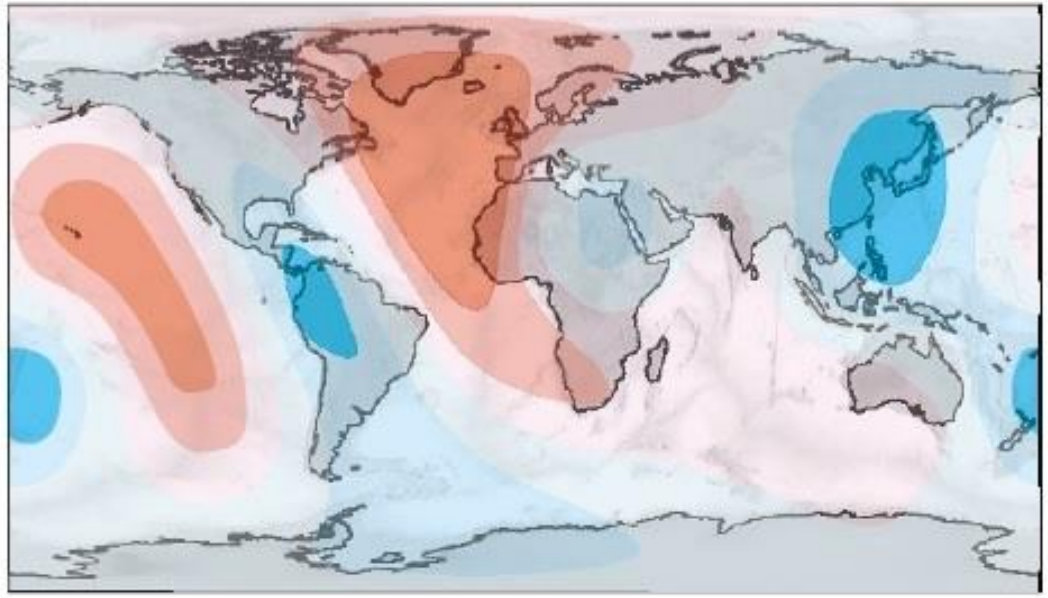

- Hot spot are concentrated in correspondence of geoid bulges

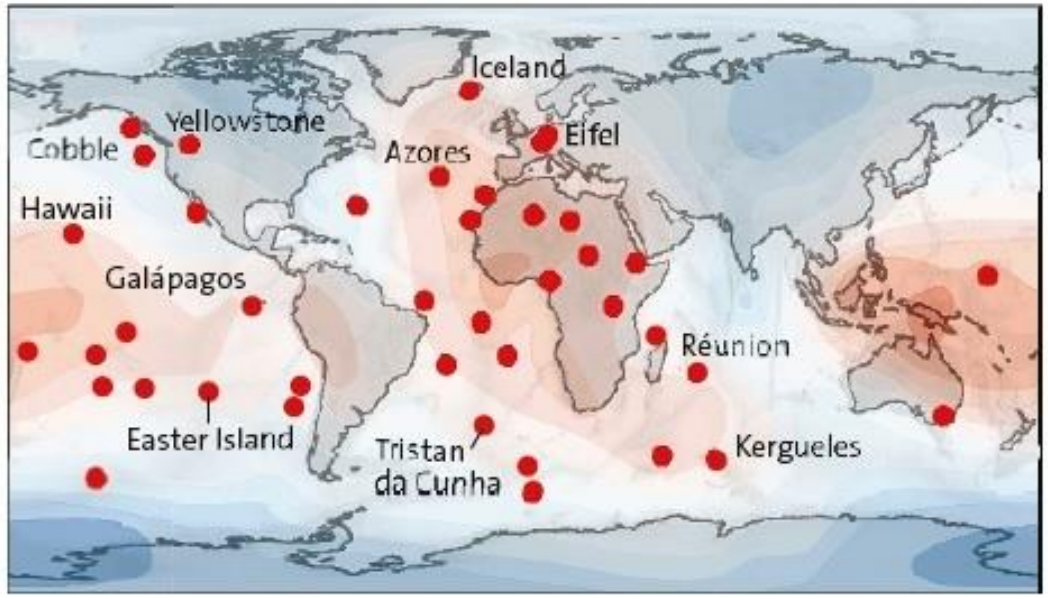

- Oceanic hot spot generate volcanic products rich of incompatible elements and high isotopic ratio of $^{87}Sr/^{86}Sr$, $^{187}Os/^{188}Os$, and $^{3}He/^{4}He$ indicating the influence of a lower mantle source.
- In particular, the $^{3}He/^{4}He$ ratio is a measure of the amount of primordial helium (^{3}He was present in the presolar nebula and is only lost from the Earth to space via degassing) relative to ^{4}He, which is primarily generated by radioactive decay of U and Th.

Hot spot tracks

Hot spots form tracks on the ocean floor in response to the motion of the ocean plate

Pacific Plate drifts over the plume at a rate of ca. 100 km in 1Myr

Hawaai (6000 km-long track)

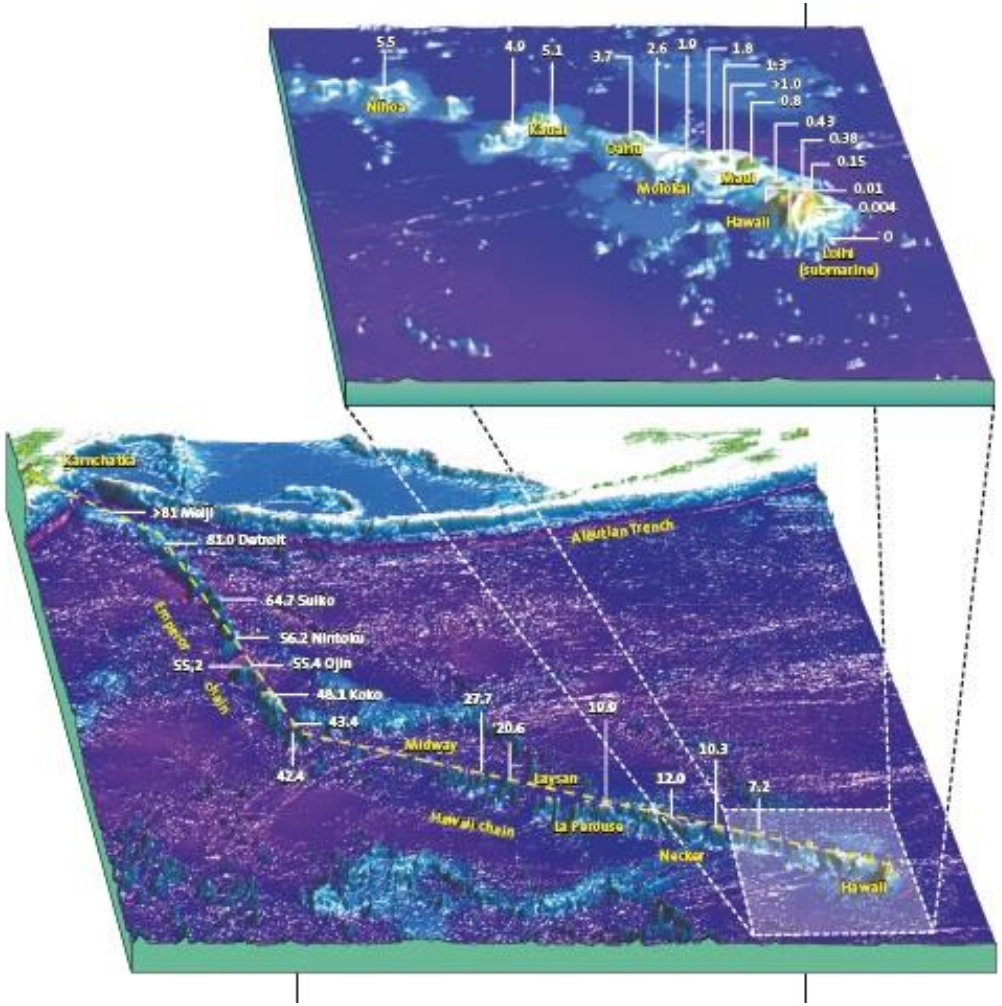

India

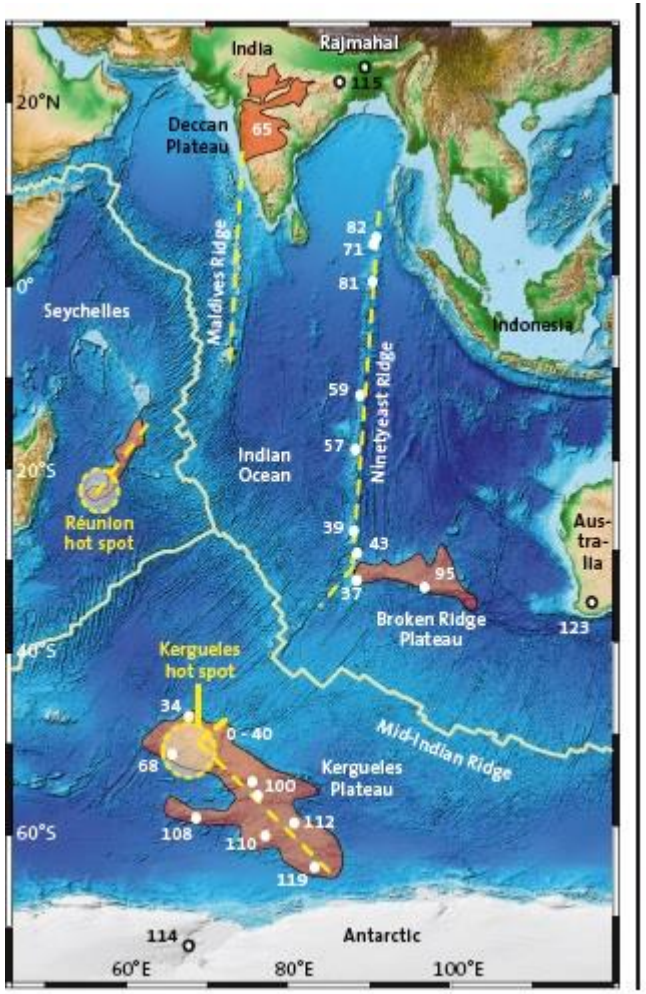

Maldives Ridge and the Ninetyeast Ridge were generated by the hot spots of Réunion and the Kergueles.

Hot spot tracks

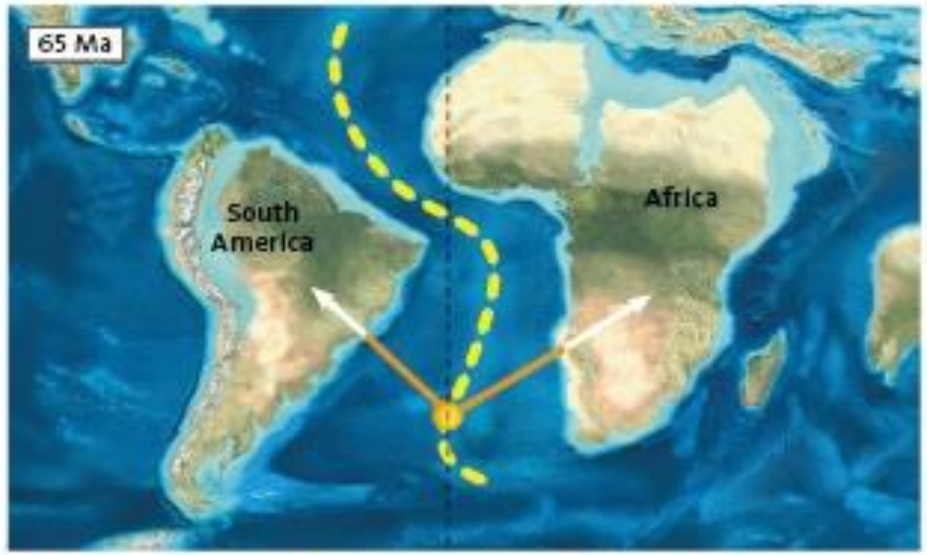

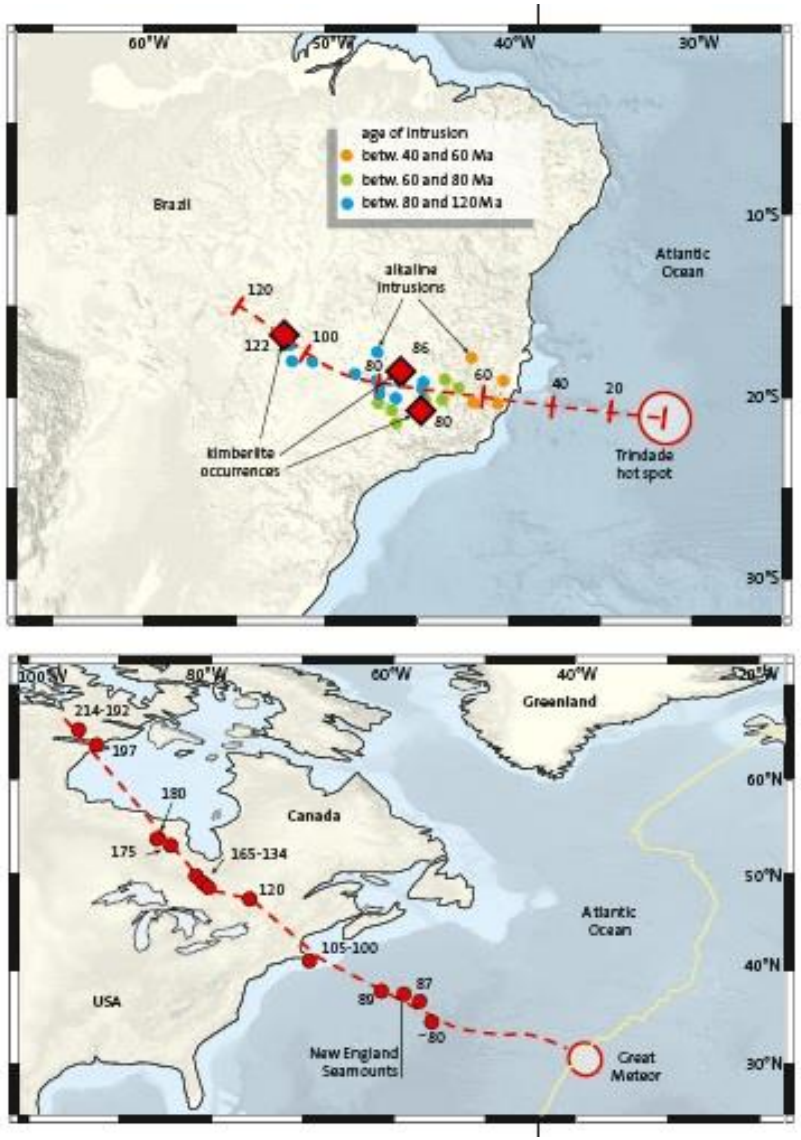

The plate boundary shifted 30 Myr, and the hot spot Tristan da Cunha tracked across only the African Plate.

Iceland hot spot

- Iceland is a product of the activity of a mantle plume that was located below Western Greenland and the Canadian Arctic.
- The young mid-ocean ridge came under the influence of the mantle plume in the Eocene ca. 30-40 Myr.

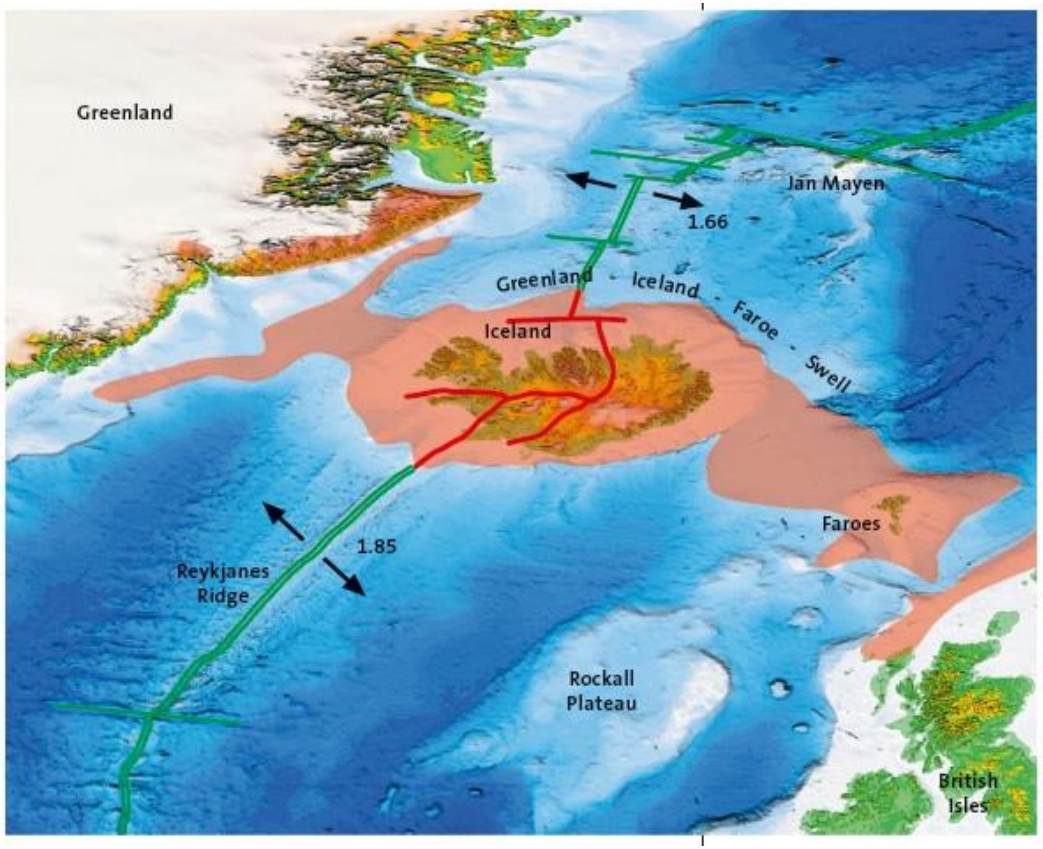

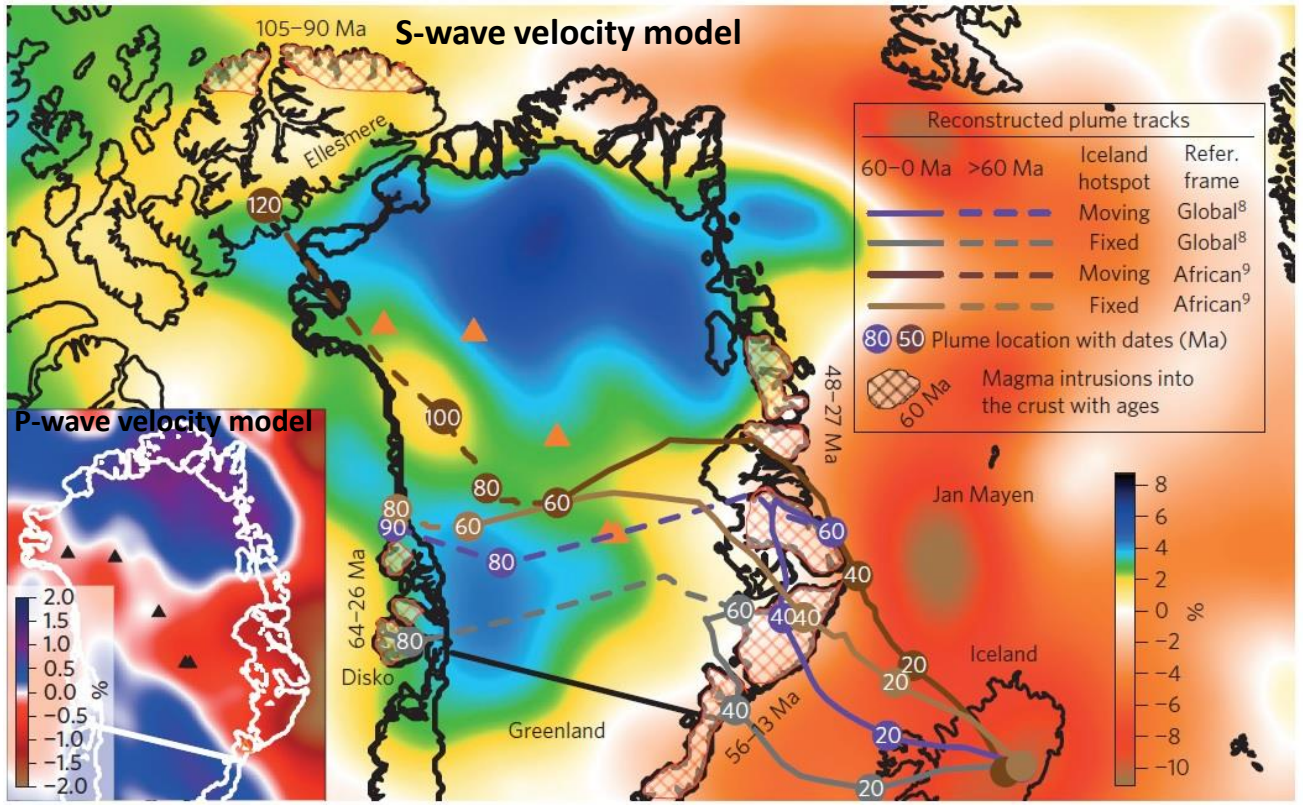

Rogozhina et al., 2016, Nature Geoscience, vol. 9

Iceland Crust

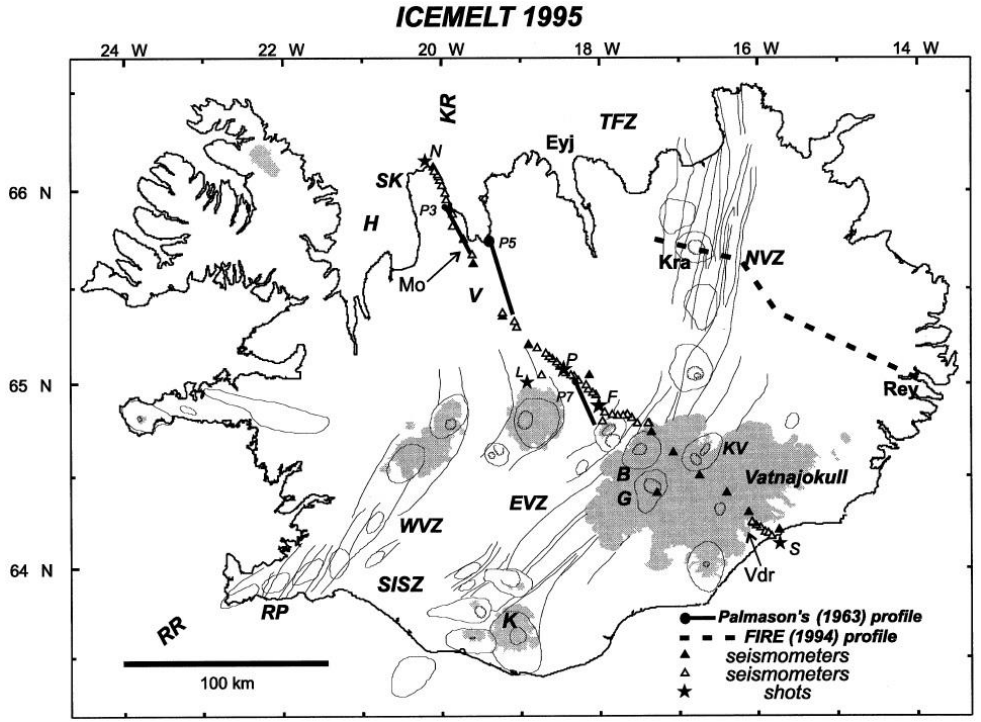

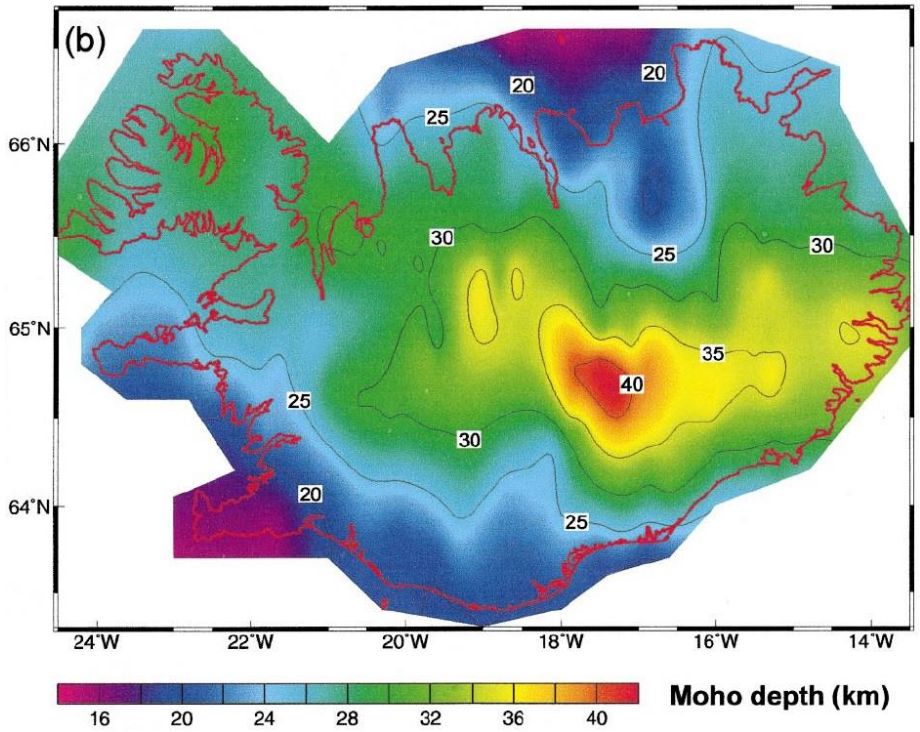

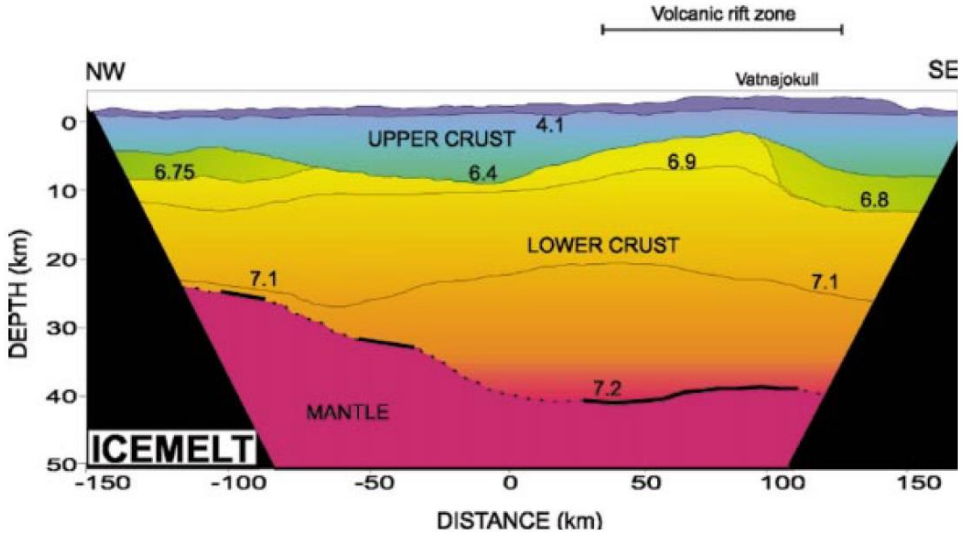

Darbyshire, 2000, EPSL, 181

Darbyshire, 1998, GJI, 135

Superswells

- Superswells represent clusters of hot spots in a restricted geographical region of anomalously high elevation, extending several hundred km beyond the area of excess volcanism, which cannot be explained by crustal thickening, examples are the Africa and the South Pacific, characterized by slow seismic velocities both in the upper and lower mantle, related to the anomalous high temperatures.
- The hot spot in the south Pacific have anomalously low seismic wave speeds in the mantle, suggesting an origin involving anomalously low densities but without substantially thinned lithosphere. The African Superswell, on the other hand, does not show a seismic anomaly in the upper mantle but rather a broad columnar zone of slow velocities in the lower mantle, both of compositional and thermal origin.
- In general, if a swell forms at a hot spot, it decreases in height with time and can no longer be detected when reaches an age of 80 Myr, (or even <50 Myr). On the other hand, the young Madeira and Canary hot spots do not show any swell.

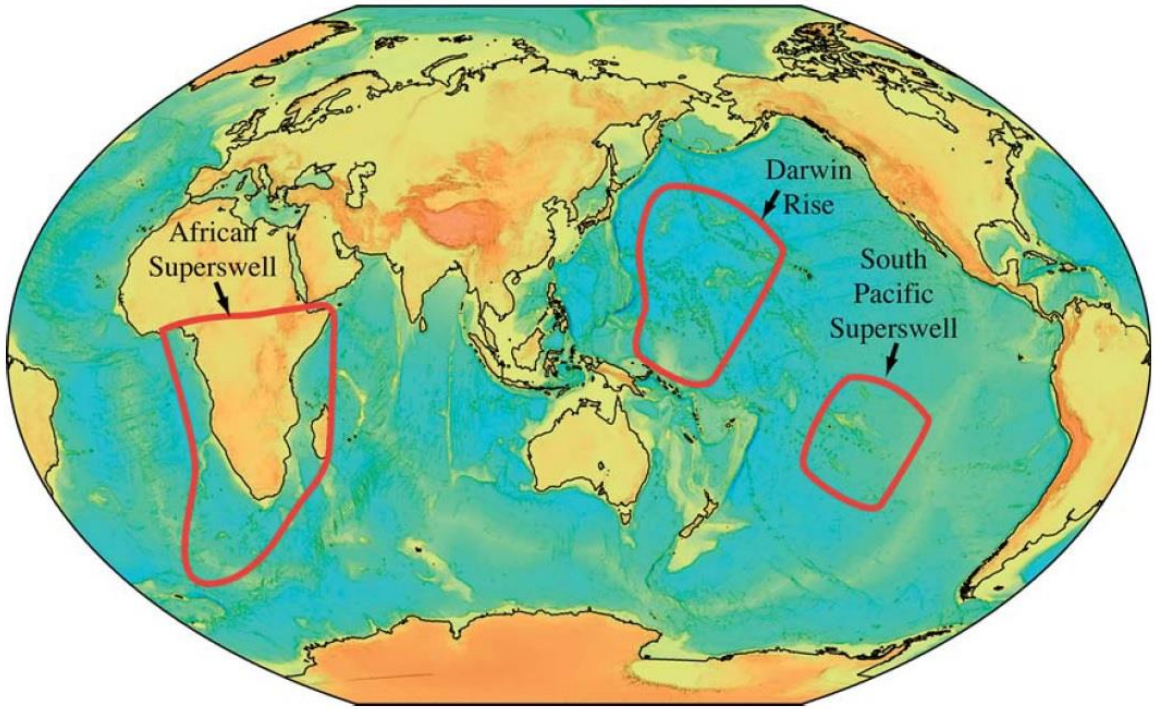

McNutt and Caress, 2007, Treatise ofGeophysics, vol. 1

Global seismic tomographic image of shear-wave velocities

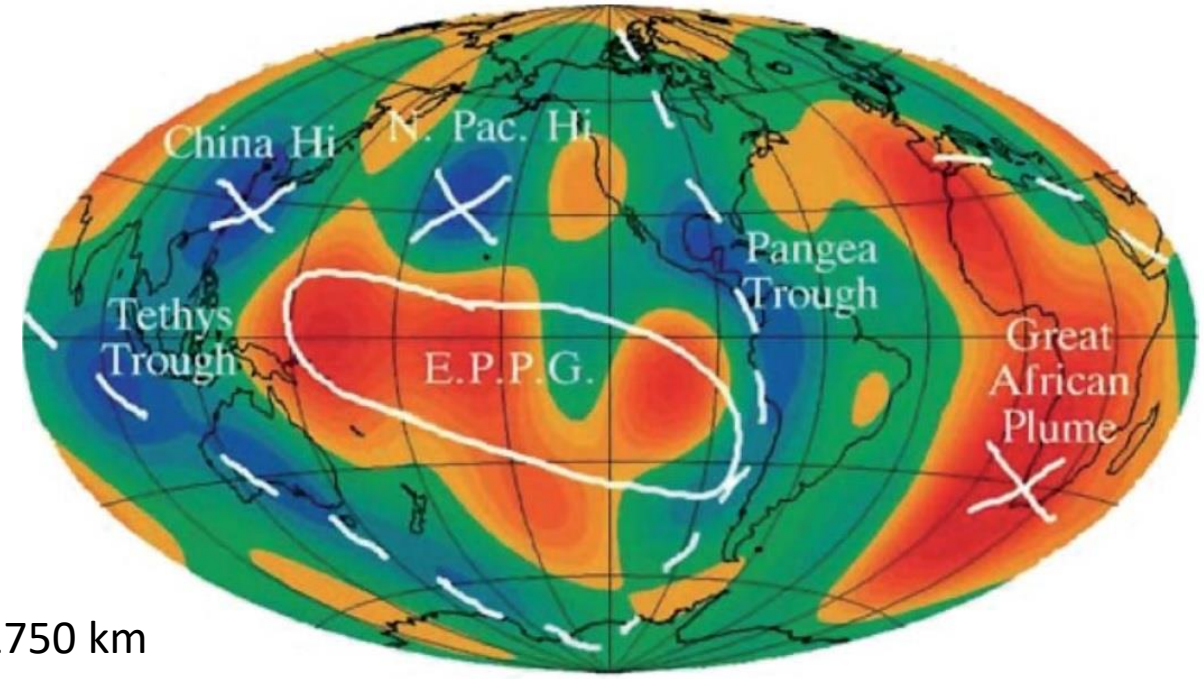

2750 km

Geophysical characteristics of hot spots

Orientation and Age

- Hot spots erupting on the Pacific Plate tend to form linear chains of volcanoes, often having a monotonic age progression. In some cases the most common age pattern is nearly synchronous volcanism at several volcanic centers along the chain, with short age progressions. However, the sequence of hot-spot eruptions is not completely random in space or time.
- Long-lived (> 50My) age-progressive volcanism occurs in 13 hot spots, defining a kinematic reference frame that is deforming at rates lower than average plate velocities. Over geologic time there has been significant motion between the Indo-Atlantic hot spots, the Pacific hot spots, and Iceland. Short-lived (<22My) age progressions occur in at least 8 volcano chains.
- The Yellowstone hot spot is the only continental hot spot showing a clear age progression. The effective speed of the hot-spot track is 4.5 cm yr^{-1}, which is interpreted to include a component of the present-day plate motion (2.5 $cmyr^{-1}$) and a component caused by the Basin and Range extension.

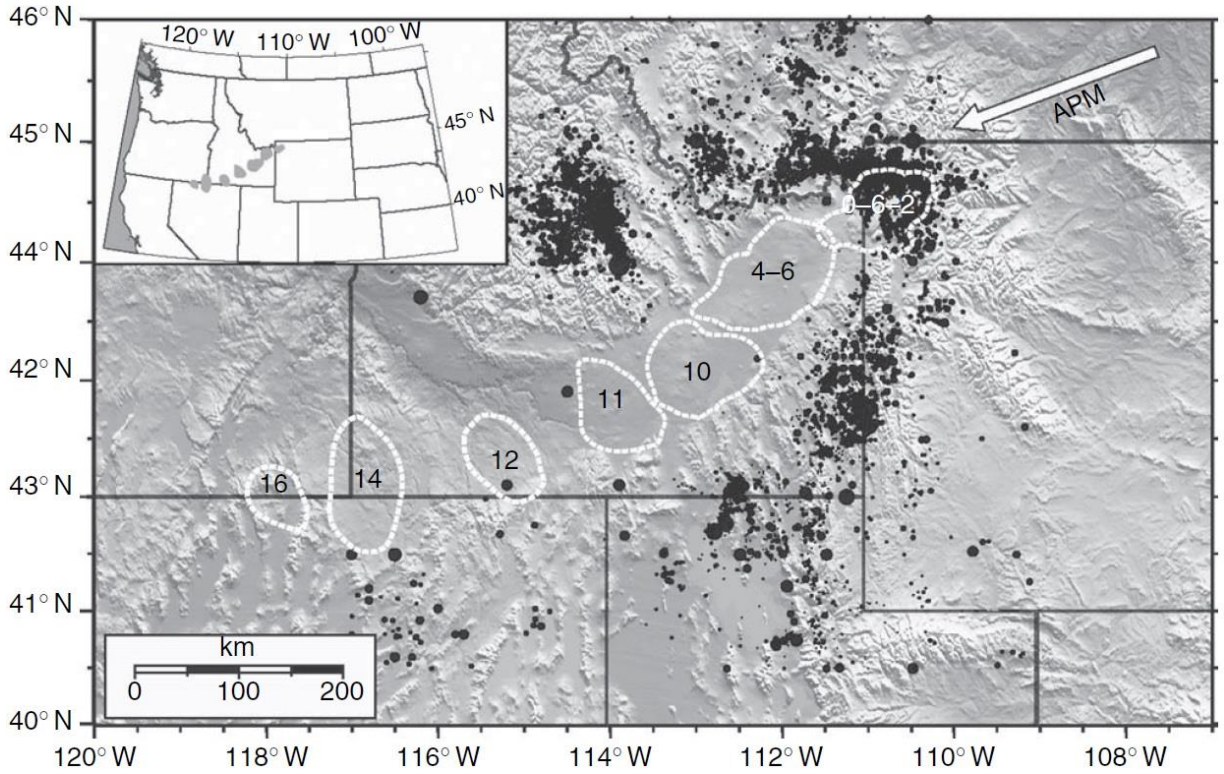

Ito and van Keken, 2007, Treatise of Geophysics, vol. 7

Geophysical characteristics of hot spots

Heat Flow

Hawaiian Islands

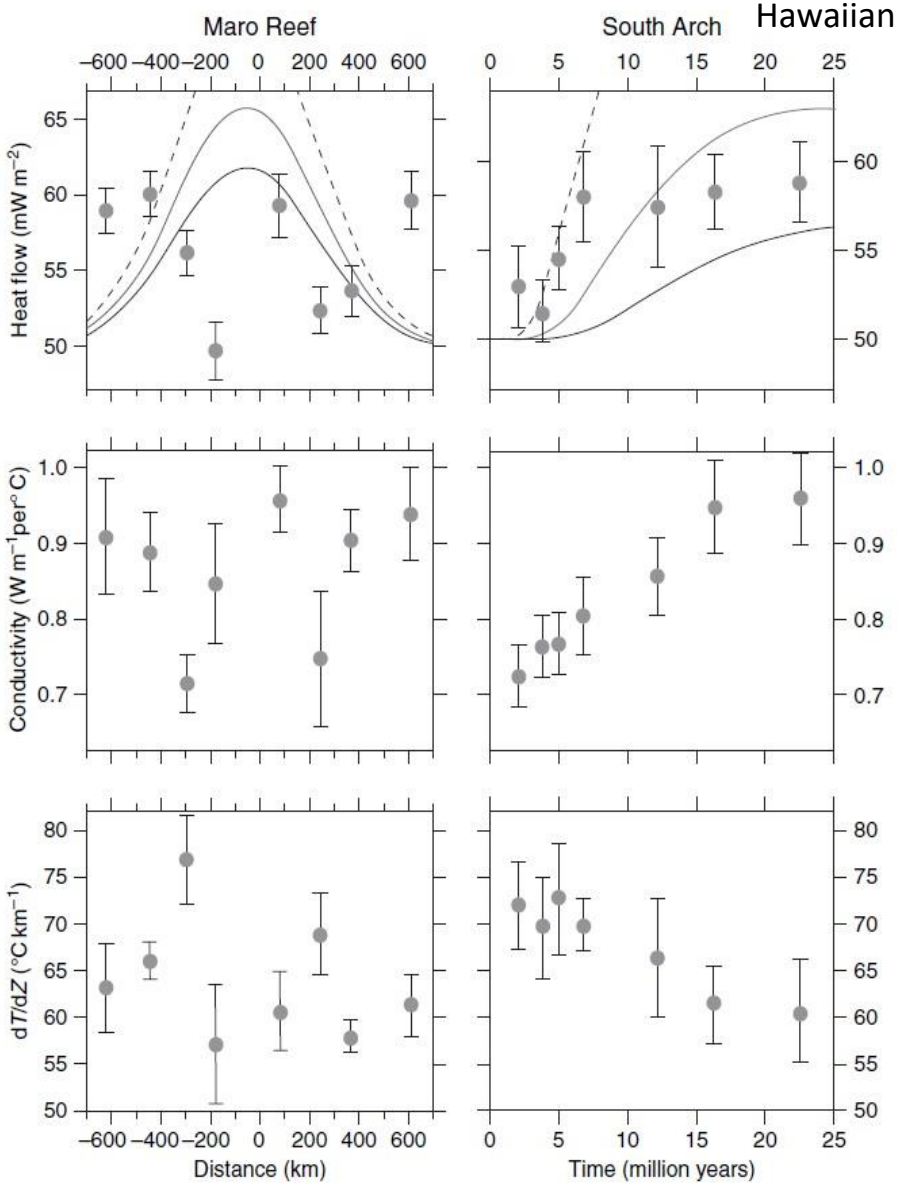

- There are modest (10-25%) heat flow anomalies associated with hot spots, suggesting that the low-density material is at least partially thermal in origin. However, the effects of near-surface fluid circulation effectively mask much of the spatial and temporal pattern of any thermal disturbance.
- Heat flow variations over Hawaiian swell controlled by near-surface processes, not plume properties: areas of high conductivity act as radiators while areas of low conductivity act as insulators, producing nonuniform conduction of heat to the seafloor that is controlled by variations in thermal conductivity.

Lines on the upper panels show the theoretical variations in heat flow expected if the hot spot reheated the lower lithosphere to asthenospheric values (1350°C) as it passed over the thermal source. The amount of thinning assumed is 60 km (solid line), 50 km (dotted line), and 40 km (dashed line).

McNutt and Caress, 2007, Treatise ofGeophysics, vol. 1

Geophysical characteristics of hot spots

Magmatic Underplating

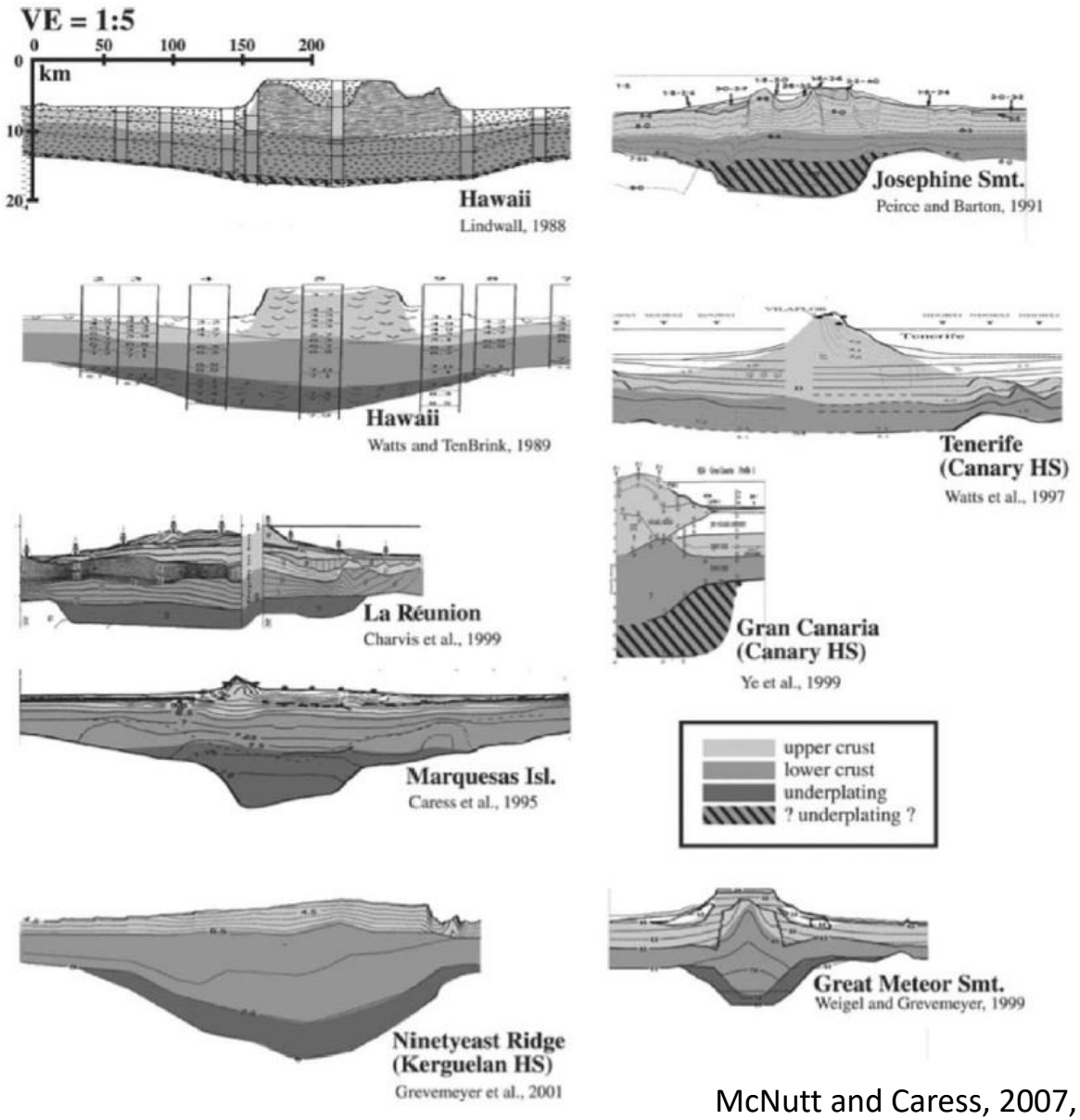

- Intrusive volcanism and underplating are characteristic for most of the volcanic provinces, which were located above a hot spot at the time of their formation.
- The seismic velocity of the underplated material suggests that the hot spot produced melt buoyant enough to rise through the upper mantle to the base of the crust, but not sufficiently buoyant to rise above the crust–mantle boundary.
- Underplating may be associated with later stages of hot-spot volcanism (e.g., Hawaai and Ninetyeast Ridge), but the existence of underplating beneath the currently volcanically active La Reunion demonstrates that subcrustal intrusions can occur during the primary edifice building stage of hot-spot volcanism.

McNutt and Caress, 2007, Treatise ofGeophysics, vol. 1

Geophysical characteristics of hot spots

Seismic Velocities

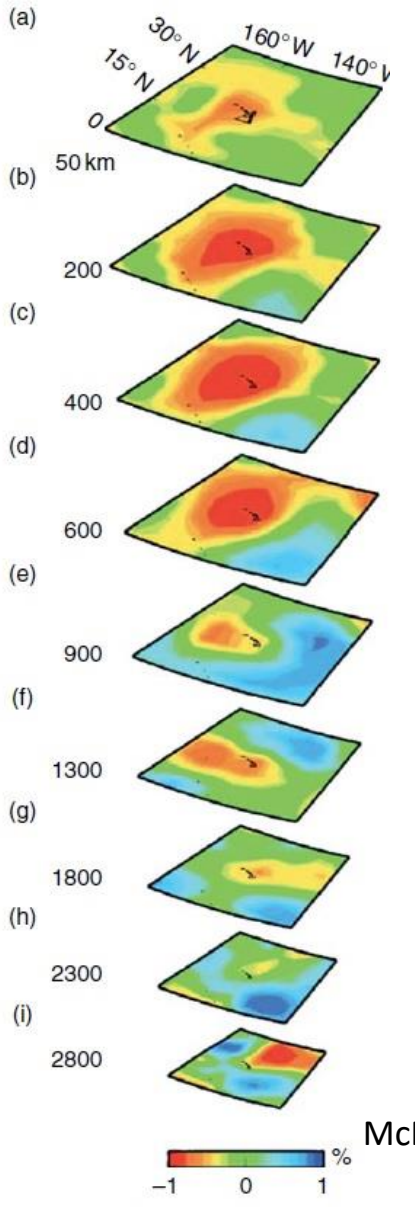

P-wave tomographic images in map view around the Hawaiian hot spot

McNutt and Caress, 2007, Treatise ofGeophysics, vol. 1

- A hot spot having a plume origin must show continuous low shear velocity in the underlying upper and lower mantle.
- There are only a few hot spots that match this criterion (Afar, Bowie, Easter, Hawaii, Iceland, Louisville, McDonald, and Samoa), out of the 37 considered.
- In several cases, the anomalous seismic structure extends well below 410 km producing a deepening of the discontinuity defining the top of the transizion zone, but not the updoming of the discontinuity of defining its bottom.
- Using broader criteria based on seismological, other geophysical, and helium isotope data, Afar, Easter, Hawaii, Reunion, Samoa, Louisville, Iceland, and Tristan are likely to be of plume origin.

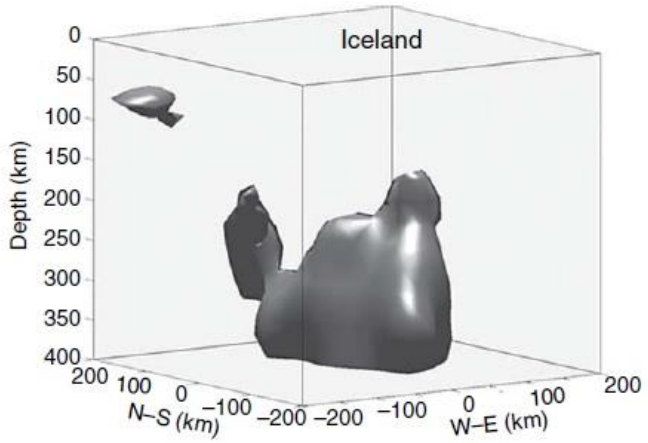

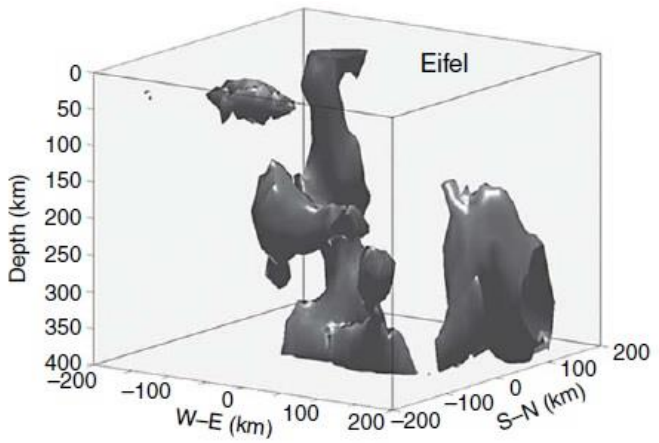

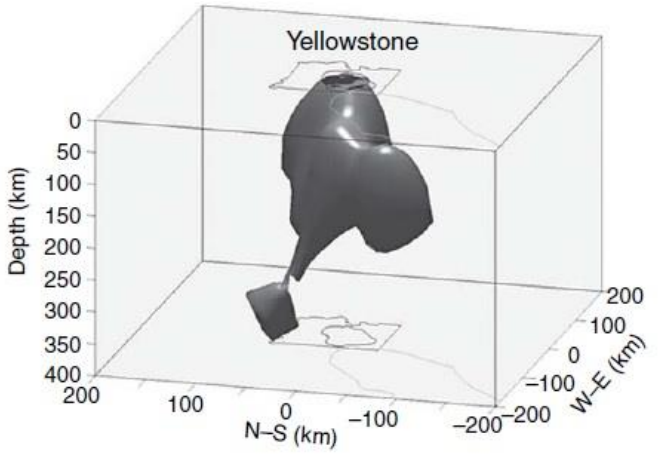

Contours of -1% P-wave velocity anomaly

Ito and van Keken, 2007, Treatise ofGeophysics, vol. 7

Azores: hot or cold spot?

- Not necessarily the mantle potential temperature beneath the hot spots is 200-300°C higher than beneath the ridge, since water and CO_2 can strongly reduce melting temperature. Thus, the excess of temperature in some hot spots like the Azores can be only ~50°C or less.
- The mantle beneath hot spots (e.g., Hawaai, Iceland, Galapagos) may also contain more fusible, mafic lithologies, such as those generated by the recycling of subducted oceanic crust forming eclogite.

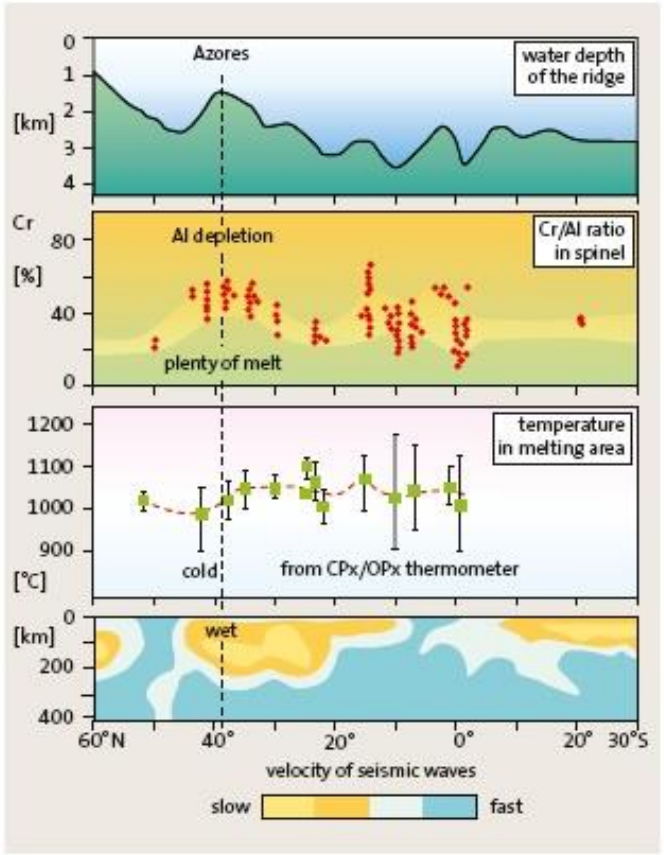

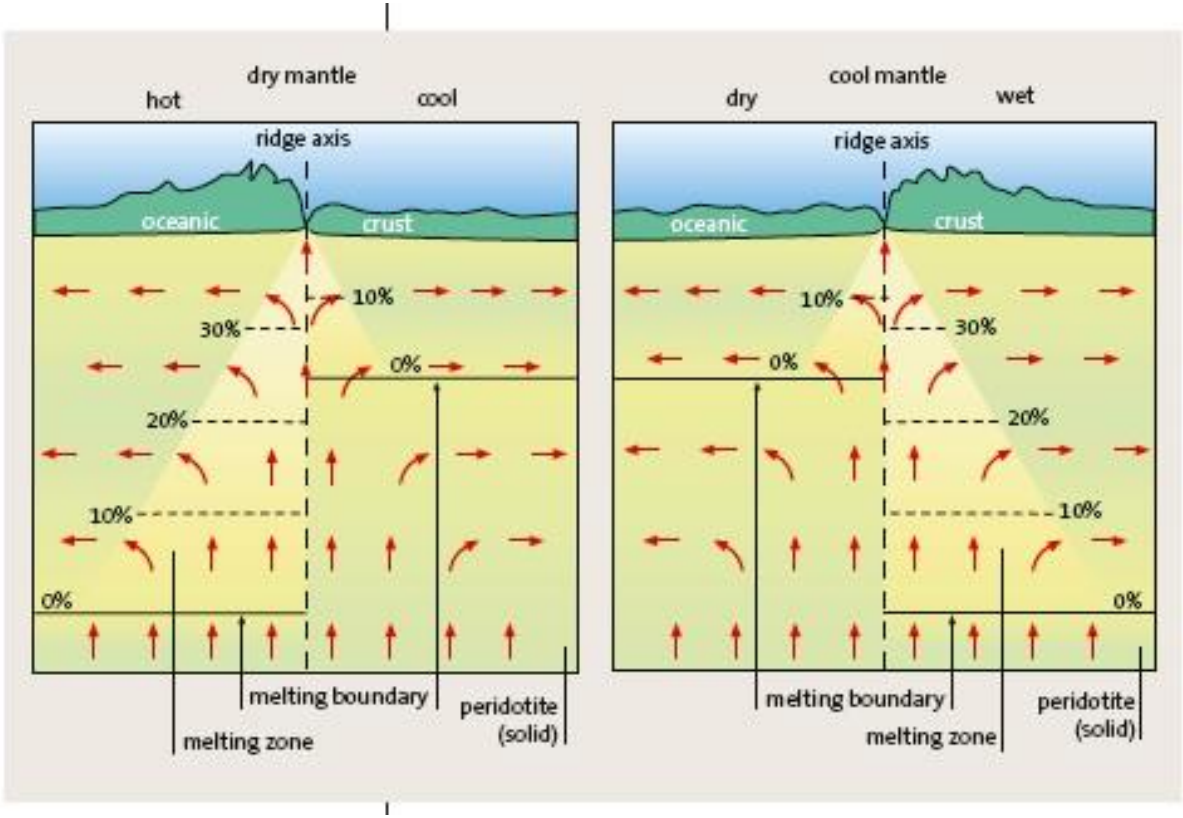

Cretaceous Superplume event

- The Cretaceous from ca. 125 Myr to 85 Myr was a time of extremes: extreme conditions were caused by the exceptionally high activity of mantle plumes that resulted in many large and unusually productive hot spots on the surface.
- The total production of oceanic crust increased, within a time interval of only a few million years, from around 20 km^3 per year to ~35 km^3 per year.

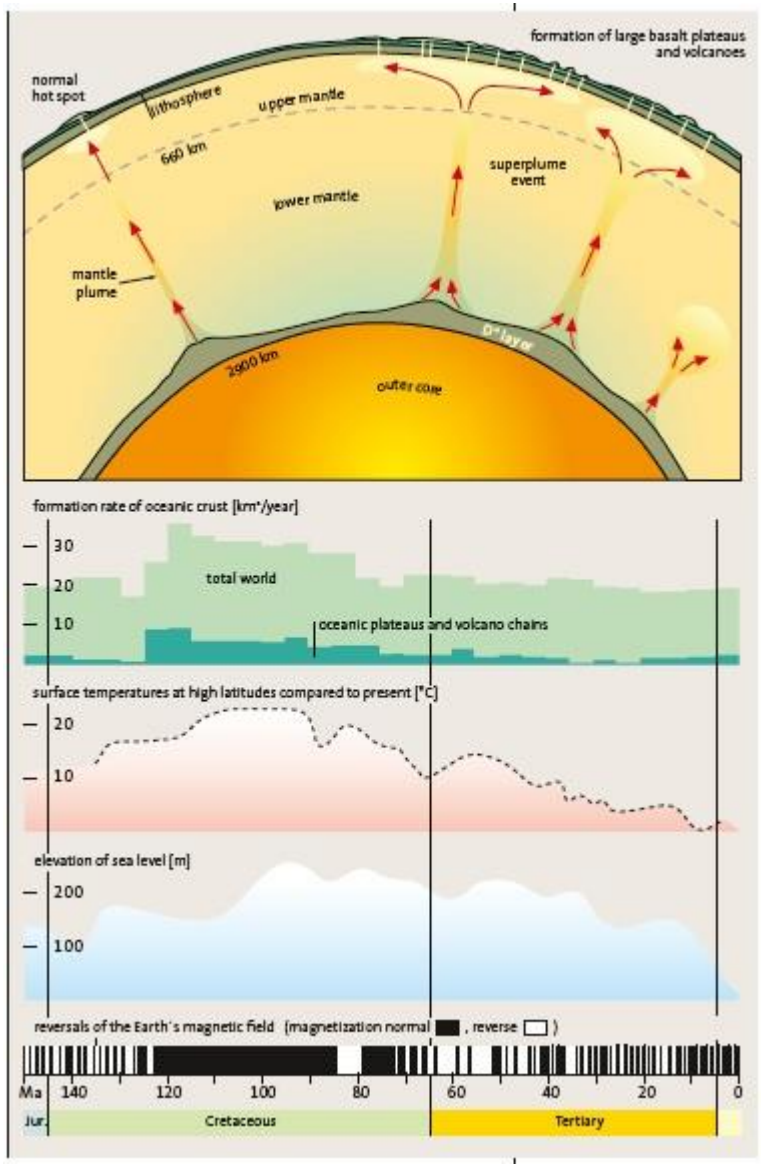

Other possible mechanisms for intraplate volcanism

Fixed hot-spot model fails to explain:

(1) Observed departures from linearity of individual volcanic chains and inconsistent orientations among multiple chains which lie on the same plate;
(2) Short-lived chains and ones which fluctuate in size;
(3) Violations of predicted along-chain age versus distance behavior;
(4) Some linear volcanic ridges in the Pacific form much more rapidly than would be predicted by fixed hot-spot model and display intermittent volcanic activity with longevities shorter than 40 Myr.

Other Hypotheses:

- Diffuse plate extension has been thought as a possible mechanism of intraplate volcanism or as alternative (1) cracking of the lithosphere under the action of thermal contraction (inconsistent with low seismic velocities beneath the volcanoes), (2) decompression melting in small-scale convective upwellings.
- In oceanic lithosphere, decompression melting may be possible only in regions where a large-scale mantle upwelling can counteract conductive cooling, keeping the mantle at its solidus temperature over some depth range.
- In the absence of a large-scale upwelling, buoyant melting may not occur spontaneously but may be triggered by some initial upwelling due to relief on the bottom of the lithosphere.
- Melting beneath spreading centers should produce a compositional lithospheric layer that is both more viscous (because of de-hydratation) and compositionally buoyant of a thickness comparable to the maximum depth of melting beneath a spreading center.

Nature of layer D’’

- The upper boundary of the layer D’’ is characterized by a velocity discontinuity, below which there may be an increase (e.g., beneath regions where there are subducting slabs) or decrease in the seismic velocities.
- Mineralogical explanations of the D” discontinuity focuses on the transformation from perowskite to the postperowskite phase.
- In a 5 to 50-km-thick layer immediately above the core–mantle boundary there is often a zone of ultra-low seismic velocities, with decreases in the shear wave velocity of 10–50% (most extensively developed beneath major hotspots). This implies partial melting with more than 15% melt.
- Lateral and vertical variations within layer D” may be caused by variations in chemical composition, mineralogic phase changes (due to the mixing of molten iron from the core with the perovskite of the mantle to form new high-pressure minerals) and/or varying degrees of partial melting and *T* differences. The result would be a chemically distinct, high-density layer but with a low viscosity.

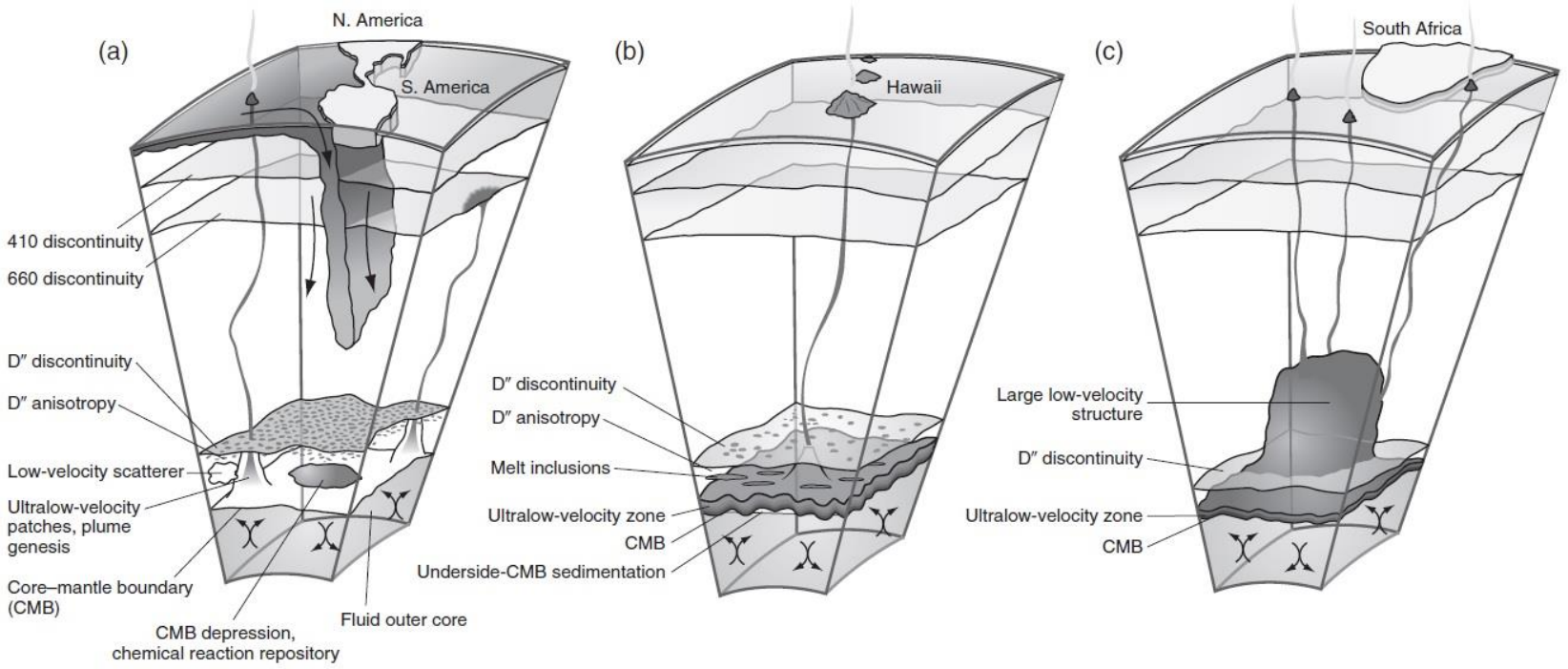

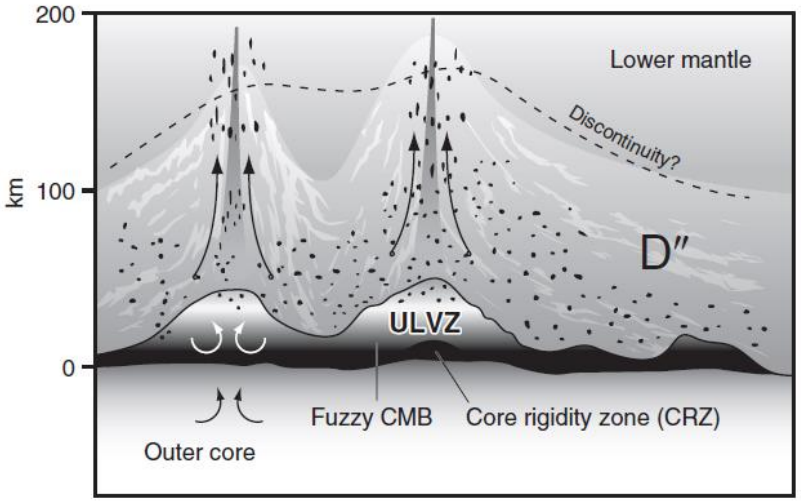

ULVZ Location

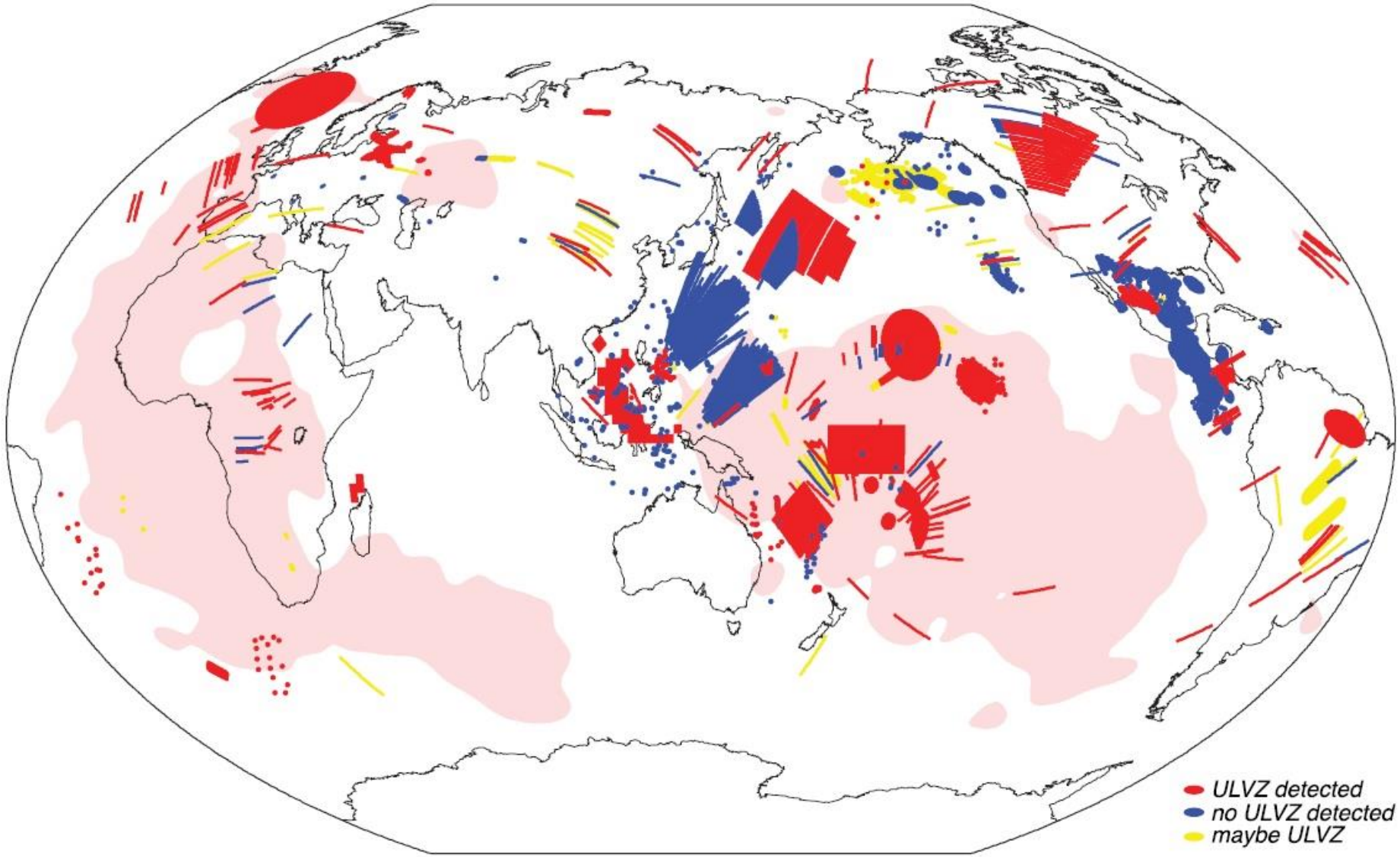

Yu and Garnero, 2018, G3, 19.

Ultra Low Velocity Zones (ULVZ)

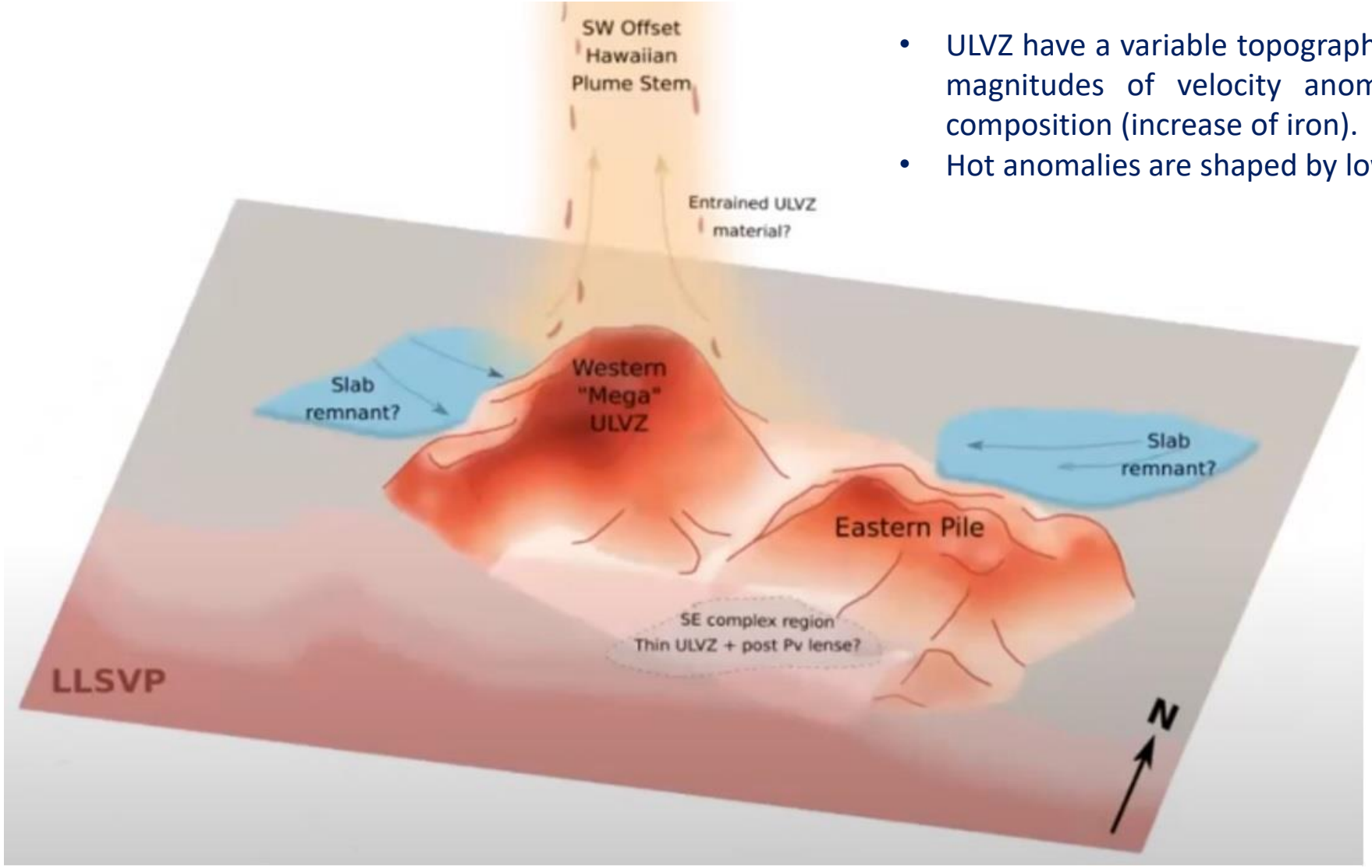

- ULVZ have a variable topography: 5-25 km, which result in different magnitudes of velocity anomalies, related to temperature or composition (increase of iron).
- Hot anomalies are shaped by lower mantle processes.

ULVZ Origins

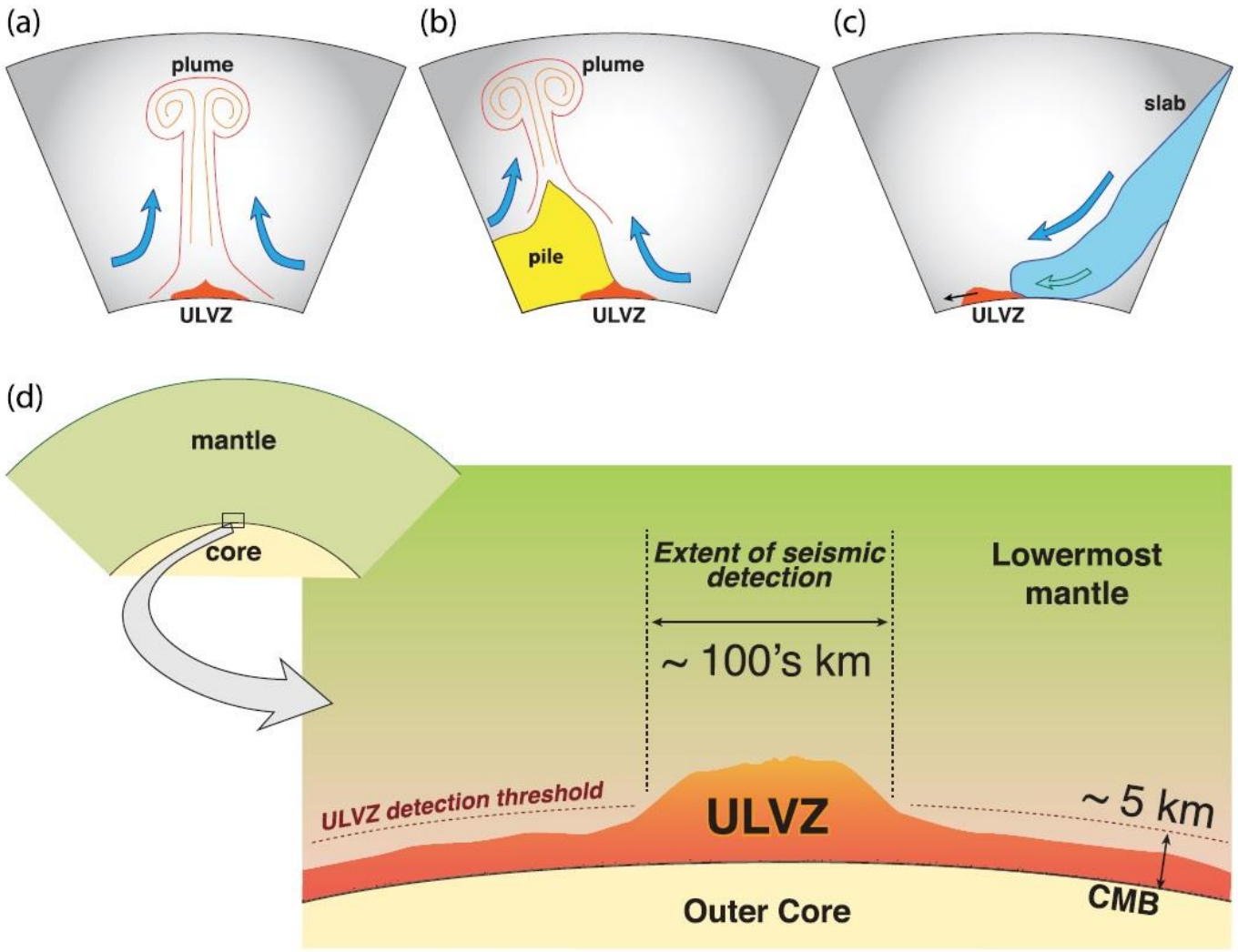

Yu and Garnero, 2018, G3, 19.

a) ULVZs have been reported to exist beneath surface hot spots, associated with mantle plumes. (b) Compositionally distinct ULVZs advect to the margins of thermochemical piles (c) ULVZs in relatively cold regions might be due to deeply subducted oceanic crust, or possible accumulated products of chemical reactions between the core and mantle.(d) The possibility of widespread thin ULVZs.

Depth source of plume

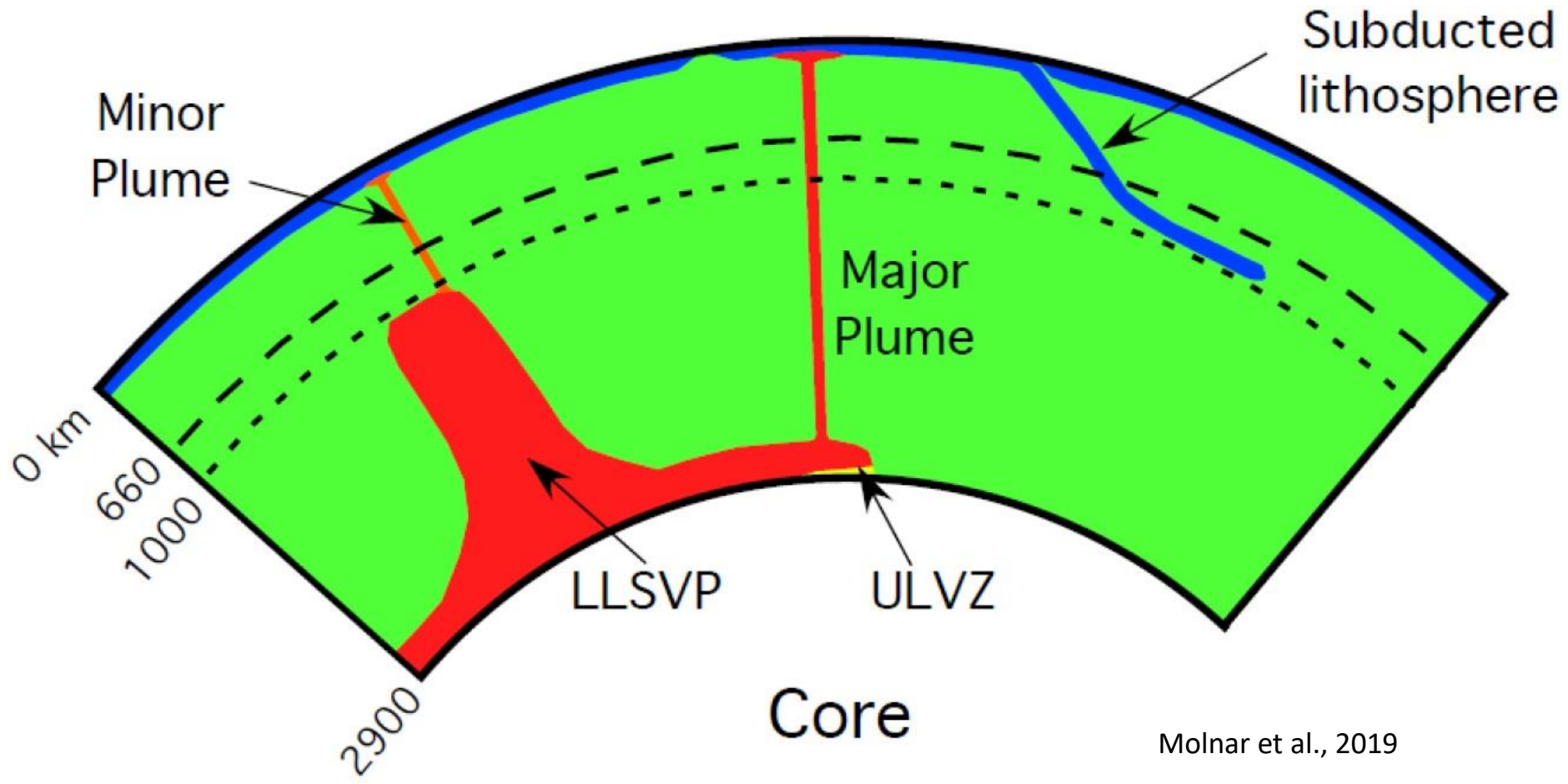

Molnar et al., 2019

- Major plumes are thought to emanate from the edges of low-shear-velocity province (LLSVP). Minor plumes may be generated from boundary layers at the tops of LLSVPs and other regions of upwelling lower mantle.

Symmetric and Asymmetric Plumes

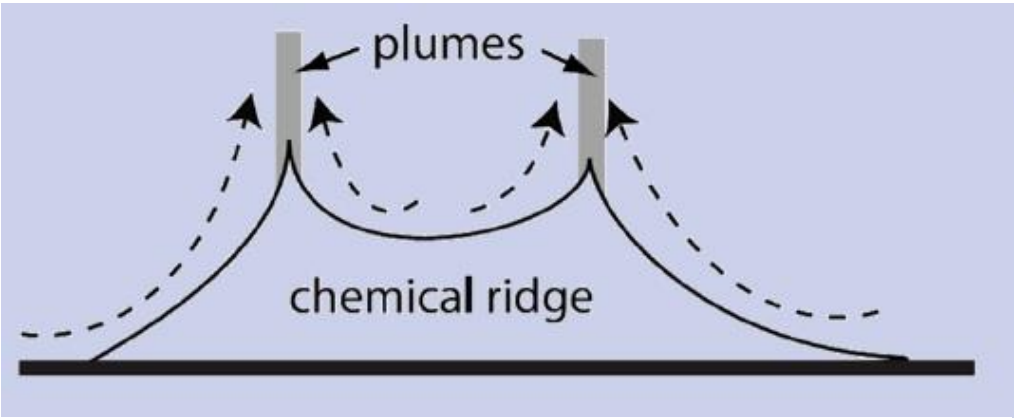

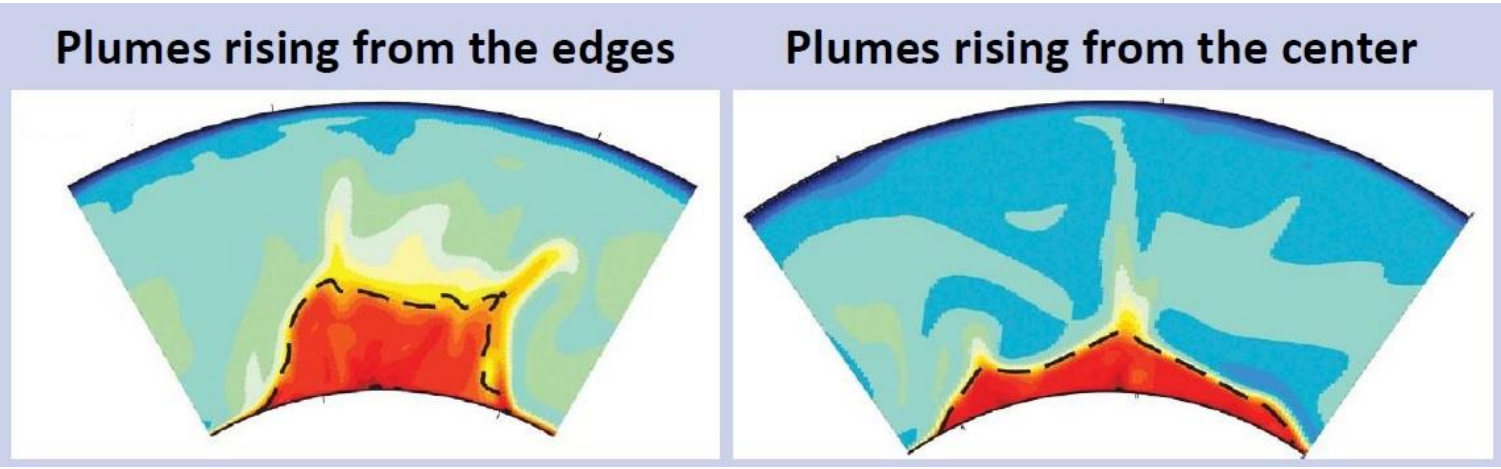

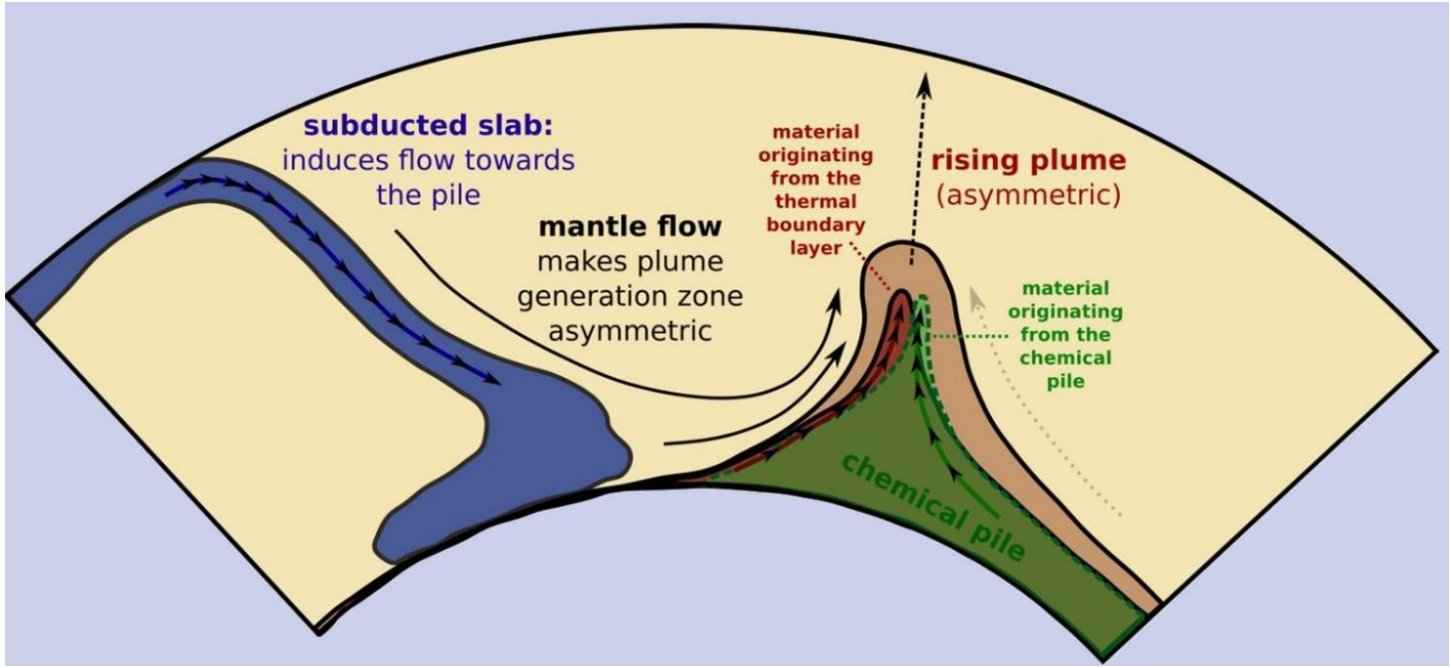

- **If the density anomaly has steep edges, the plumes will rise preferentially near the edges.**
- **The mantle flow and the subducting slabs influence the symmetry of the pumes.**

Rise and deformation of plumes through a flowing mantle

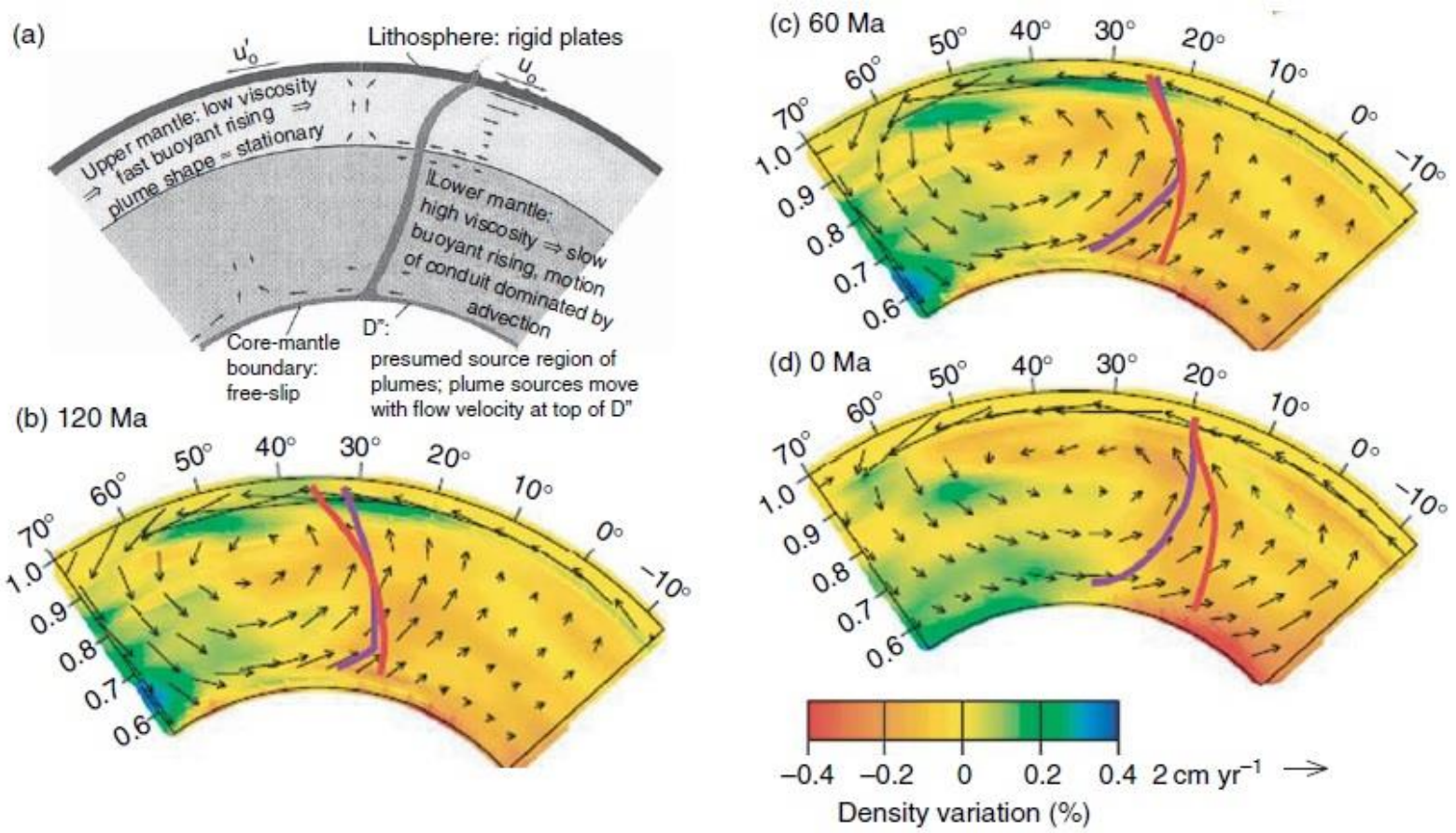

Predicted mantle flow (arrows), density variations (colors), and deformation of the Hawaiian plume rising from the CMB at a location that is fixed (purple, initiated 150 Myr), or moving with the mantle (red, initiated 170 Myr).

Ito and van Keken, 2007, Treatise of Geophysics, vol. 7

A plume is simulated by inserting a vertical conduit in the mantle at a specified time in the past. Velocities at each point along the conduit are the vector sum of the ambient mantle velocity and the buoyant rise speed of the conduit:

- Plume conduits therefore deform with time and where they intersect the base of the lithosphere defines the location of the hot spots.

Plumes and Heat Loss

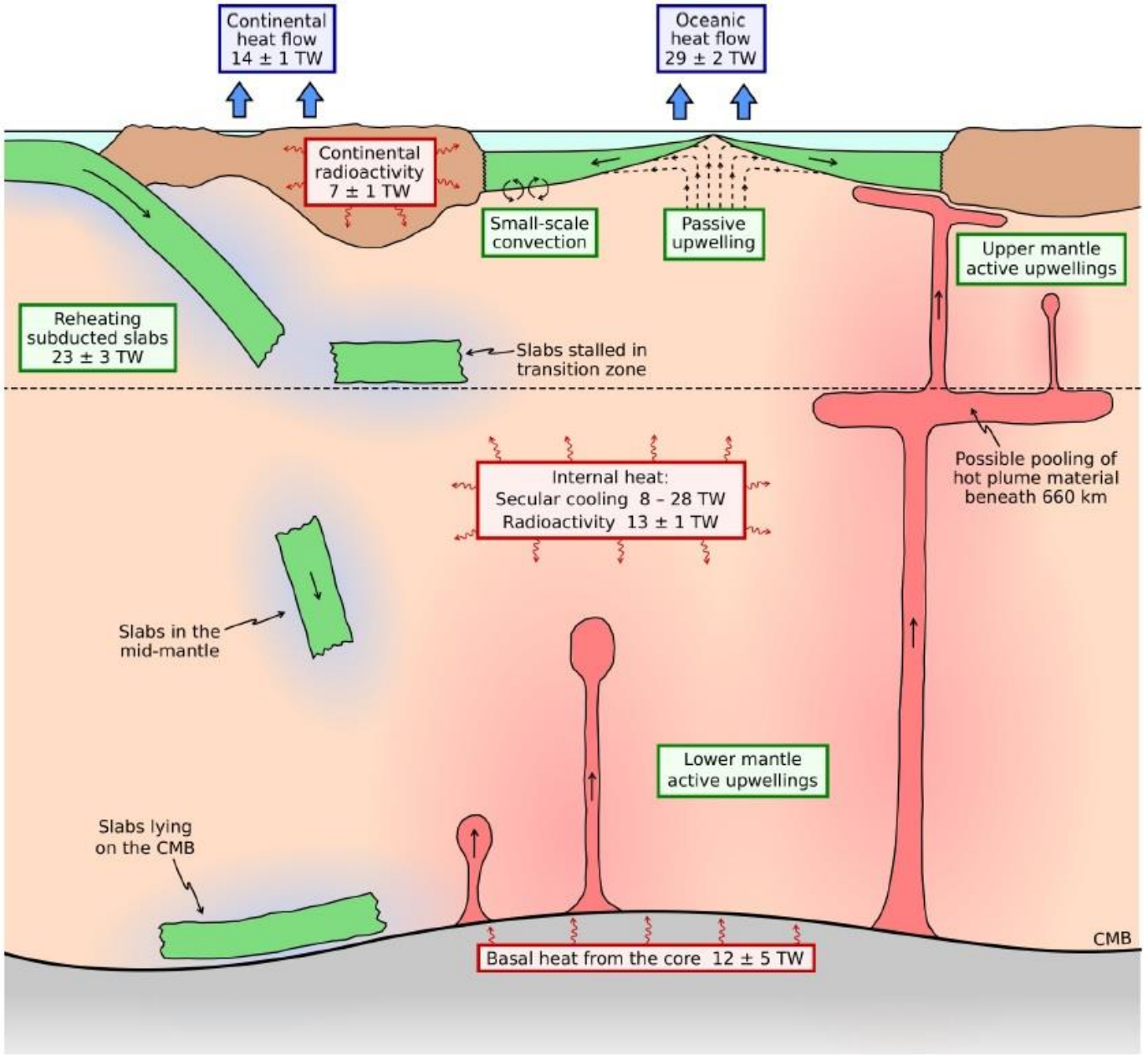

Hoggard et al., 2020, EPSL, 542

Plume generation

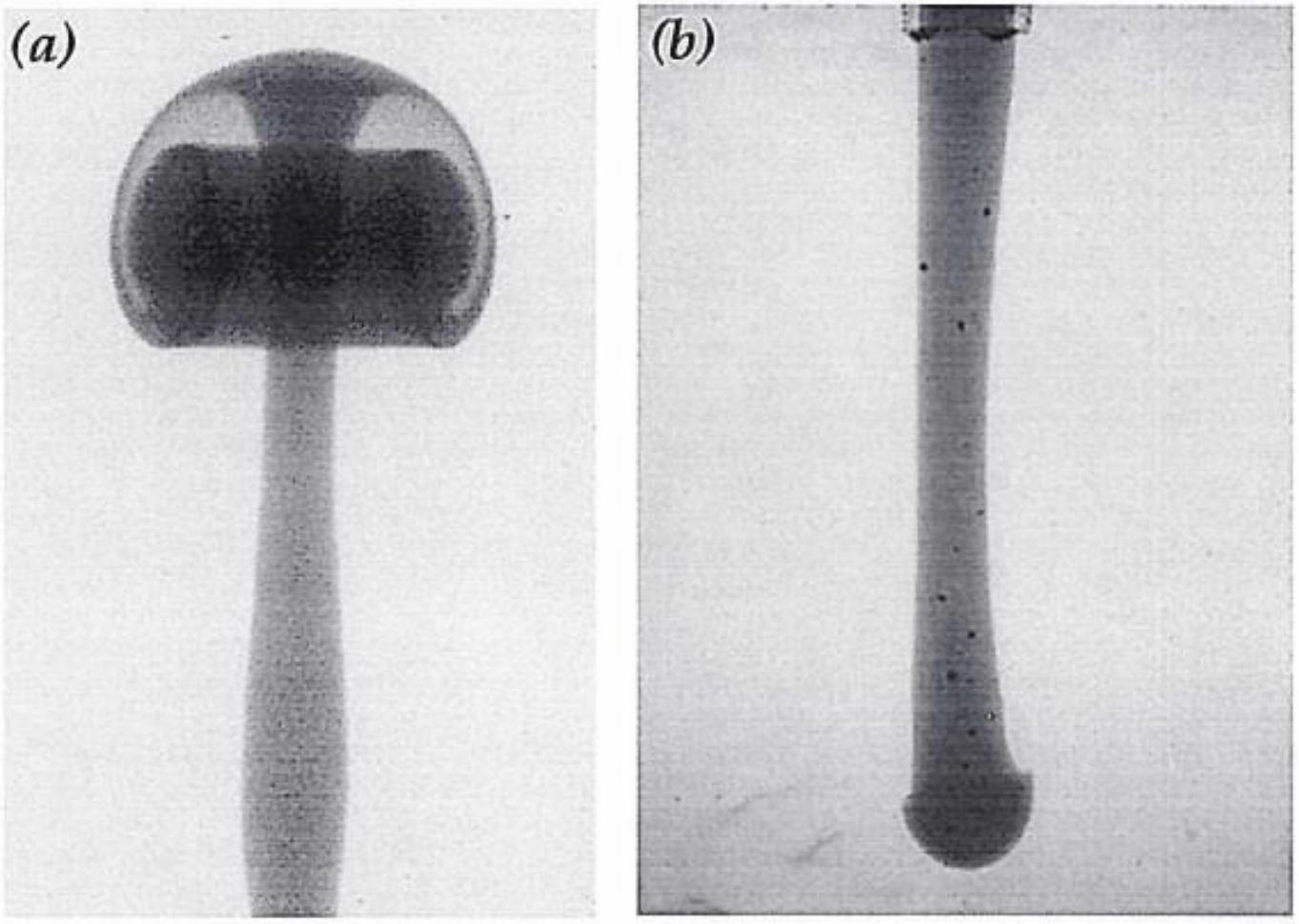

(a) The buoyant fluid is hot, and the plume viscosity is about 1/300 times that of the surrounding fluid (the column has a large, nearly spherical head at the top with a very thin conduit or tail connecting it to source).

(b) The injected fluid is cooler and thus denser and more viscous than the ambient fluid (the diameter of the buoyant columns is fairly uniform over its height).

Physical Characteristics of the Plume

- **Plume's diameter depends on (1) the volume flux and temperature excess of the source (2) thermal and viscosity properties of the lower mantle into which plume starts to ascend.**
- **Plume's head grows by entrainment as it ascends through the mantle (then as a function of distance travelled).**

Plume heads slow down by the viscosity of the surrounding mantle:

- **Expansion of the head (slower upward motion compensated by the faster tail)**

$$\mu = a \exp\left(\frac{E + pV}{RT}\right)$$

μ=viscosity
a=constant
P=pressure
v=activation volume

Activation enthalpy: H=E+pV

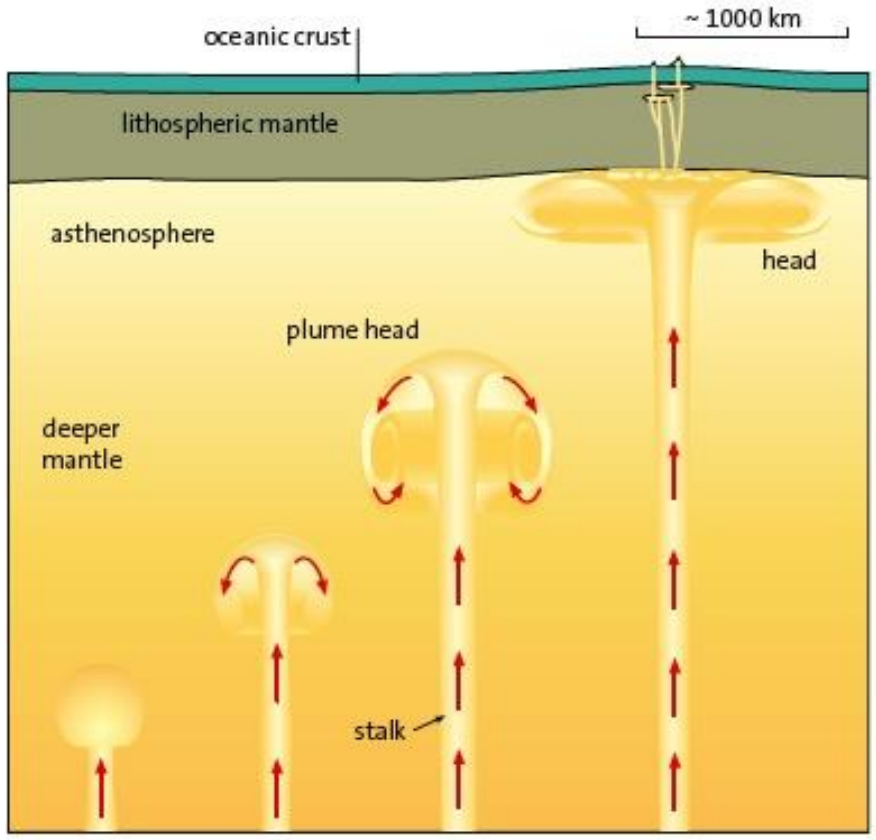

Plume Velocity and Energy Flux

Hot plume material loses heat to the surrounding fluid by diffusion (plume grows wider as it rises).

Laminar Regime: $$W \propto \frac{R^2 \Delta\rho g}{\mu} \propto \frac{R^2 \rho_o \alpha \Theta g}{\mu}$$

W = plume velocity, μ = viscosity, R = radius, Θ = temperature anomaly at height *z* above the source

Plume Energy Flux

P=Plume energy flux $$P \propto \rho_o C_p W \Theta R^2$$

$$W \propto \sqrt{\frac{\alpha g P}{\mu C_p}}$$

W does not depend on *z*, which indicates that the plume rises at a constant velocity.

Since radius increases with height due to diffusion: $$R \approx \sqrt{\kappa t} \qquad t \propto z/W, \qquad R \propto \sqrt{\kappa \frac{z}{W}}$$

Since the plume dimensions change with height, Reynolds number varies with height (increases approching the surface):

$$\mathrm{Re}(z) = \frac{\rho W R}{\mu} \propto z^{1/2}$$

Reynolds Number for Laminar

$$\mathrm{Re} = \frac{\rho W R}{\mu} \propto z^{2/3}$$

Reynolds Number for Turbolent

Close to the source Reynolds number is small and the flow cannot be turbolent

Plume and Surrounding Mantle

Plume tails become thinner by decreasing plume's viscosity

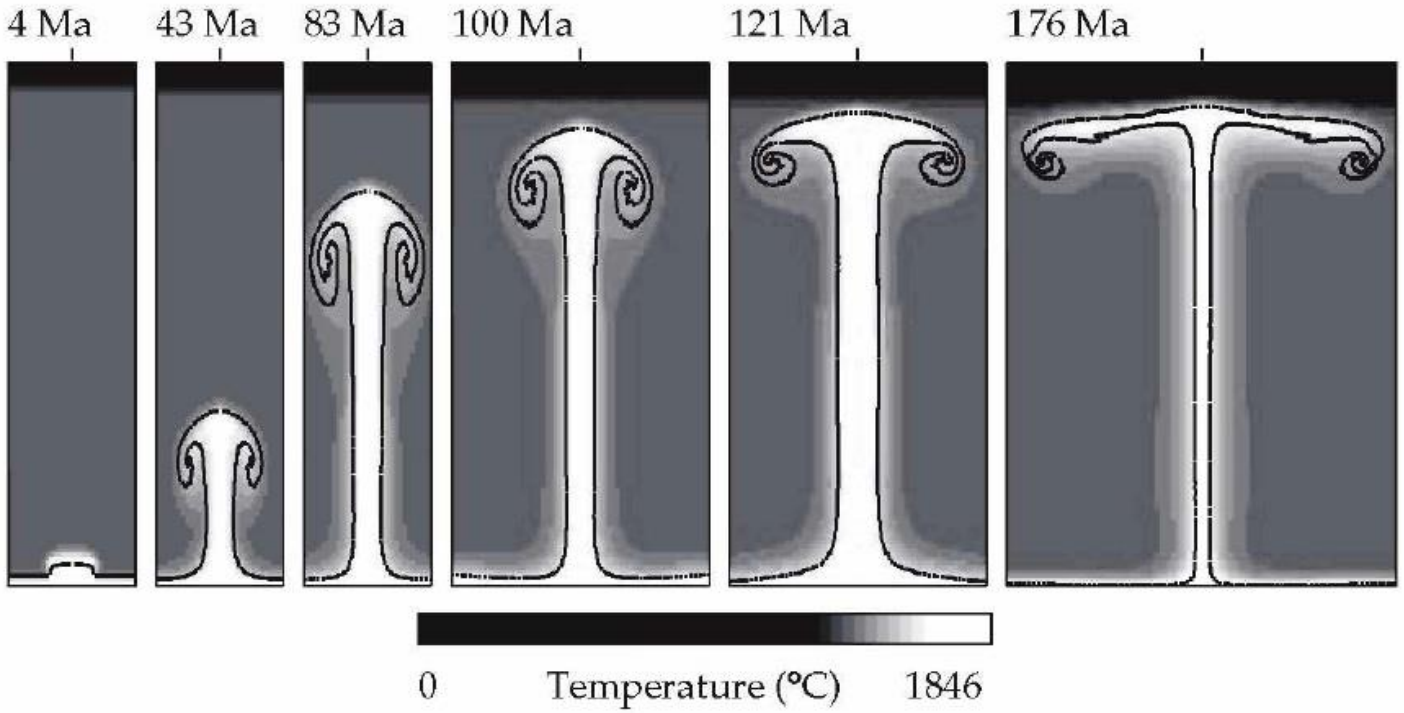

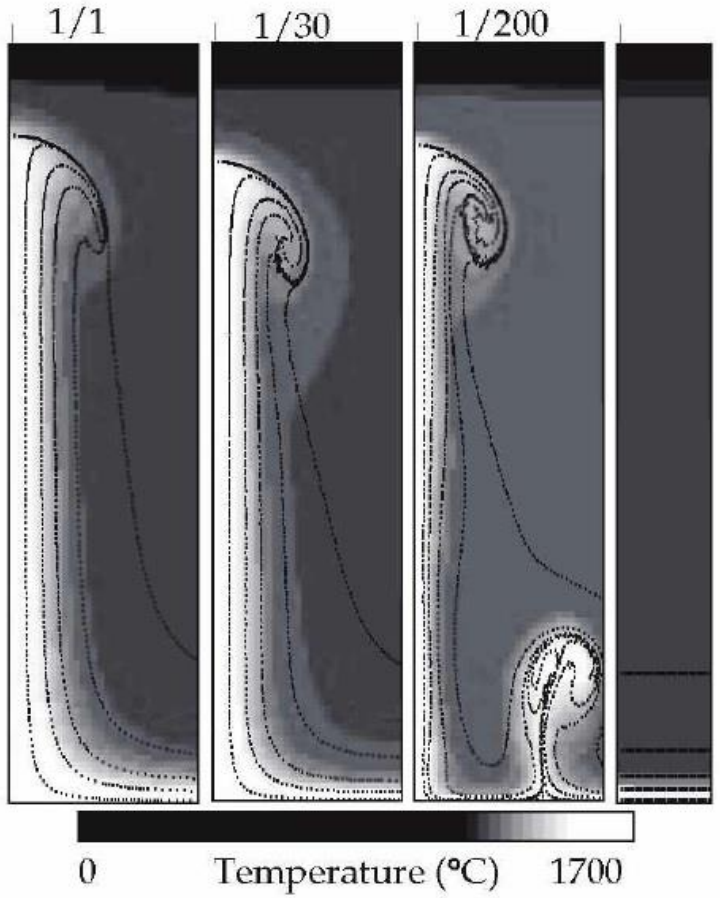

- Plume heads have a larger buoyancy which is more capable of penetrating resistance than a narrow column.
- The rise speed of the plume is proportional to its buoyancy and is inversely proportional to viscosity.

Mantle Phase Transformations and Clapeyron Slope

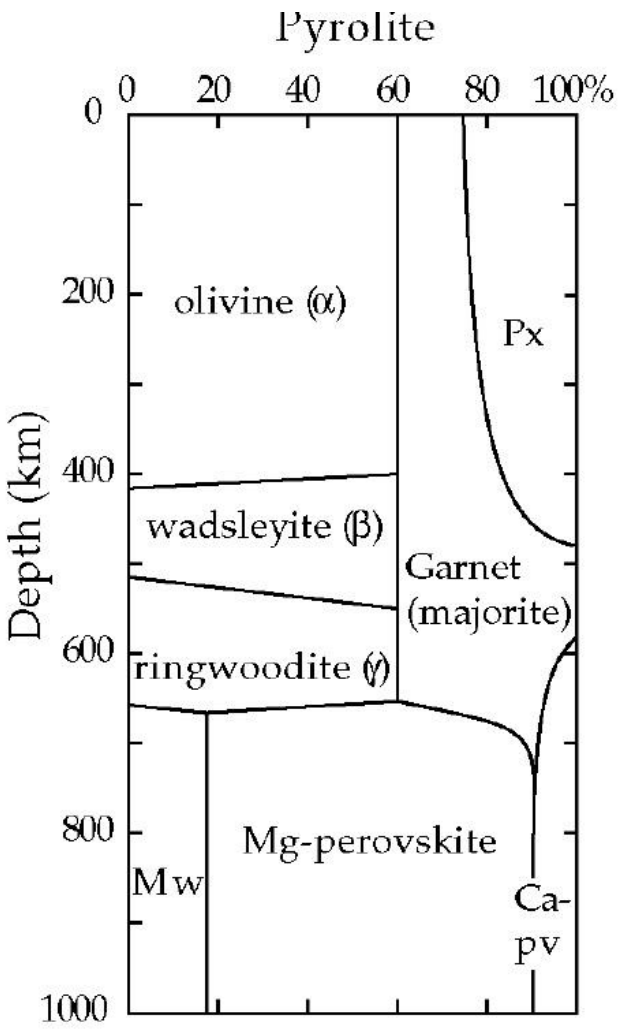

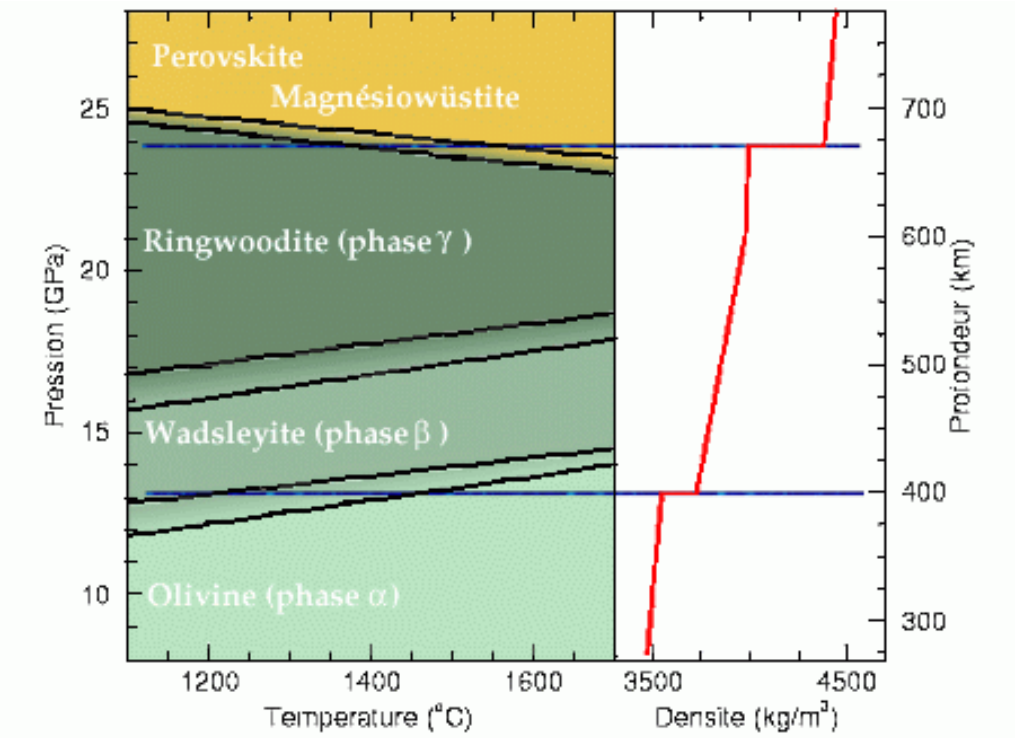

Phases transformation at 410 km:

- Olivine -> wadsleyite reaction has a positive Clapeyron slope of ~3 MPa/K (esothermic reaction)
- Pyroxene ->garnet majorite transformation may have a strongly negative slope (net effect unclear).

Phases transformation at 660 km:

- Ringwoodite -> perovskite + magnesiowüstite transformation has a negative Clapeyron slope of ~ -2 MPa/K (endothermic reaction).
- Garnet -> perovskite transformation may have a strongly positive Clapeyron slope (about 4 MPa/K) and a substantial density increase, yielding a negative buoyancy in opposition to the transformation of the ringwoodite component (net effect unclear).

The effect of a phase transformation may be significant in 2D, constant viscosity model, but less significant in 3D and with *T* dependent viscosity

Plume and Surrounding Mantle

Influence of mantle viscosity and a phase transformations on the plume

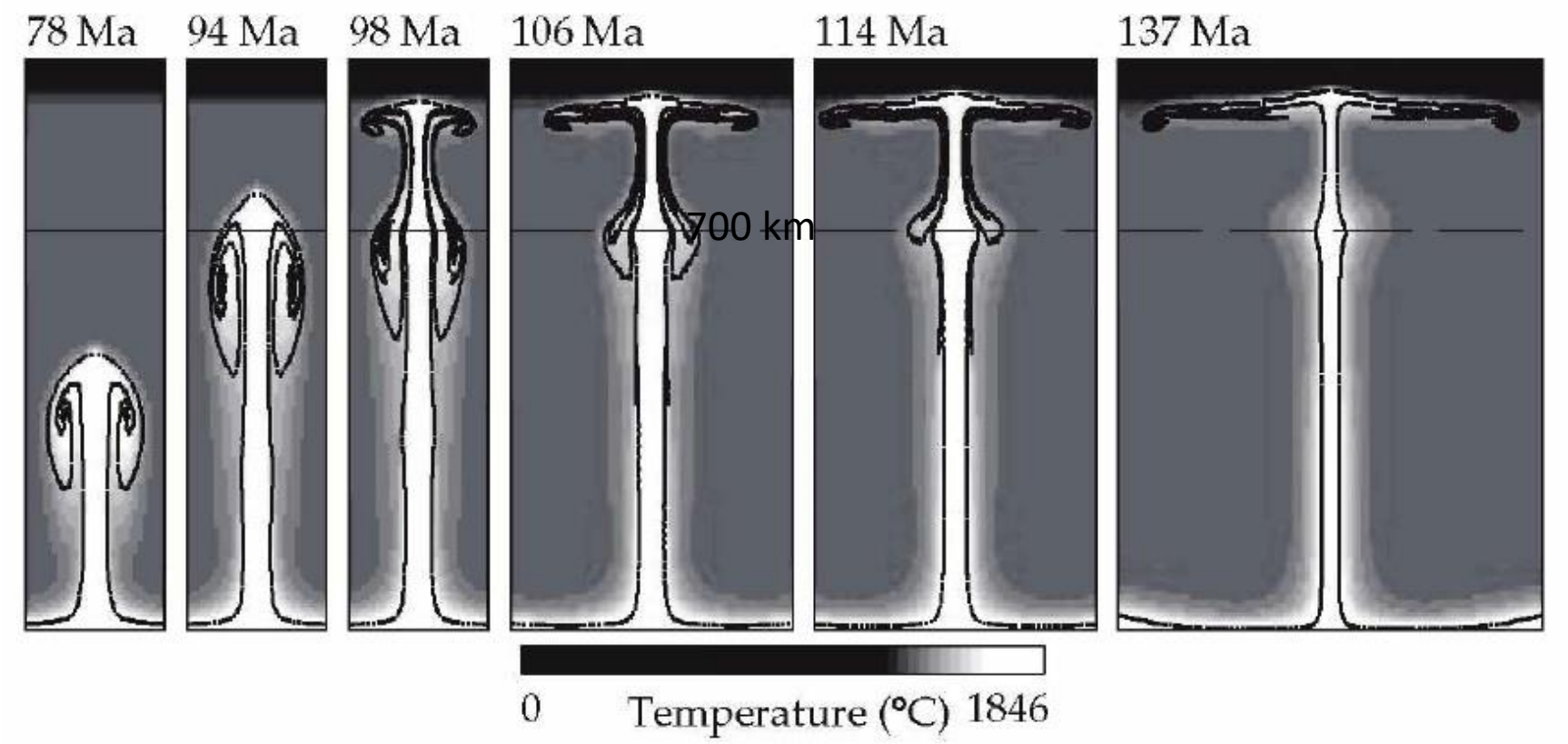

- The viscosity increases by a factor of 20 at 700 km and exponentially by a factor of 10 below.
- The effect of a phase transformation at 700 km depth is simulated with a moderately negative Clapeyron slope of -2MPa/K.

Plume and Surrounding Mantle

Effects of depth dependence of viscosity and a phase transformation on the plume

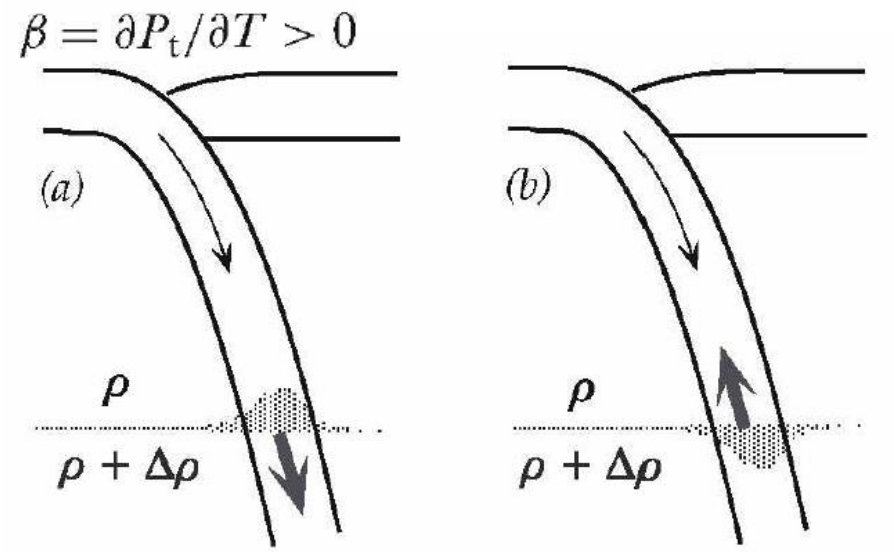

Exothermic = *T* increases of 90 K **Endothermic= *T* decreases of -90 K**

- A positive Clapeyron slope causes a negative buoyancy force (broad arrow) that would add to the negative thermal buoyancy of the cold slab, aiding its descent.
- A negative Clapeyron slope delays the transformation to greater pressure and depth within a descending slab, producing a positive buoyancy that would oppose the slab's descent.
- In cold subducted lithosphere *T* may be too low for the thermally activated reactions to occur. Thus, the phase would persist metastably, producing a positive buoyancy that would always oppose the descent of the slab.
- In contrast, a hotter anomaly causes the exothermic phase change at 410 km to occur deeper and the endothermic phase change at 660 km to occur shallower, assuming that the olivine system dominates the phase changes.

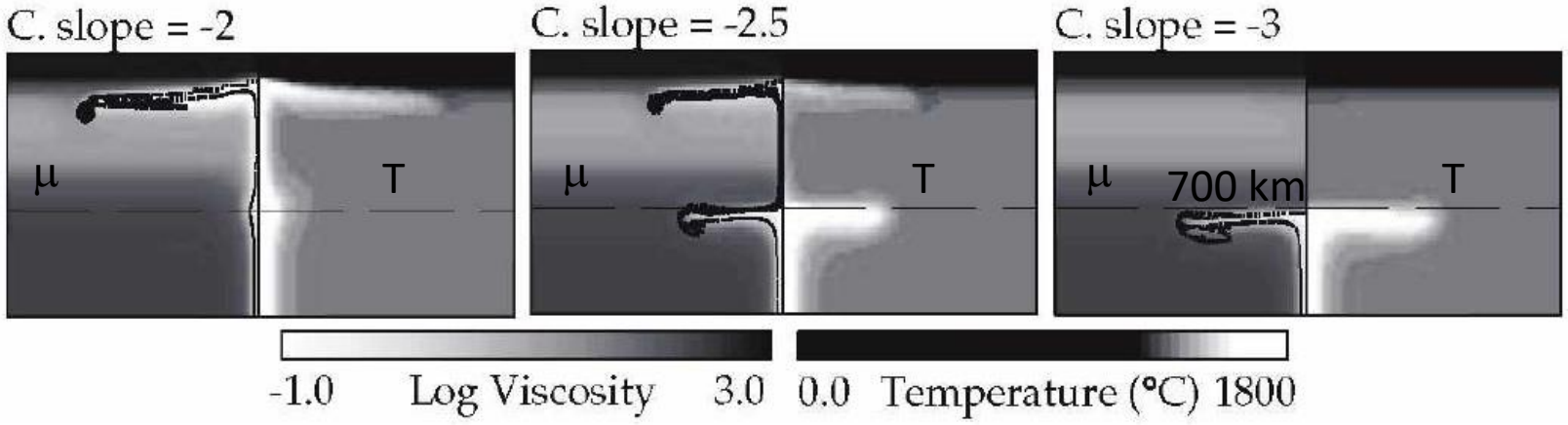

- In a hot rising column of mantle a positive Clapeyron slope would cause the transformation at a greater depth, yielding a positive buoyancy that would enhance the column's rise, while a negative Clapeyron slope would inhibit its rise.

Plume Thermal Conditions

- The heat goes partly outwards, to form the thermal boundary layer around the head, and partly inwards, to further heat the entrained material.
- The thickness, δ, of the thermal boundary layer adjacent to the hot plume head depends on the time the adjacent fluid is in contact with the passing plume head.

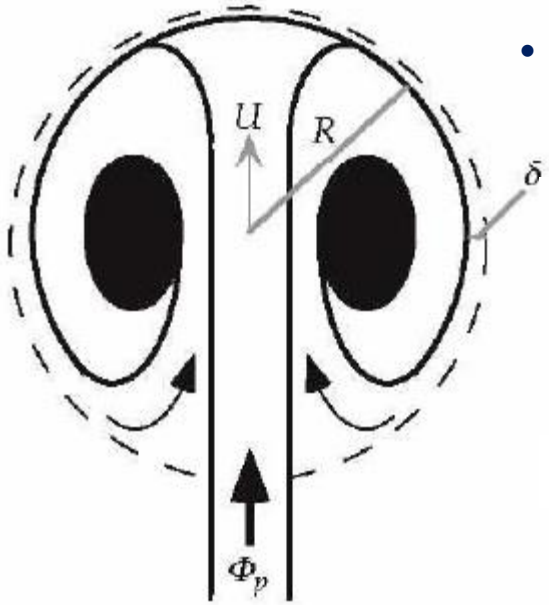

$$\delta = \sqrt{\kappa t} = \sqrt{\frac{2\kappa R}{U}}$$

ϕ_e=The rate at which boundary layer fluid flows through the horizontal cross-sectional area of the boundary layer near the head's equator (volumetric rate entrainment).

$$\Phi_e = 2\pi R \delta U \qquad t = 2R/U \qquad U = \frac{g\rho\alpha\Delta T R^2}{3\mu}$$

U=(rising velocity for a low-viscosity sphere)

$\phi_P = \pi r^2 U$

(ϕ_P=volumetric flow rate at which the swell volume is created)

The velocity v of a sphere is obtained balancing the Buoyancy force (B) with the Resistance force (R)

$$B = -4\pi r^3 g\Delta\rho/3 \qquad \tau = c\mu v/r \qquad R = -4\pi r^2 \cdot c\mu v/r = -4\pi c r \mu v$$

$$B + R = 0 \qquad 4\pi c r \mu v + 4\pi r^3 g\Delta\rho/3 = 0 \qquad v = -g\Delta\rho r^2/3c\mu$$

The rate of increase of the head radius due to entrainment is: $\frac{\partial R}{\partial t} = \frac{\Phi_e}{4\pi R^2}$

For μ=10^{22} Pa s, ΔT=100 °C, R=500 km, U = 7 x 10^{-10} m/s = 20 mm/yr, δ=40 km, we obtain Φ_e =2.7km^3/yr and a $\frac{\partial R}{\partial t}$ = 1 mm/yr= 1 km/Myr

Dynamic Topography

Vertical displacement of the Earth's surface generated in response to flow within the mantle

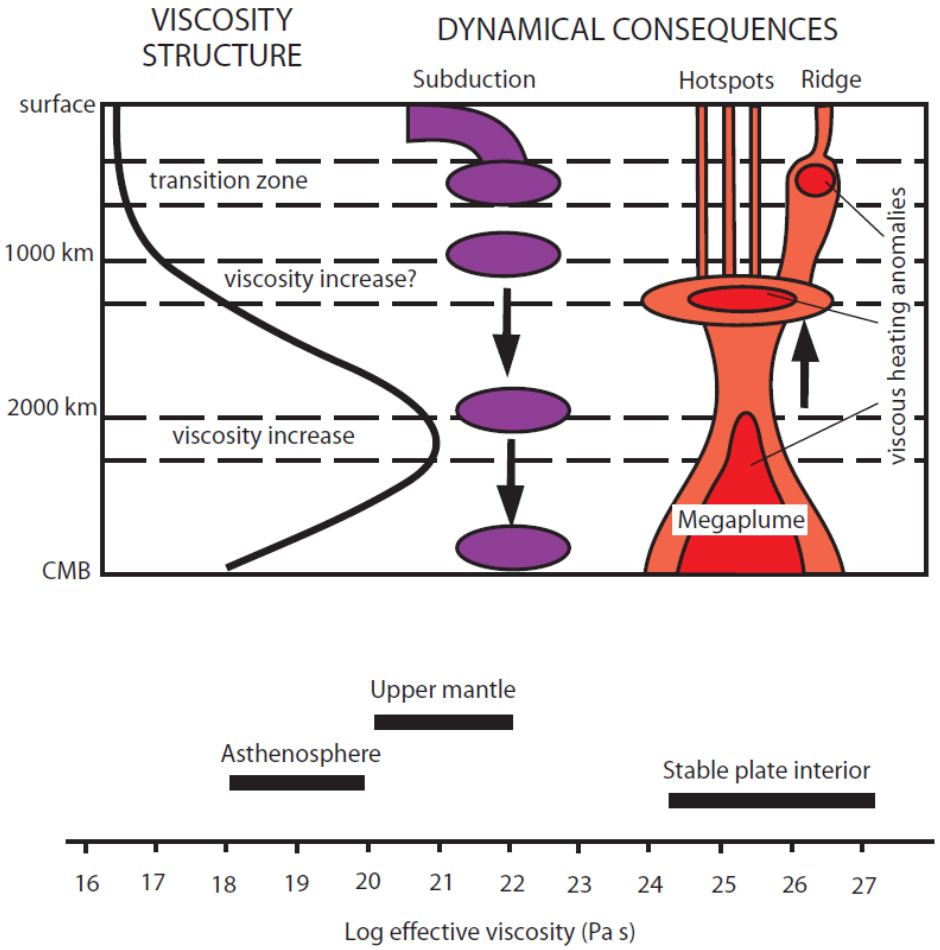

- Dynamic topography is transient and is usually of the order of few hundred meters (300-500 m).
- Response time of the mantle to a disturbance depends on its viscosity and wavelengths of the anomalous body.
- It is estimated by removing from the topography the isostatic effects of lithospheric thickness changes and thermal subsidence.

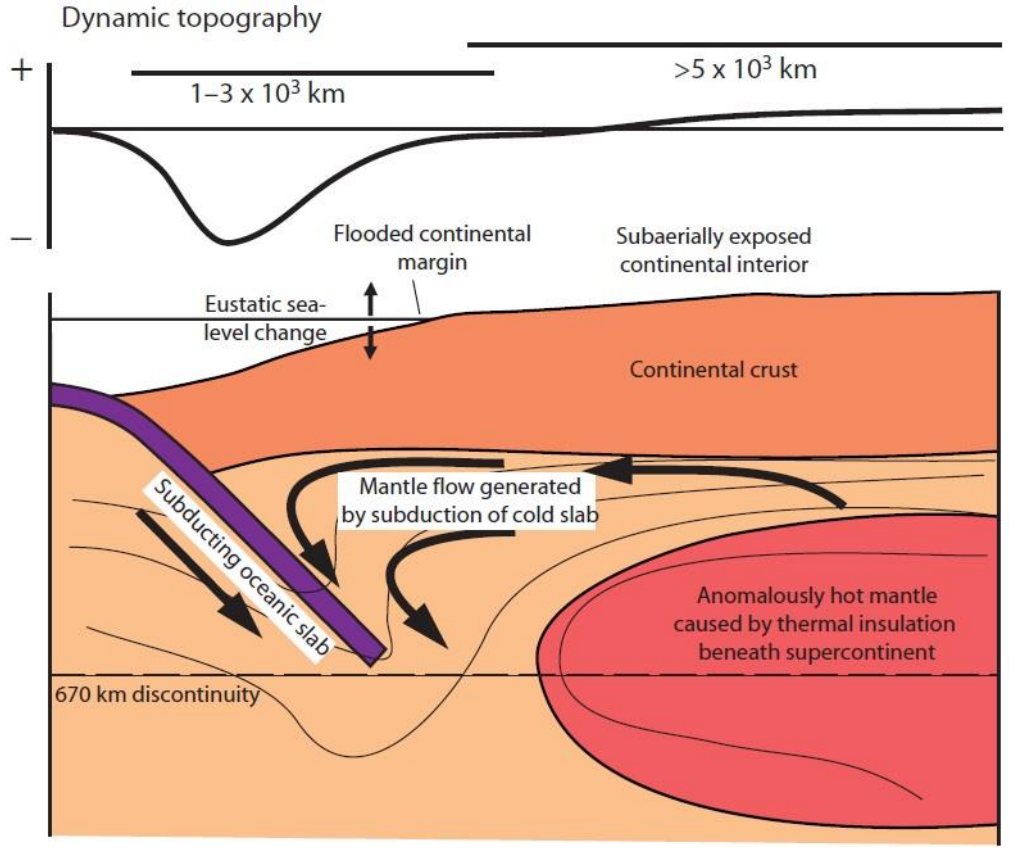

Dynamic Topography

- Buoyancy in a fluid layer deflects both the top and the bottom surfaces of the fluid and the combined weight of the topographies balances the internal buoyancy.
- The amount of deflection of each surface depends on the magnitude of the viscous stresses transmitted to each surface, which depends on the distance from the buoyancy to the surface and viscosity.

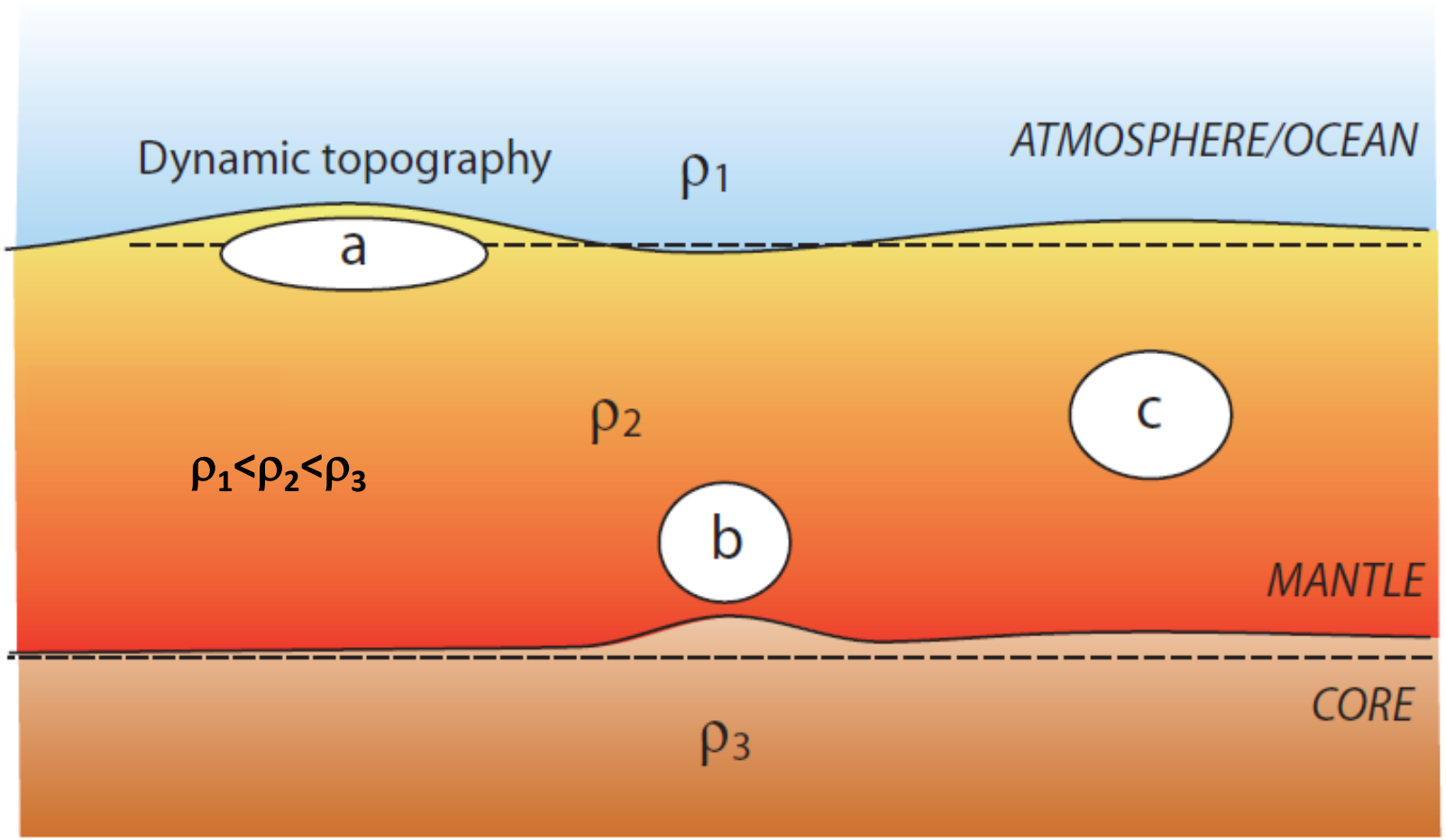

Plume and Dynamic Topography

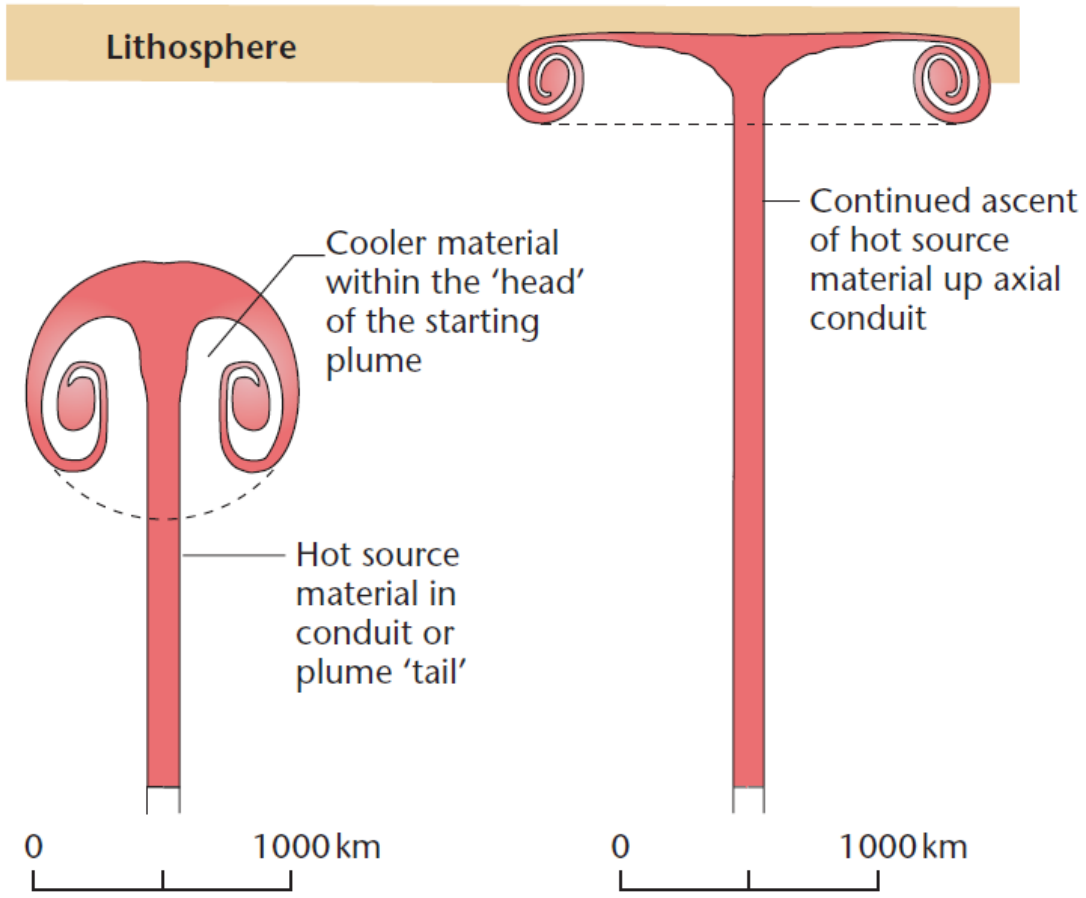

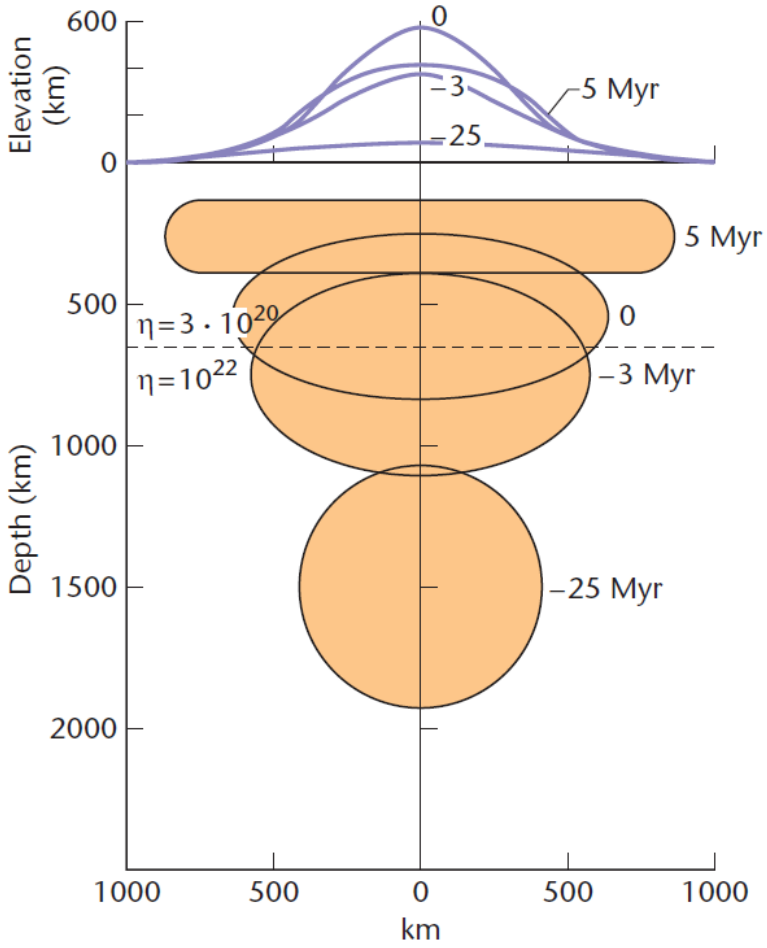

Buoyancy flux: 3×10^4 N s^{-1} ΔT=300 K

- Surface is weekly uplifted if the plume head is within the lower mantle (-25 Myr).
- Surface uplift takes place rapidly when the head's plume reaches the asthenosphere.
- Maximum uplift depends on (1) penetration of the hot plume into the cold lithosphere (2) a volume increase caused by melting (when it reaches shallow depths).

Plume and Dynamic Topography

Hawaiian Ridge

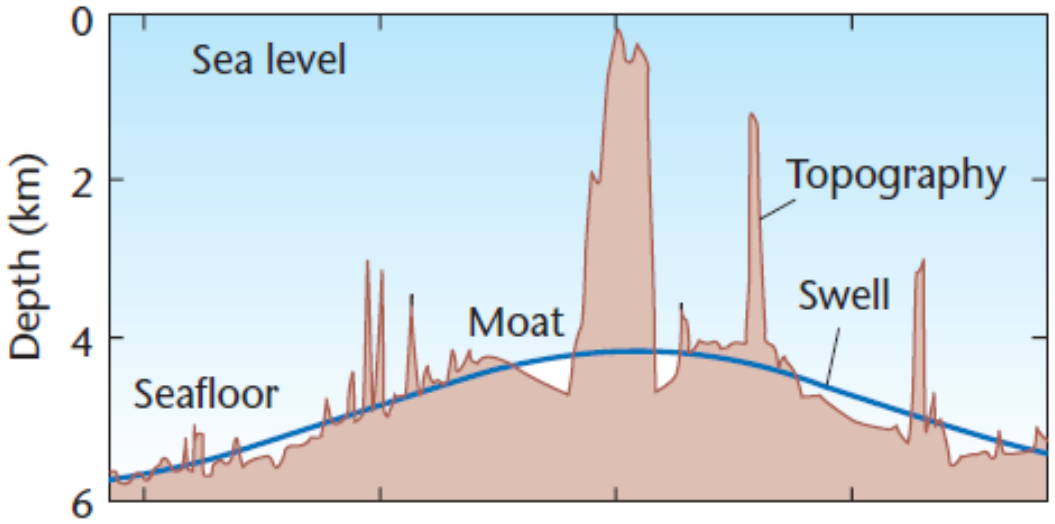

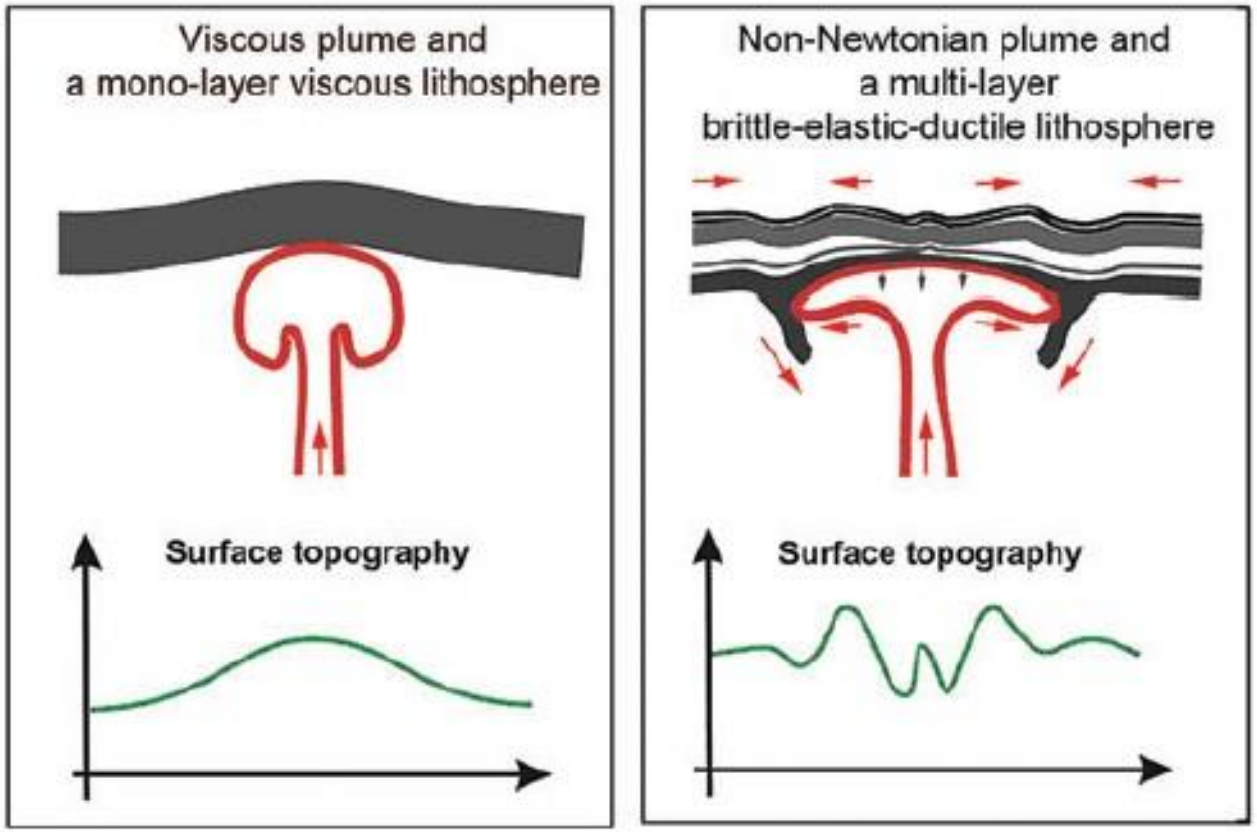

Burov and Cloetingh, 2009, Geophys. J. Int., 178

- The conventional models predict only long-wavelength (controlled by the plume head size) isostatic topography due to plume impact.
- Accounting for plate rheology and multilayer lithosphere structure yields a more complex response, with several short-wavelengths generated by intraplate deformation, tectonic-style deformation at surface and strong lithospheric mantle erosion at depth.

Plume beneath a craton (Tanzania Craton)

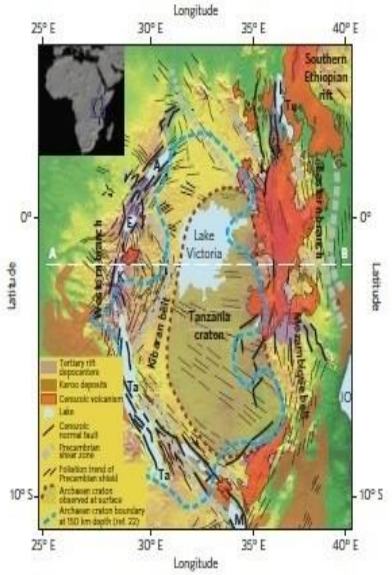

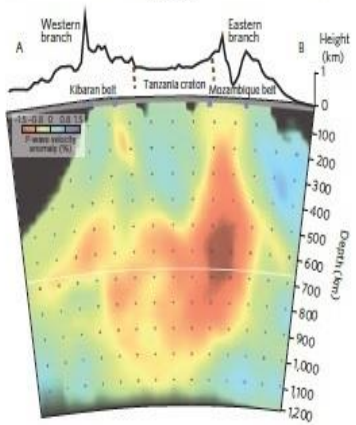

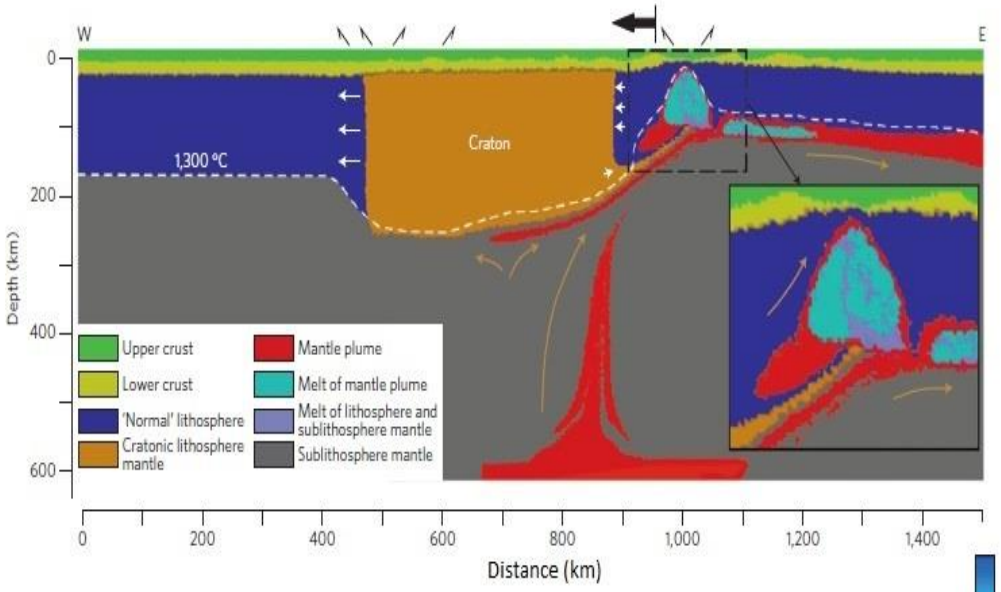

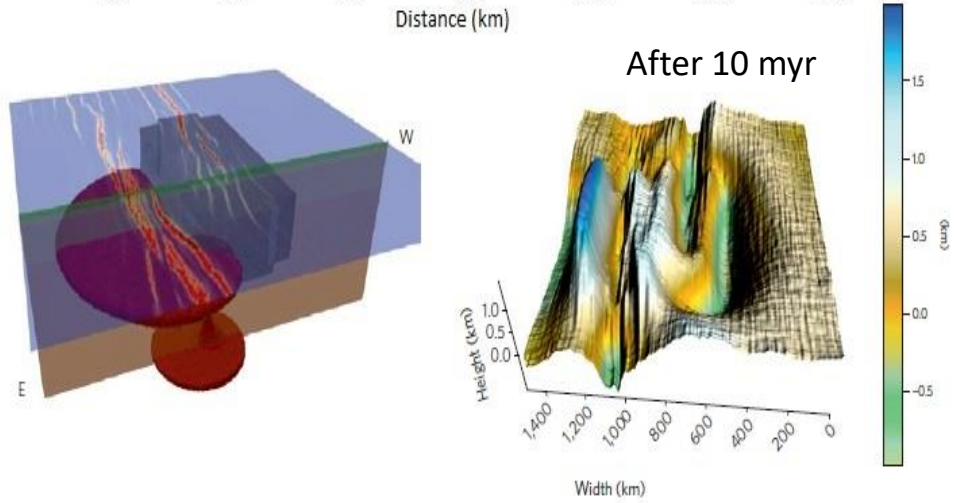

- **The Tanzanian craton is surrounded on both sides by active rift branches**: **(1)** the magma-poor western rift exhibits low-volume volcanic activity, large (M>6.5) magnitude earthquakes, and hypocentre depths reaching 30–40 km, and **(2)** the magma-rich eastern rift is characterized by a broad zone of shallow (5–15 km) and lower magnitude seismicity, but voluminous Cenozoic volcanism.
- Surface topography first reacts by domal uplift, soon after (<1Myr) replaced by subsidence and coeval initiation of long and narrow rifted basins on either side of the craton.
- These basins form above a thinning lithosphere, creating channels for the subsequent migration of mantle plume material.

Koptev et al., 2014, Nature Geoscience

The plume is deflected by the cratonic keel and preferentially channelled along one of its sides, leading to the coeval development of magma-rich and magma-poor rifts along opposite craton sides, fed by melt from a single mantle source.

Buoyancy flow rate and heat flow rate

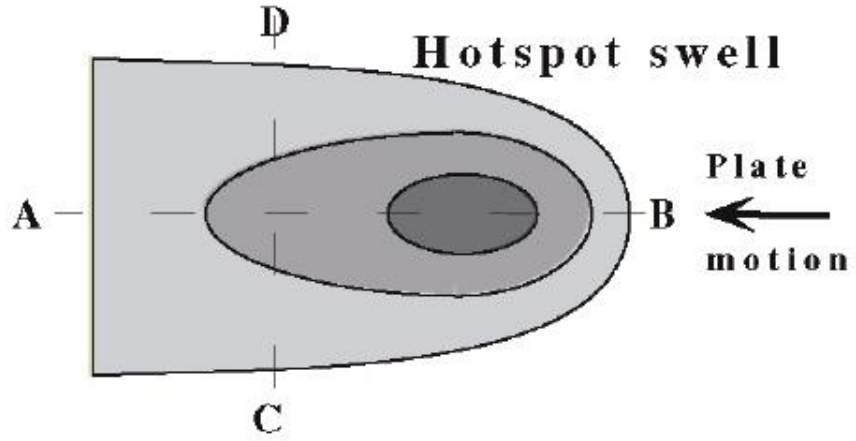

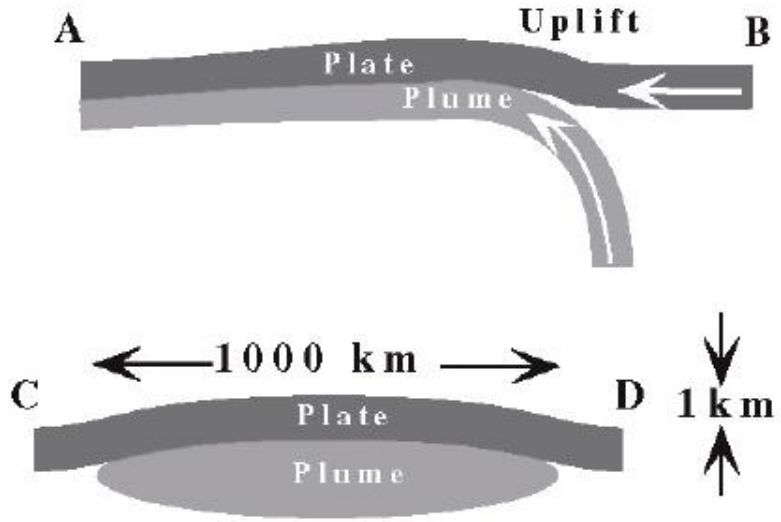

There is a close isostatic balance between the weight of the excess topography created by this uplift and the buoyancy of the plume material under the plate.

Buoyancy flow rate: $b = g\Delta\rho \cdot \pi r^2 u$ $\Delta\rho = (\rho_p - \rho_m)$

$\Delta T = T_p - T_m$ $\rho_p - \rho_m = \rho_m \alpha \Delta T$ $b = g\rho_m \alpha \Delta T \pi r^2 u$ *r*=radius of vertical cilinder *u*=average velocity

The addition to swell topography each year is equivalent to elevating by a height h = 1 km a strip of sea floor with a width w = 1000 km (the width of the swell) and a length $v\delta t$ = 100 mm.
The rate of addition to the weight (negative buoyancy) of the new swell is: $W = g(\rho_m - \rho_w) wvh = b$

(the effective difference in density is between the mantle, ρ_m, and see water, ρ_w)

Heat flow rate: $Q = \pi r^2 u \rho_m C_P \Delta T$ $Q = C_P b / g\alpha$

Volumetric flow rate and heat flow rate

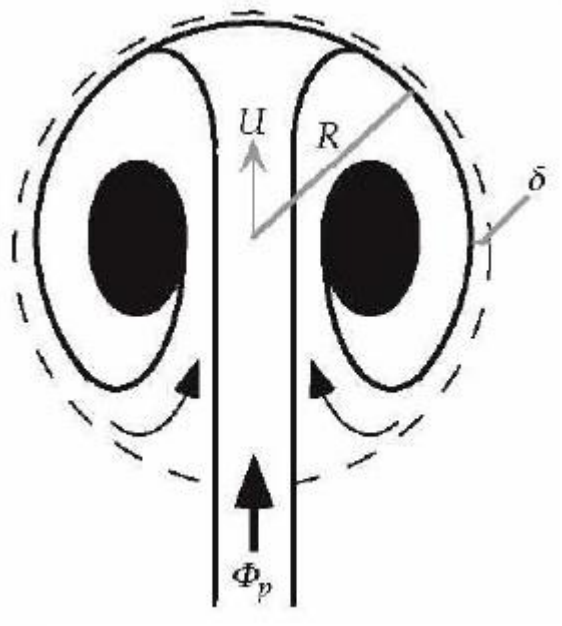

The volumetric flow rate is related to the buoyancy flow:

$$\Phi_p = b/g\rho_m\alpha\Delta T \qquad b=g\rho_m\alpha\Delta T\pi r^2 u$$

b is also related to the rate at which the swell volume is created, ϕ_s, to the rate of addition to the weight , *W:*

$$W = g(\rho_m - \rho_w)wvh = b$$

$$\Phi_s = wvh = W/g(\rho_m - \rho_w) = b/g(\rho_m - \rho_w)$$

The plume volumetric flow rate is related to the swell volumetric rate of creation through:

$$\Phi_p = \Phi_s(\rho_m - \rho_w)/\rho_m\alpha\Delta T$$

$\phi_P=\pi r^2 u$

(ϕ_P=volumetric flow rate at which the swell volume is created)

u=average velocity in the conduit

e.g.: ϕ_s = 0.1 km^3/yr, ρ_m = 3300 kg/m^3, ρ_w = 1000 kg/m^3, α = 3x 10^{-5} /°C, and ΔT = 300 °C
$\phi_p = \phi_s(\rho_m - \rho_w)/\rho_m\alpha\Delta T$ = 7.5km^3/yr (75 times the rate of uplift of the swell)

The magmas usually show evidence of being derived from 5-10% partial melting of the source, which means that about 80-90% of the plume material does not melt at all.

Plume Thermal Perturbation

The emplacement of a plume below an oceanic plate perturbs the temperature, heat flux, and topography.

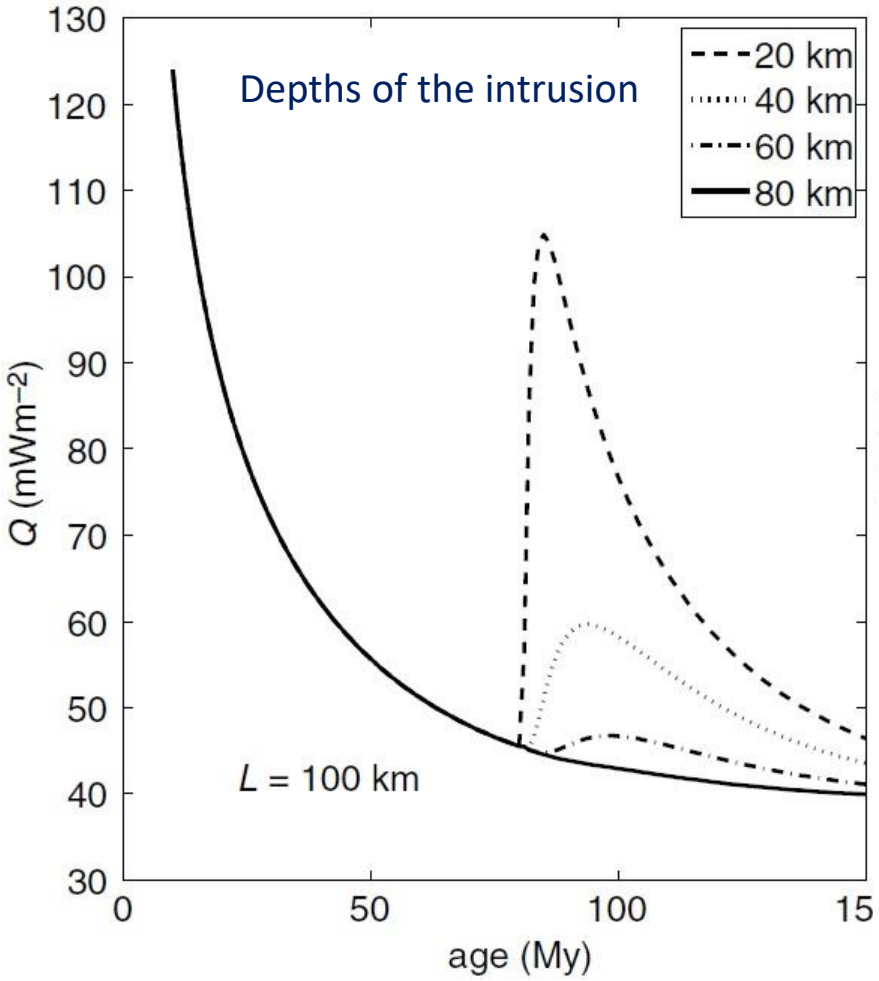

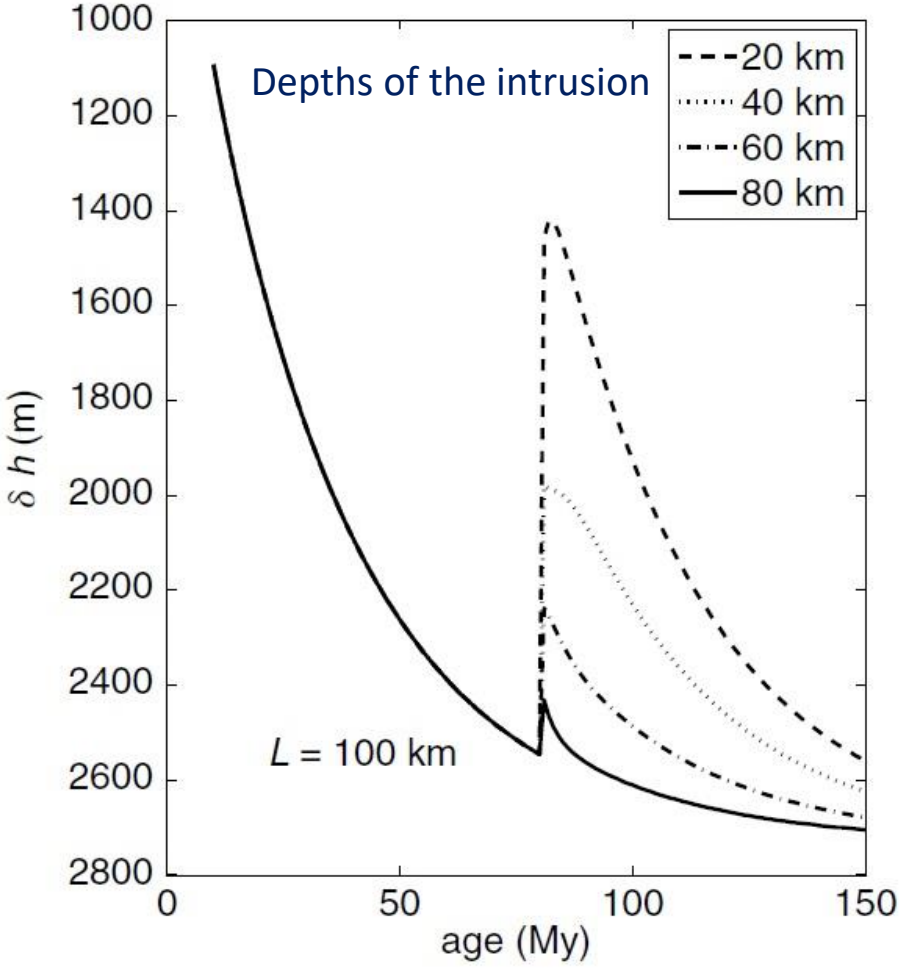

A swell height of δh relative to sea floor of the same age must be supported by the thermal expansion of the lithospheric column $\delta h = \alpha h \langle \Delta T \rangle$, where $\langle \Delta T \rangle$ is averaged over the entire lithospheric column.

This corresponds to an input of heat $\rho_m C_p h \langle \Delta T \rangle$:

$$\Delta Q = \frac{\rho_m C_p \delta h}{\alpha}$$

Variation of the heat flux (a) and bathymetry (b), following replacement of the lowermost lithosphere by hot material at 80My.

The maximum of heat flux anomaly (usually < 10mWm^{-2}) is retarded by several Myr, while the bathymery changes instantanealy.

Melt generation during continental extension

- For a thermally normal asthenosphere (T_p = 1300°C), no melting occurs unless stretching exceeds values of 2.0.
- The contribution of heat flow from melt cooling lasts several years after the rift episode and even for larger periods than the characteristic thermal time or the solidification time of the melt layers

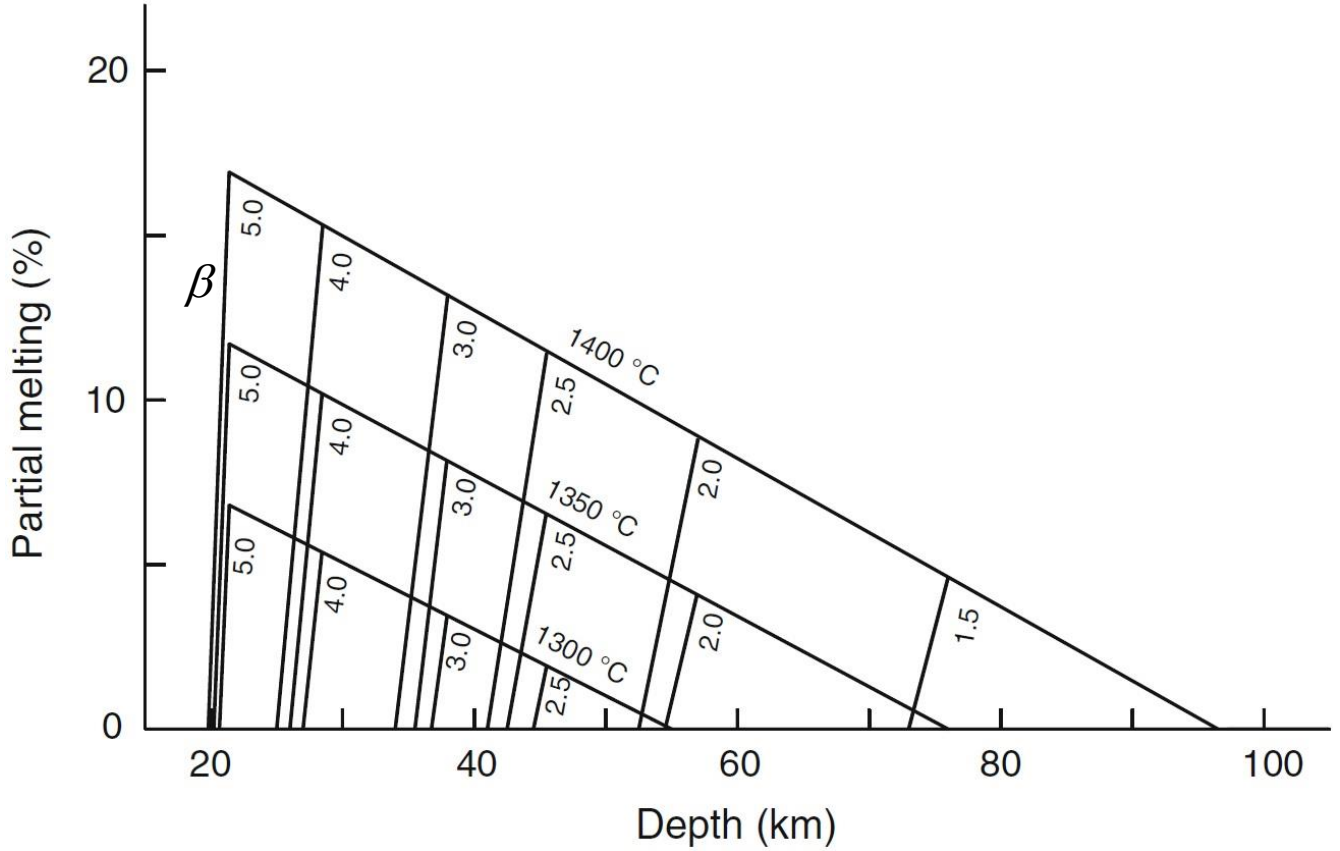

Partial melting as a function of depth at various amounts of extension β (1.5, 2.0, 2.5, 3.0, 4.0 and 5.0) and for asthenosphere T_p (1300, 1350, and 1400 °C)

Melt generation during continental extension

Amount of melt generated during the lithospheric stretching depends on the T_P of the asthenosphere (T that the asthenosphere would have if brought to the surface adiabatically without melting) and amount of stretching.

For β=2, T_p= 1400°C (due to plume activity), and L= 100 km, $Thick_{MELT}$= 2 km

Large T_p increases the amount of MgO and decreases NA_2O (from alkali basalts to tholeites)

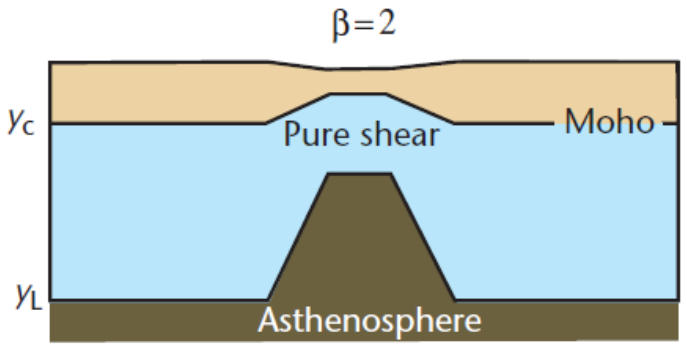

In absence of plume

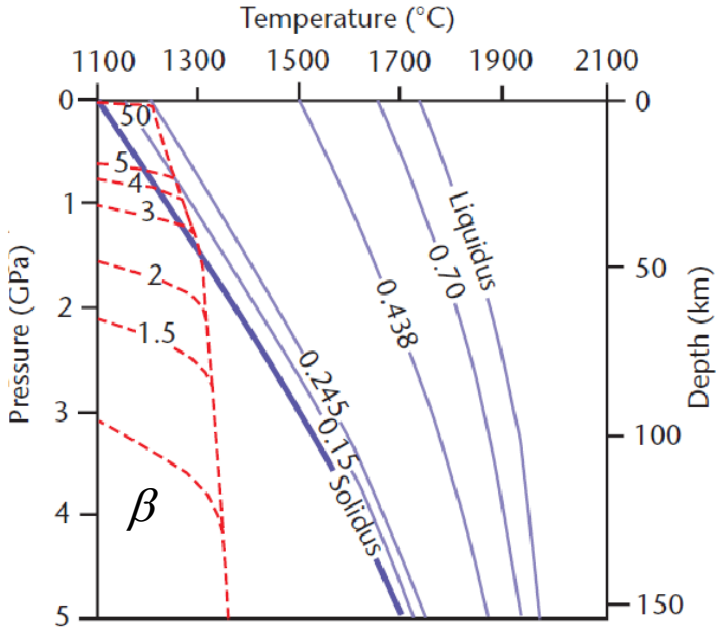

T_p= 1280°C L=100 Km ν=4x10^{15} m^{2}s^{-1}

In presence of plume

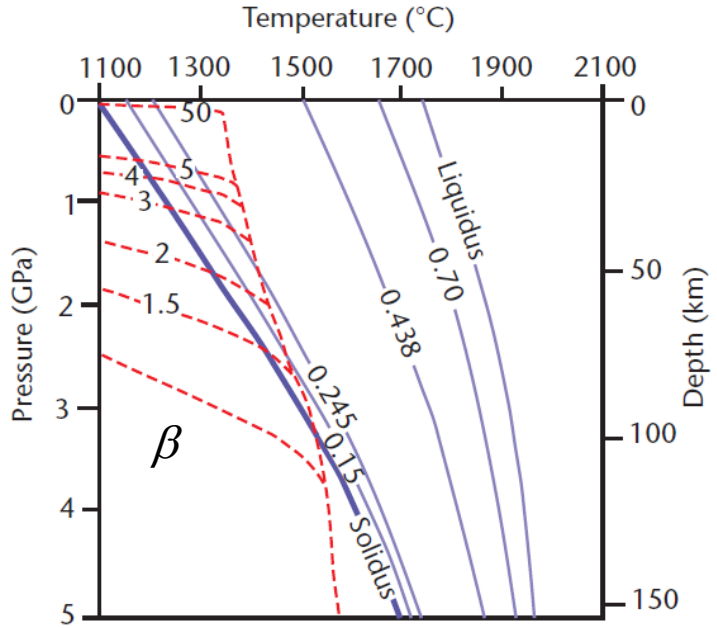

T_p= 1480°C L=100 Km ν=4x10^{15} m^{2}s^{-1}

Radial viscous fingering generated by plumes

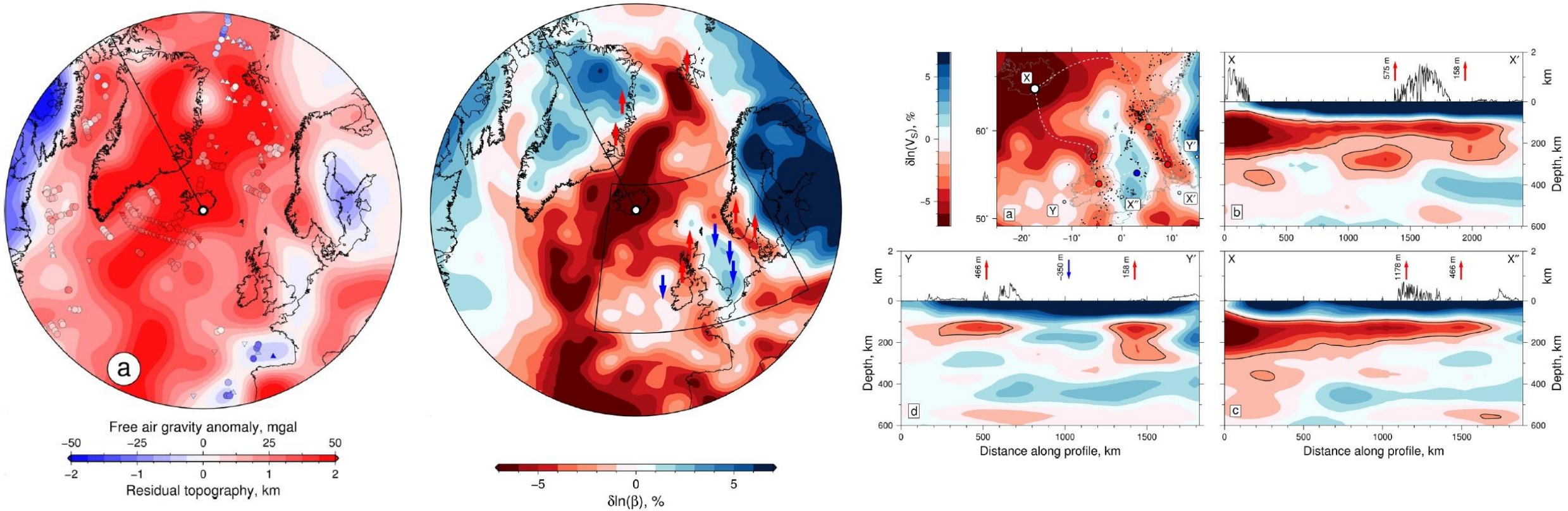

Schoonman et al., 2017, EPSL 468

There are narrow, slow velocity fingers (low velocity anomaly > 2%) that protrude beneath the fringing continental margins (British Isles and western Norway)

Radial viscous fingering generated by plumes

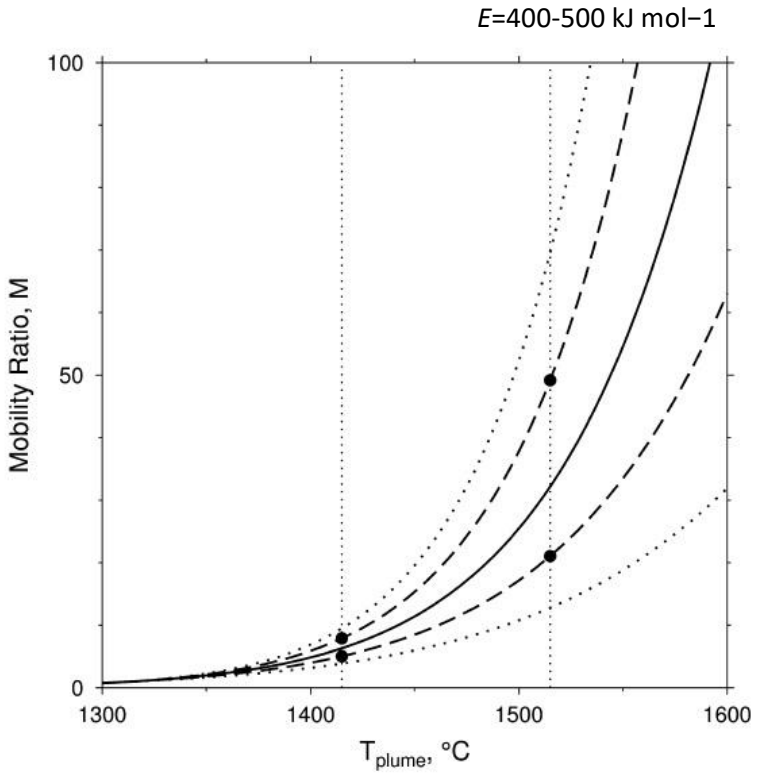

Schoonman et al., 2017, EPSL 468

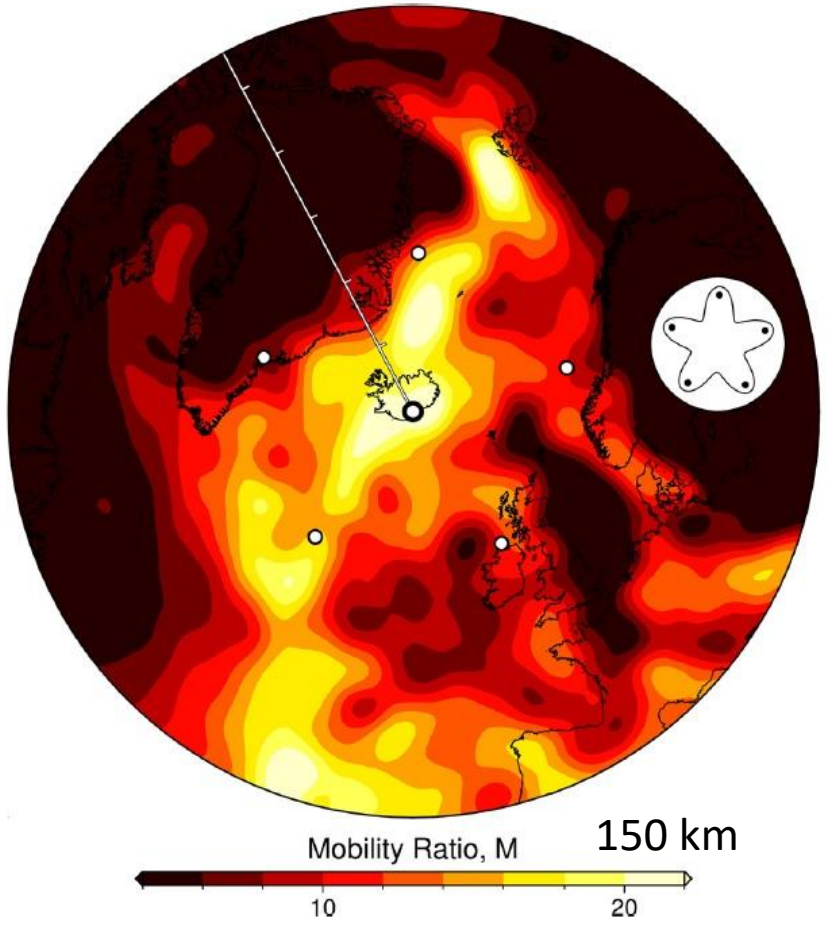

$$M = \frac{\eta_r}{\eta} \qquad \eta = \eta_r \exp\left\{\frac{E}{R}\left(\frac{1}{(T+273)} - \frac{1}{(T_r+273)}\right)\right\}$$

η_r= mantle viscosity

η= plume viscosity

Tr=mantle temperature

T= plume temperature

Saffman-Taylor instability: When a less viscous fluid displaces a more viscous fluid, the boundary between the two fluids can become unstable and promote viscous fingering.

Radial viscous fingering generated by plumes

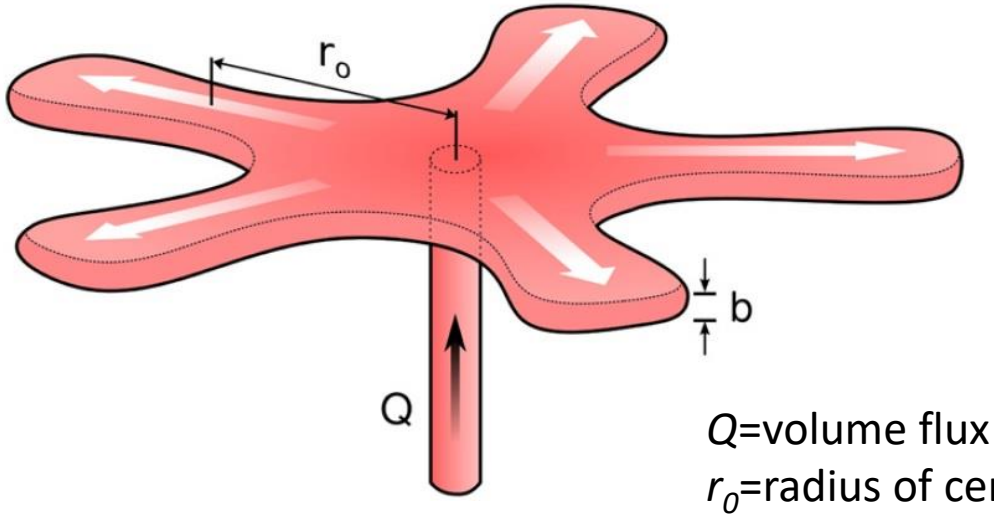

Q=volume flux
r_0=radius of central portion of plume
b=thickness of the layer

Schoonman et al., 2017, EPSL 468

Radial fingers are generated by a phenomenon known as the Saffman–Taylor instability

- Wavelength and number of fingers are controlled by the mobility ratio (i.e. the ratio of viscosities η_m/η_p), by the Péclet number (i.e. the ratio of advective and diffusive transport rates), and by the thickness of the horizontal layer into which fluid is injected.

- Iceland plume has an irregular planform due to small-scale convective circulation (radial fingers) that can generate and maintain surface deformation on short length scales.

Radial viscous fingering generated by plumes
(experimental analysis)

$$B = \rho_m \alpha \bar{T} S Y (L + A/2)$$

$$Q = \frac{\delta \rho g W S_{AO}^3 S_{BO}}{Y \eta_p}$$

$$Pe = \frac{Q}{b\kappa}$$

S_{AO}=maximum thickness of plume material at center of rift
S_{BO}=depth to base of plume material at distal end of rift
W= width of rift
η_p=viscosity of the asthenosphere.

S = full spreading rate (e.g. 16.5 mm/yr)
L =thicknesses of the lithosphere
A =thicknesses of the asthenosphere
Y = along-strike distance supplied by plume

B=Buoyancy flux
Q=Volume flux

Plume	Radius (km)	ΔT (°C)	B (Mg s^{-1})	b (km)	M	$Pe \times 10^4$
Iceland	1200	150	27	100	24	2.06
Hawaii	500	250	5	120	68	0.20
Cape Verde	390	190	2	130	31	0.09
Yellowstone	1000	80	17	100	4.4	2.44

Schoonman et al., 2017, EPSL 468

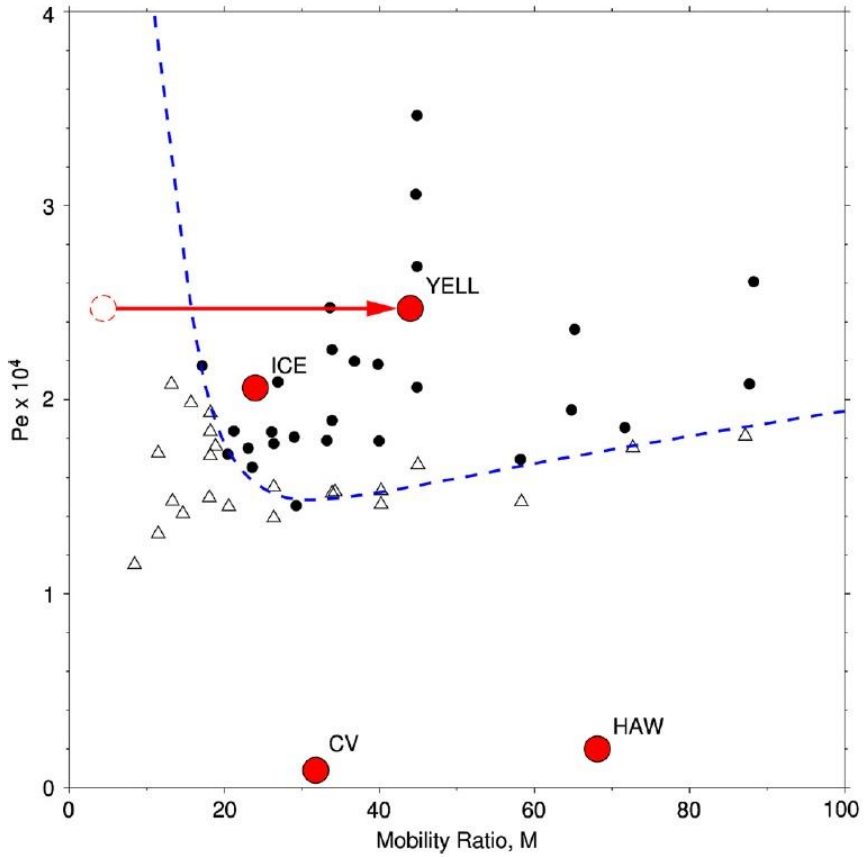

- Absence of fingering is principally a consequence of smaller buoyancy fluxes (Hawaiian and Cape Verde plumes).
- Yellowstone plume has likely a high mobility because of the presence of minor fractions of hydrous melt (this plume has an excess asthenospheric T of not more than 55–80◦C).

Thermals

Plume: a constant energy *E* is released for ~ 100 Myr and thus a narrow upwelling structure extends vertically.

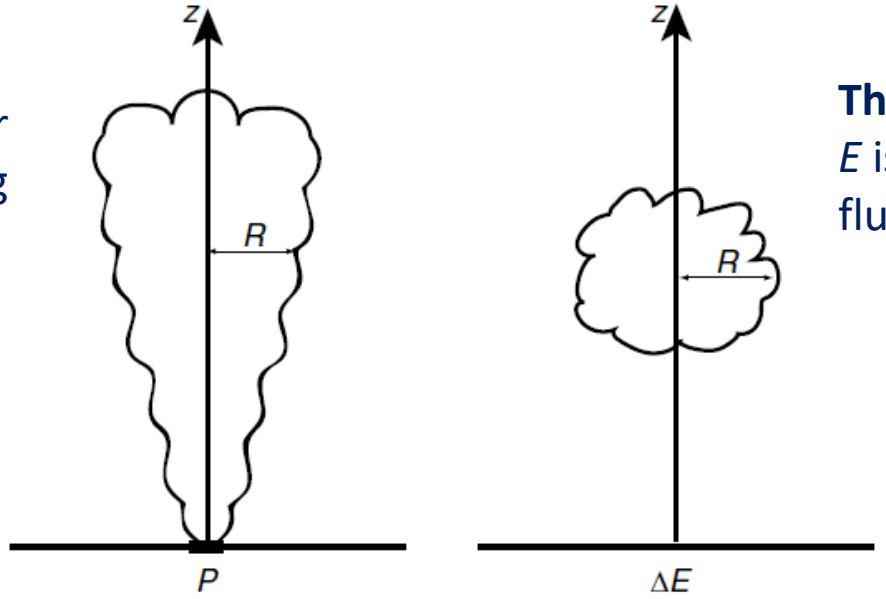

Thermal: A fixed amount of energy *E* is released and a volume of heated fluid detaches from the source.

$$\Delta E = \rho_o C_p \Delta T V$$ ΔE is the energy needed to heat a volume *V* of fluid to temperature *To* +ΔT

The thermal grows due to diffusion or turbulent entrainment, but the total amount of energy transported remains costant:

B=Buoyancy force

$$B = g(\rho_o - \rho)V = \rho_o g \alpha \Delta T V = \frac{g\alpha}{C_p}\Delta E$$

$$\mathrm{Ra}_E = \frac{\rho_o g \alpha \Delta T V}{\kappa \mu} = \frac{g \alpha \Delta E}{C_p \kappa \mu}$$

Ra_E: strength of the flow, analougus to Rayleigh number

LIPs (Large igneous provinces): Large Magma Volume in few Myr

Possible origin: higher basaltic composition in the plume head from subducted oceanic slab

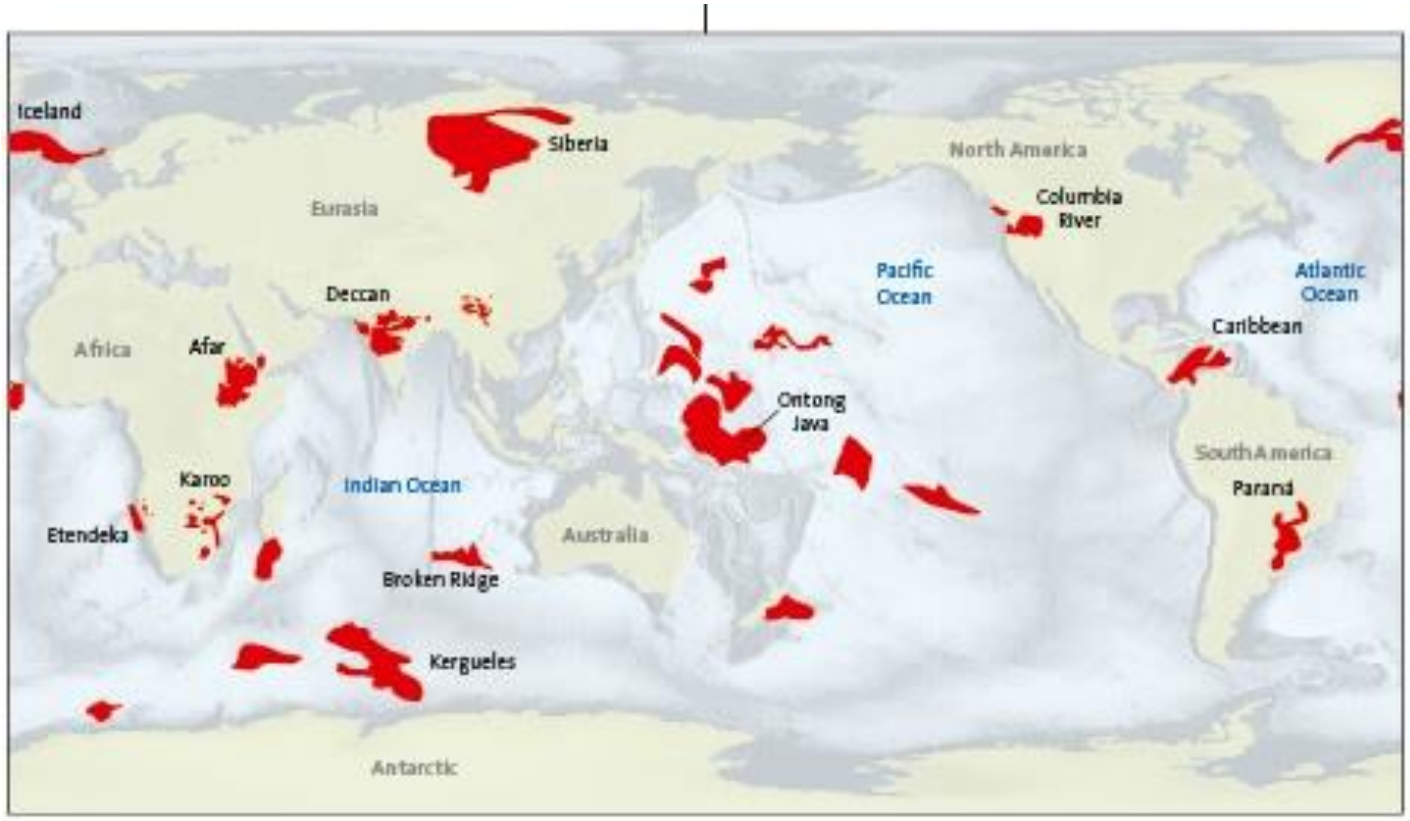

They extend up to 2000 km across, several km thick, 10 million km^3 of volcanic products

- Siberian Flood Basalts > 4 mln. km^3
- Deccan Traps ~2 mln. km^3
- North Atlantic Province >2-4 mln.km^3
- Columbia River Province ~ 0.3 mln. km^3
- Onthong-Java Plateau > 40mln. km^3

LIPs (Large igneous provinces)

Melt volume from a plume head model

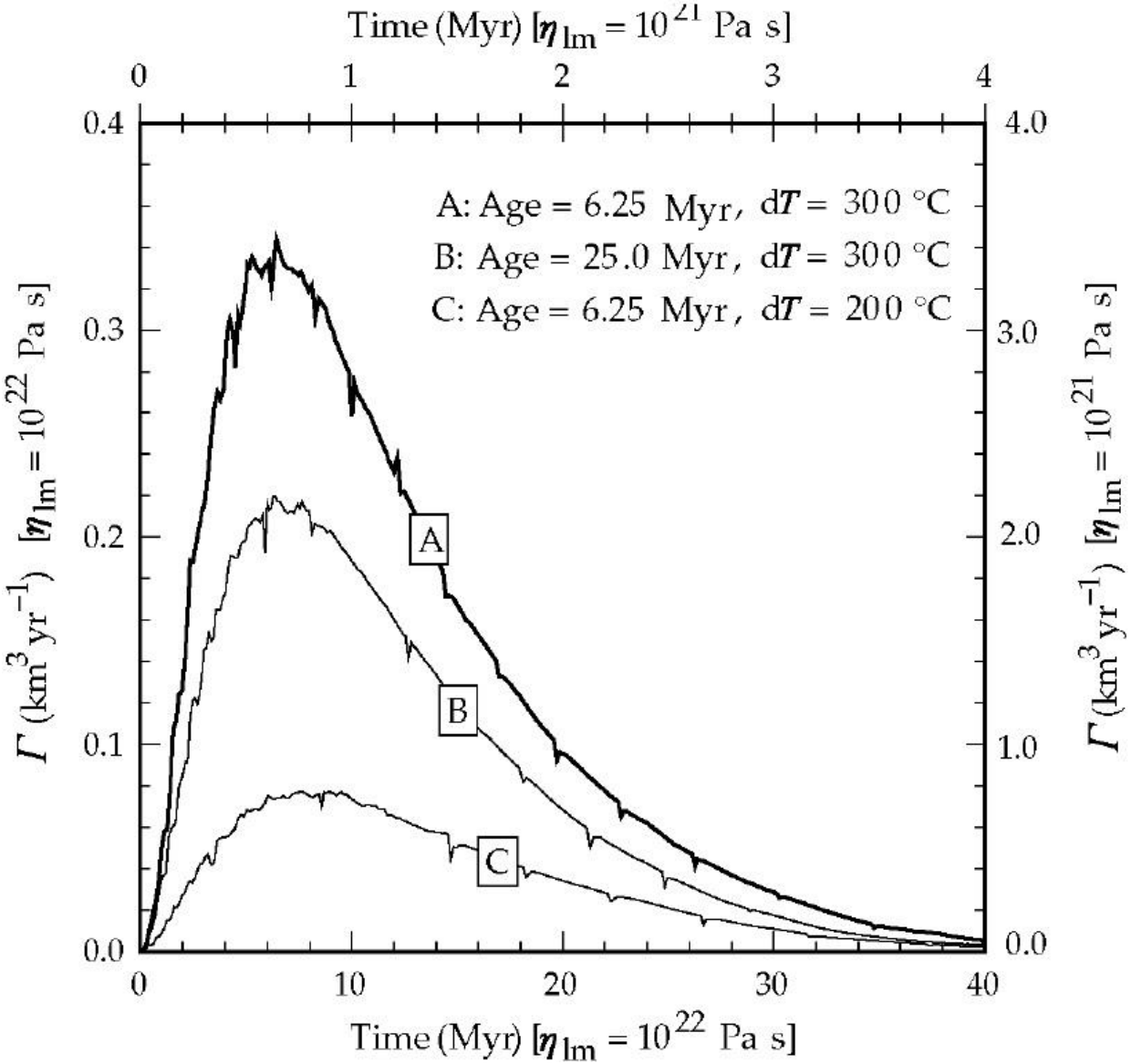

LIPs often predate continental break-up

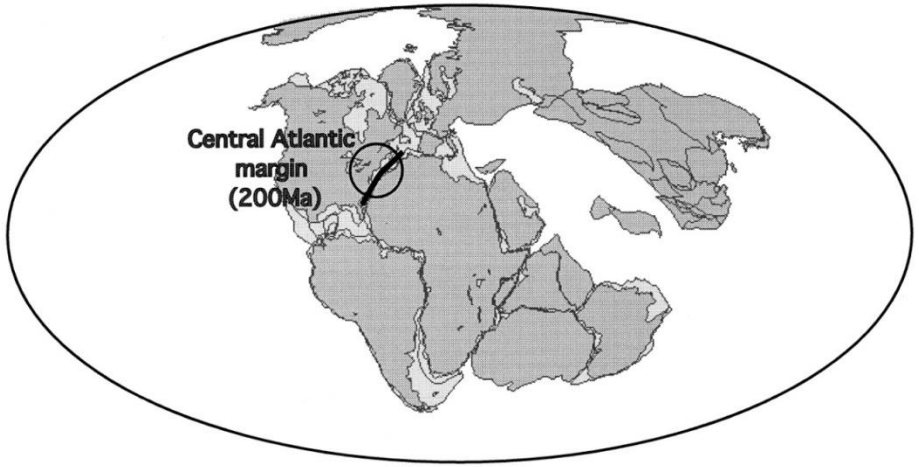

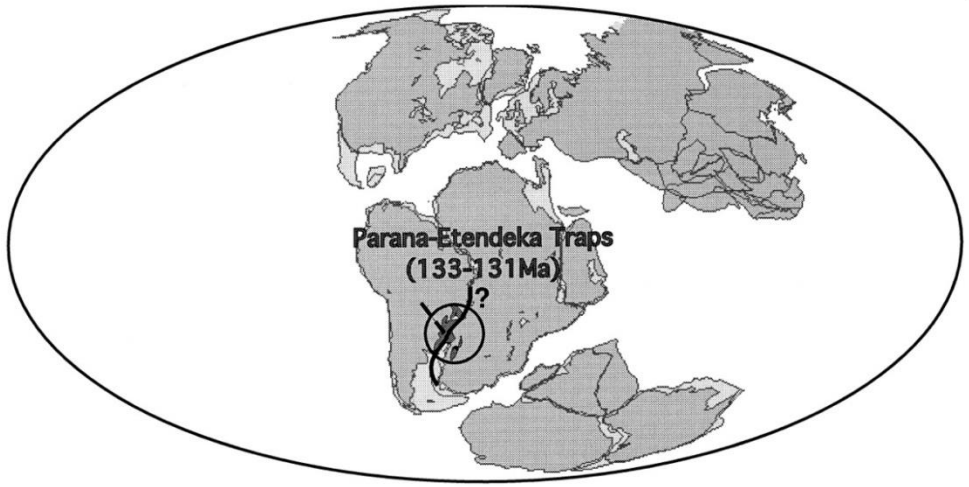

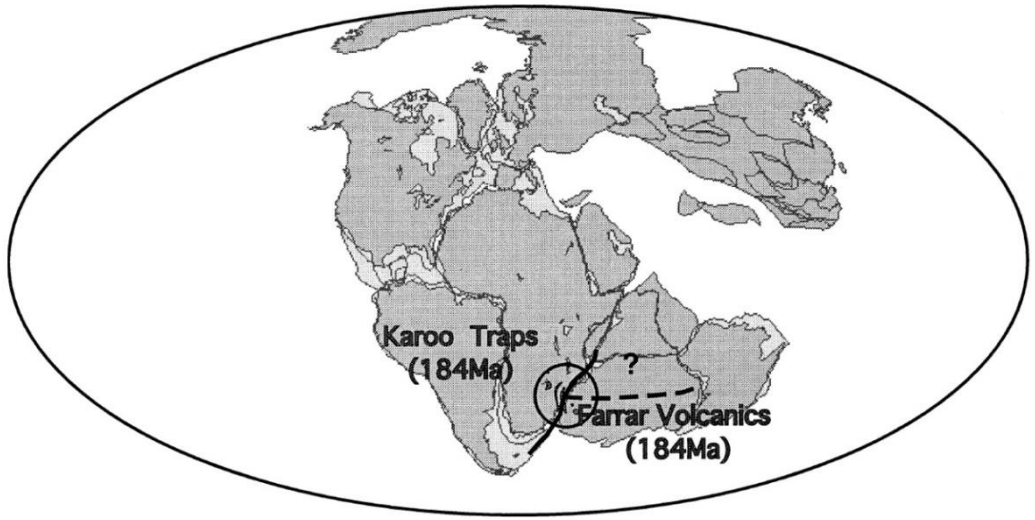

LIPs often predate continental break-up

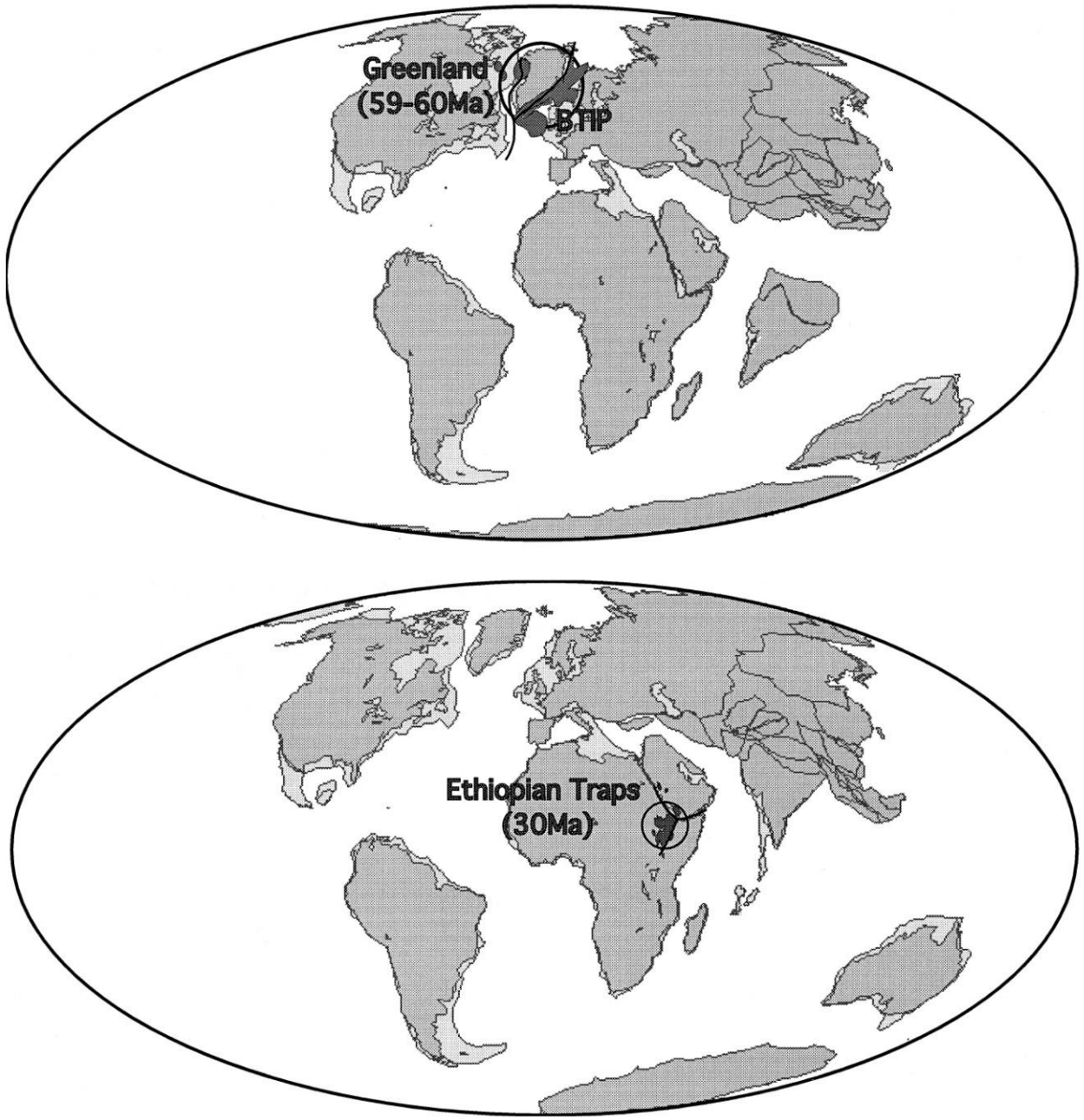

Connection of LIPs to mantle plume

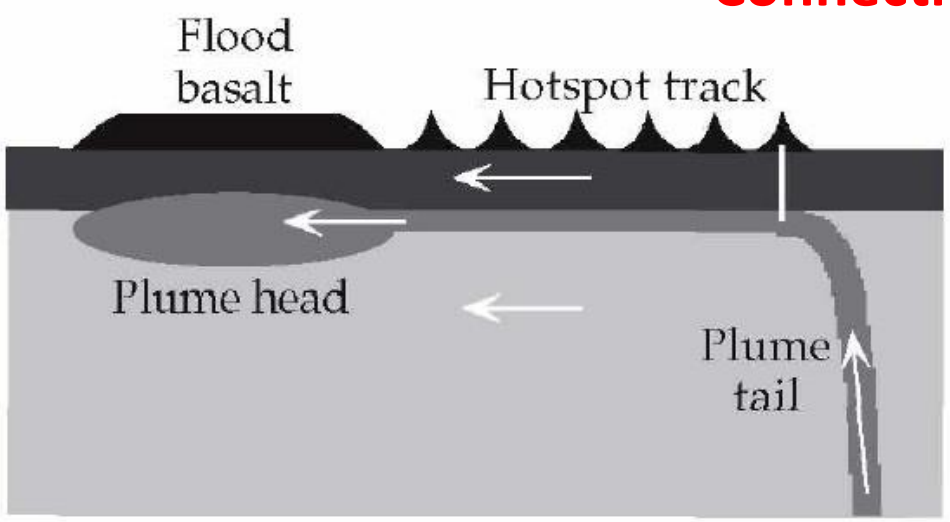

At least six examples have strong geographical, geochronological, and geochemical connections between hot-spot volcanism and flood basalt provinces: (1) Iceland and the North Atlantic Volcanic Province; (2) Kerguelen, and Bunbury, Naturaliste, Rajmahal (E. India), Broken Ridge, and Ninetyeast Ridge; (3) Reunion and Deccan, W. Indian, Chagos–Laccadive, Mascarenas, Mauritius; (4) Marion and Madagascar (Storey *et al*., 1997); (5) Tristan da Cunha and Paranà, Etendeka, Rio Grande, Walvis Ridge; (6) Galapagos and Caribbean.

- **The observation of large plume heads followed by thin tails in fluid dynamical experiments has traditionally been used to explain the LIP-hotspot connection**: the hottest material of rising plume heads will erupt first, which explains high MgO basalts early in the LIP record. Furthermore, the arrival of the plume at the surface will lead to uplift and extension, often observed in the geological record of LIPs.
- The viscosity change can also completely break apart a starting mantle-plume head into multiple plumes, perhaps contributing to multiple flood basalt episodes.

Alternative hypothesis to the plume origin of the LIPs:

(1) Excess heat can build below continents during tectonic quiescence and/or supercontinent formation, causing the massive eruptions during continental breakup (it addresses the correlation between LIPs and continental breakup and the lack of connection of some continental LIPs to hot-spot trails).
(2) Delamination of continental lithosphere and secondary convection at rifted margins have been forwarded to generate LIPs near continents (it addresses the lack of connection of some continental LIPs to hot-spot trails).
(3) Compositional, rather than thermal effects cause excess melting, for example, more fertile mantle such as eclogite and/or water in the source (it addresses the lack of uplift of some LIPs, like OJP and the lack of connection of some continental LIPs to hot-spot trails).
(4) Meteorite impact could be responsible for the emplacement of LIPs, since the decompression of mantle following impact may generate extensive melting with less uplift than expected from a hot plume head and without a connection to a hot-spot track (but no evidence).
(5) Oscillatory instabilities in starting plumes can be caused by the competing effects of thermal and chemical buoyancy.

LIPs Main Characteristics

LIPs source has high temperature

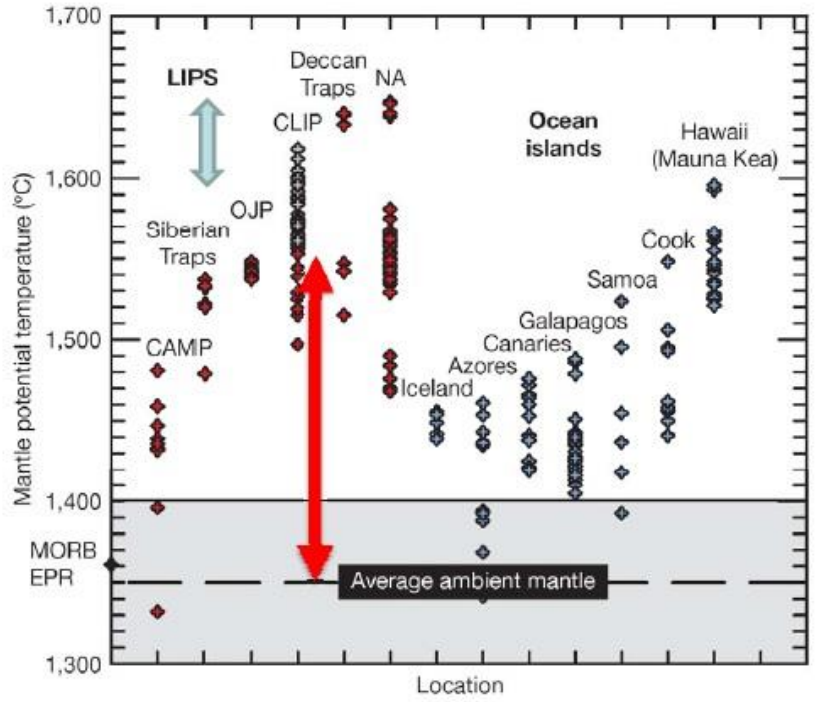

Herzberg and Gazel, 2009

LIPs correlate with mass extinction events

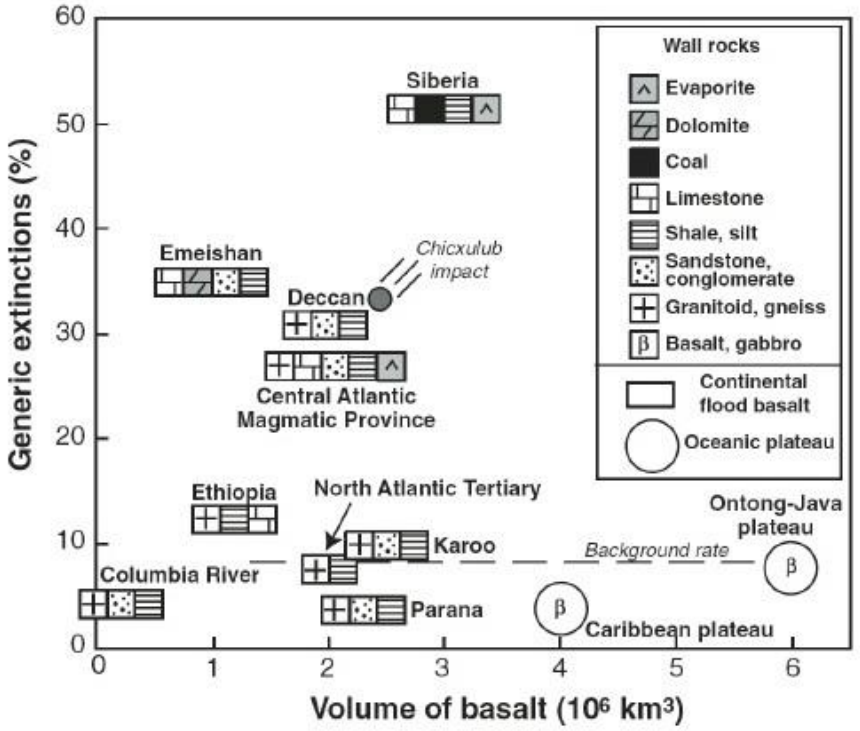

No Correlation with LIPs volume

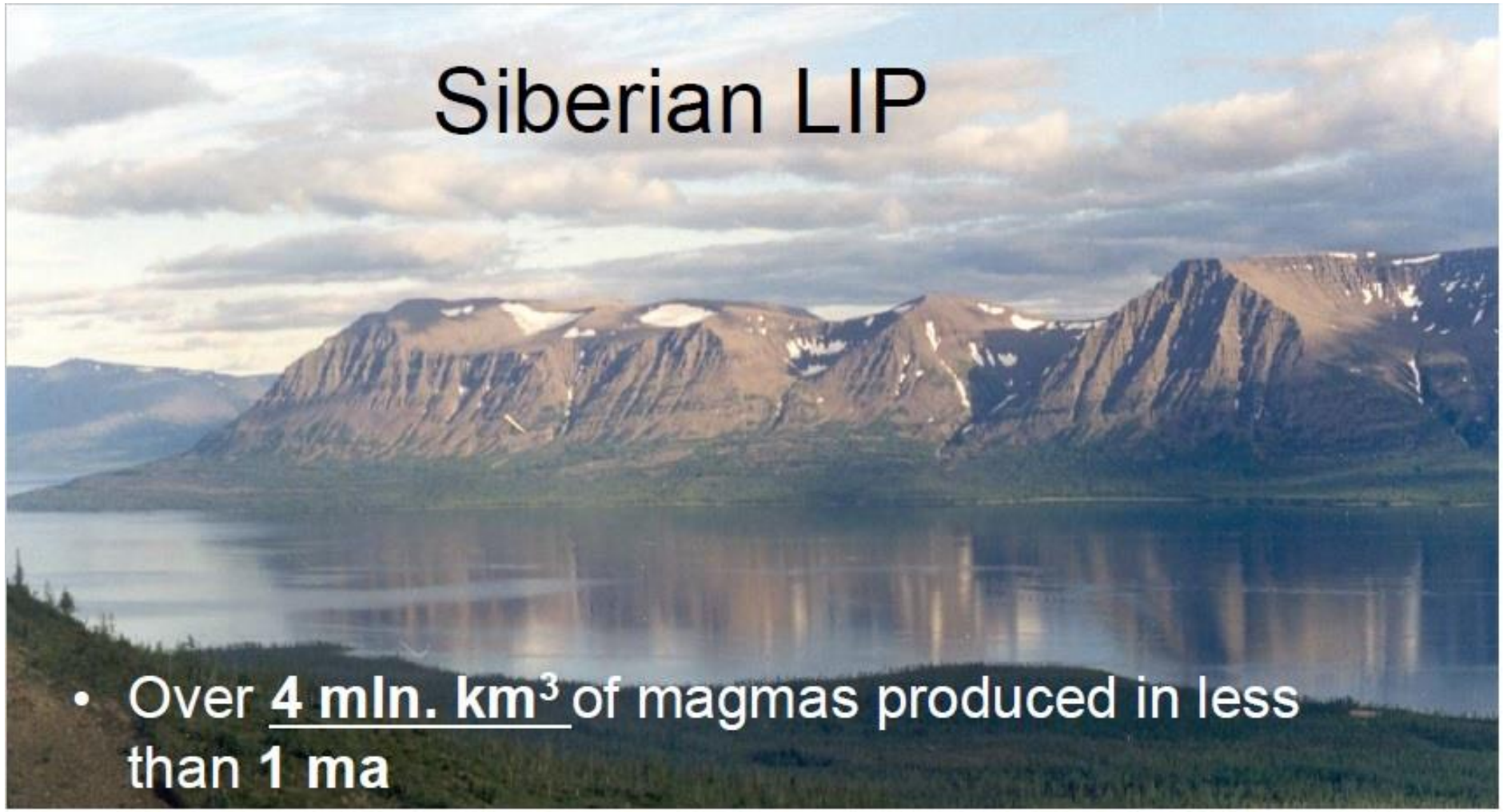
Siberian LIP
• Over 4 mln. km³ of magmas produced in less than 1 ma

Siberian Traps

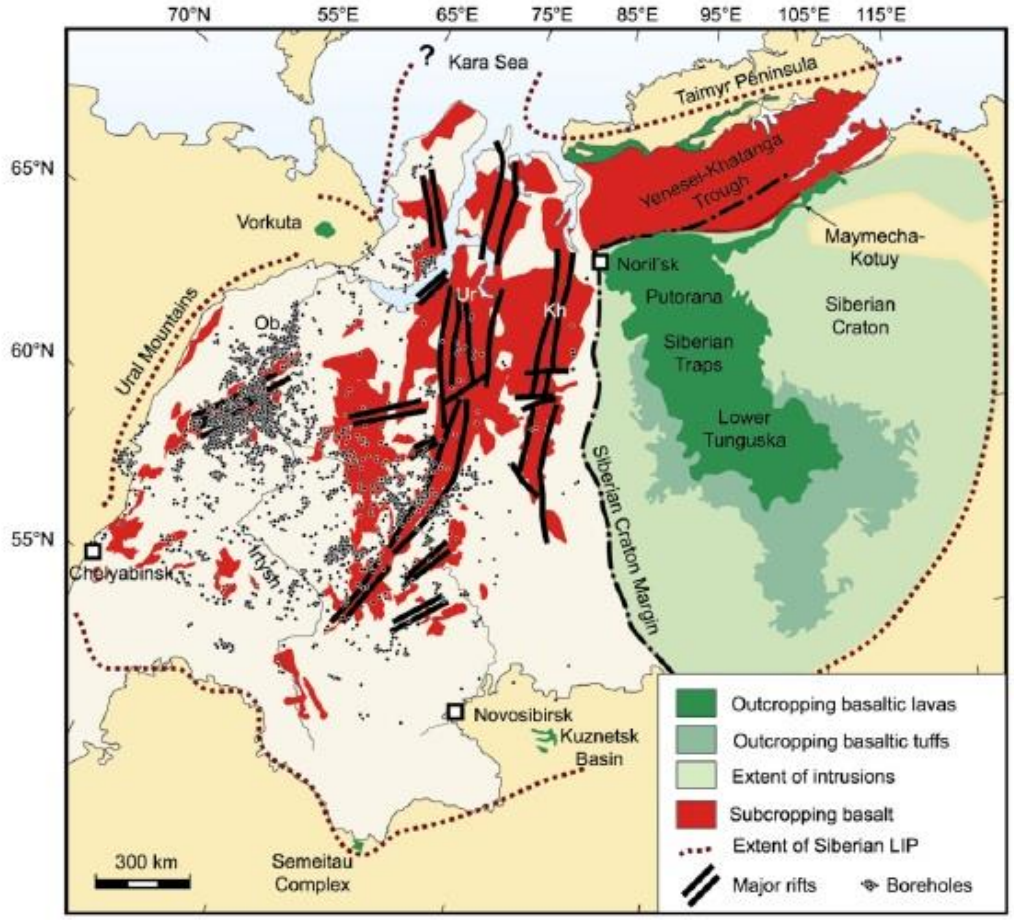

- Why no pre-magmatic uplift?
- Why large volume of magmas erupted at thick cratonic lithosphere without extreme extension?
- How lithosphere was thinned by >50 km during only few 100 thousand years?
- What was the source of large volumes of CO_2 and other gases that triggered P-T mass extinction?

White and Saunders (2005) Reichow et al, 2009

Piroxenite formation

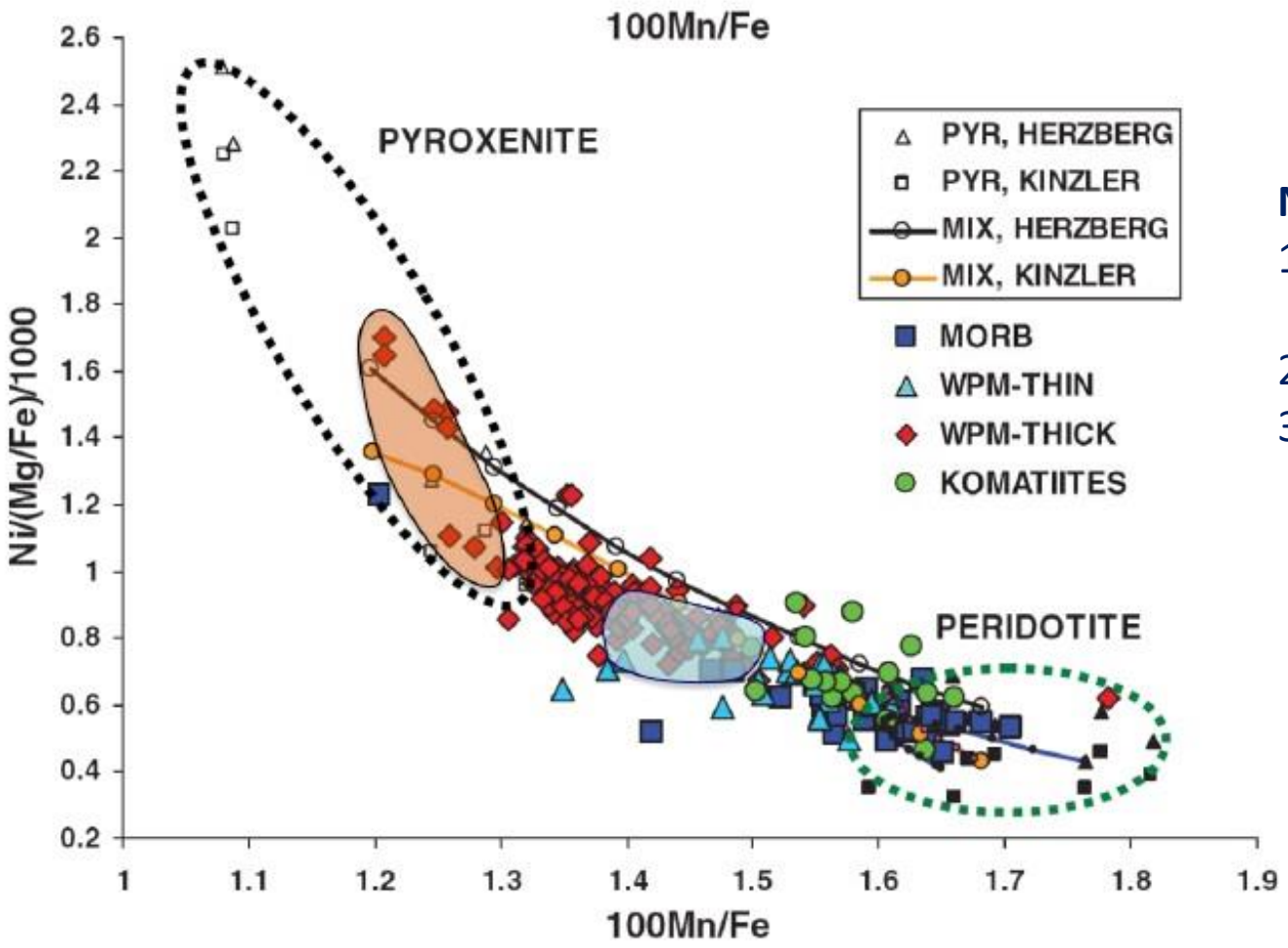

Ni excess and Mn depletion is interpreted as:

1. the result of the contribution of olivine free pyroxenite lithology in their source.
2. Effect of clinopyroxene crystallization.
3. Contribution of core material to the mantle source.

Sobolev et al, *Science*, 2007

Piroxenite formation

Crustal recycling

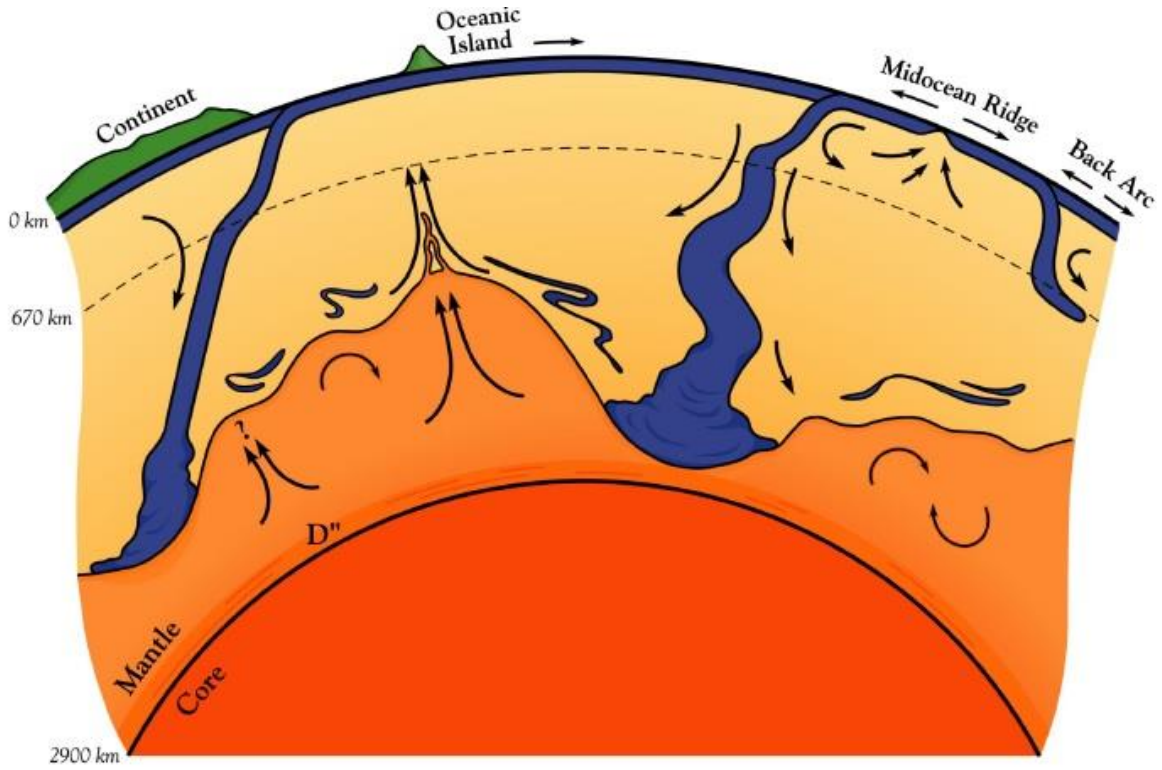

Kellogg et al., 1999

- In subduction at P > 2.5 GPa, the basaltic and gabbroic portions of the oceanic crust are transformed completely to eclogite (clinopyroxene and garnet) with a free SiO_2 phase.
- In the ascending, the silica-oversaturated eclogite starts melting at higher pressures than the peridotite and produces high silica melt, which reacts with olivine from peridotite, producing pyroxenes and garnet.

Eclogite

Piroxenite formation

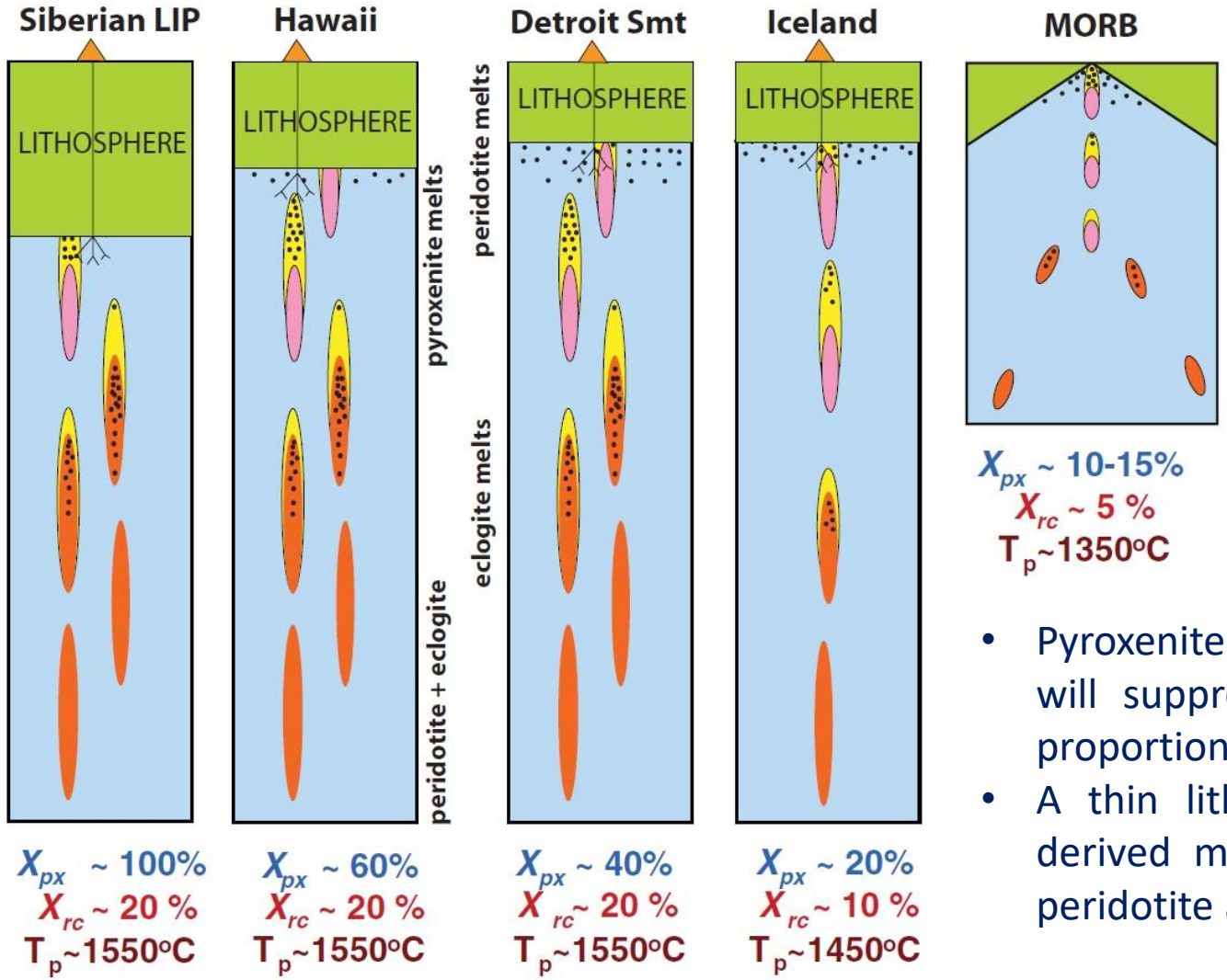

Blue = upwelling peridotitic mantle
Red=recycled oceanic crust (eclogite with free SiO_2 phase)
Black dots = melting
Yellow= reaction zones forming hybrid pyroxenite
Pink= refractory restite after eclogite melting

- Pyroxenite melts at higher *P* than peridotite, a thick lithosphere will suppress low-depth peridotite melting and favor a high proportion of pyroxenite derived melts.
- A thin lithosphere favors a higher proportion of peridotite-derived melt because of the increasing degree of melting of peridotite at shallower depths.

Sobolev et al, *Science*, 2007

Plume numerical models

Model Setup

- Plume potential temperature Tp=1600°C
- Eclogite content in plume 10-20wt% (15wt%)
- Initial lithospheric thickness = 130 km

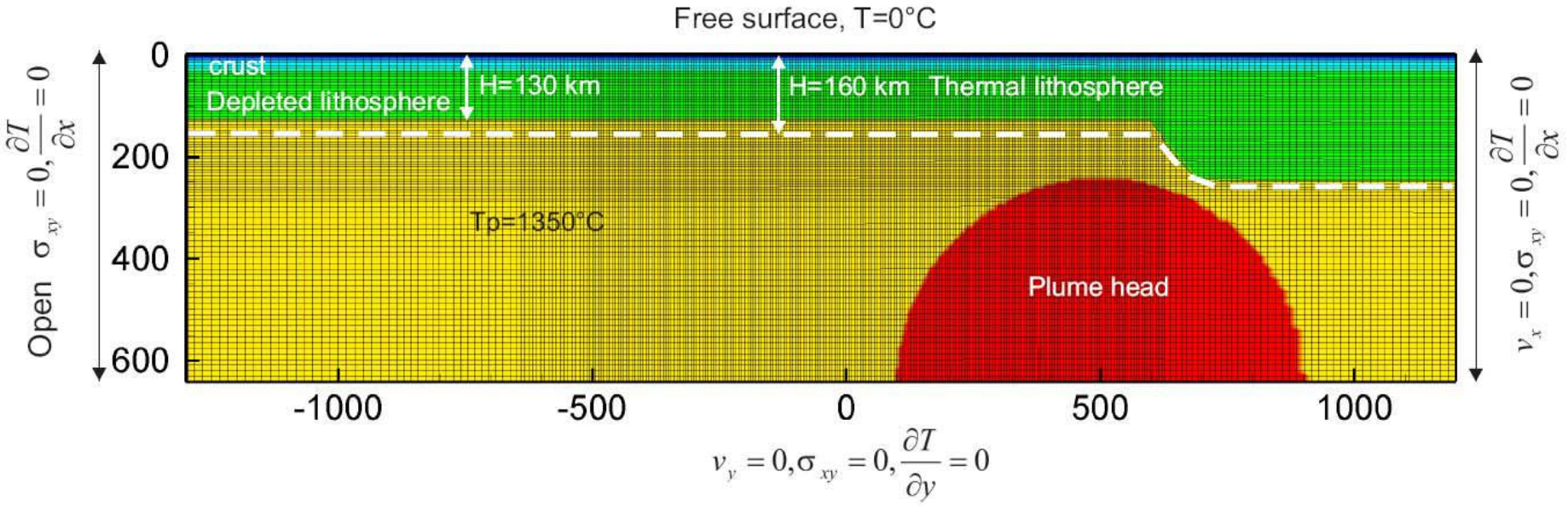

Finite element size is 5 X 5 km in the best resolved part of the model

Sobolev et al., 2011, Nature

Plume numerical models

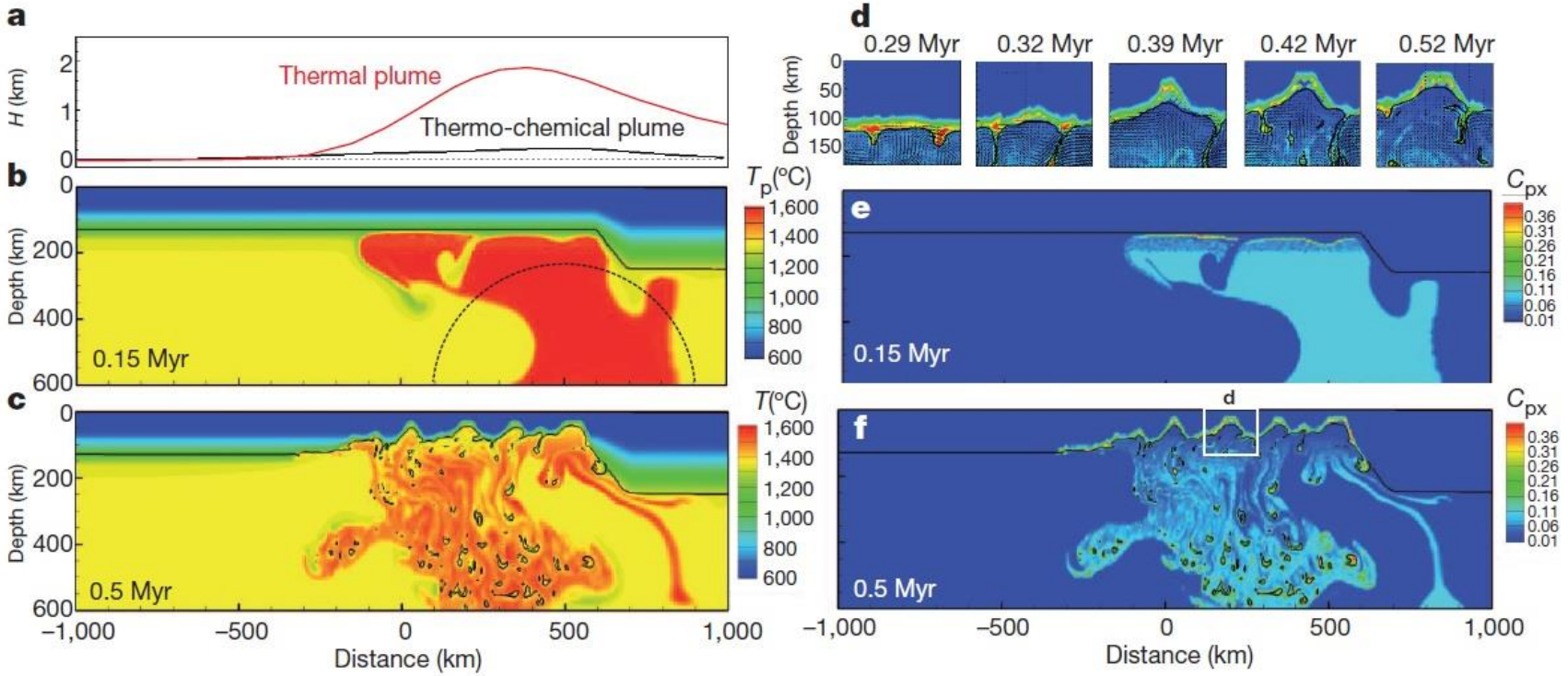

Sobolev et al., 2011, Nature

Magma intruded into the crust = 6–8 x10^6km^3

Large fraction (15 wt%) of dense recycled material is present within the plume, its buoyancy is strongly decreased, resulting in little regional uplift (250 m).

1. The plume head erodes the lowest part of the thermal lithosphere and rapidly spreads below the more refractory depleted lithosphere.
2. Plume ascent leads to progressive melting of recycled eclogitic material in the plume and to the formation of reaction pyroxenite, which melts at depths of 130–180 km (well before the peridotite).
3. The melt intrude into the lower lithosphere, cools and crystallizes to dense eclogite. It also strongly heats, weakens and mechanically erodes the lithosphere, promoting Raleigh–Taylor instabilities.
4. Enriched in eclogite, the lithospheric material in the boundary layer above the plume escapes to the sides of the plume and then downwards, allowing the plume to ascend.
5. The plume reaches its minimum depth of about 50 km crystallizing to a garnet-free assemblage, having a density lower than that of the ambient mantle (no formation of Raleigh–Taylor instabilities).

Effect of plume on the intensity of the lithospheric destruction

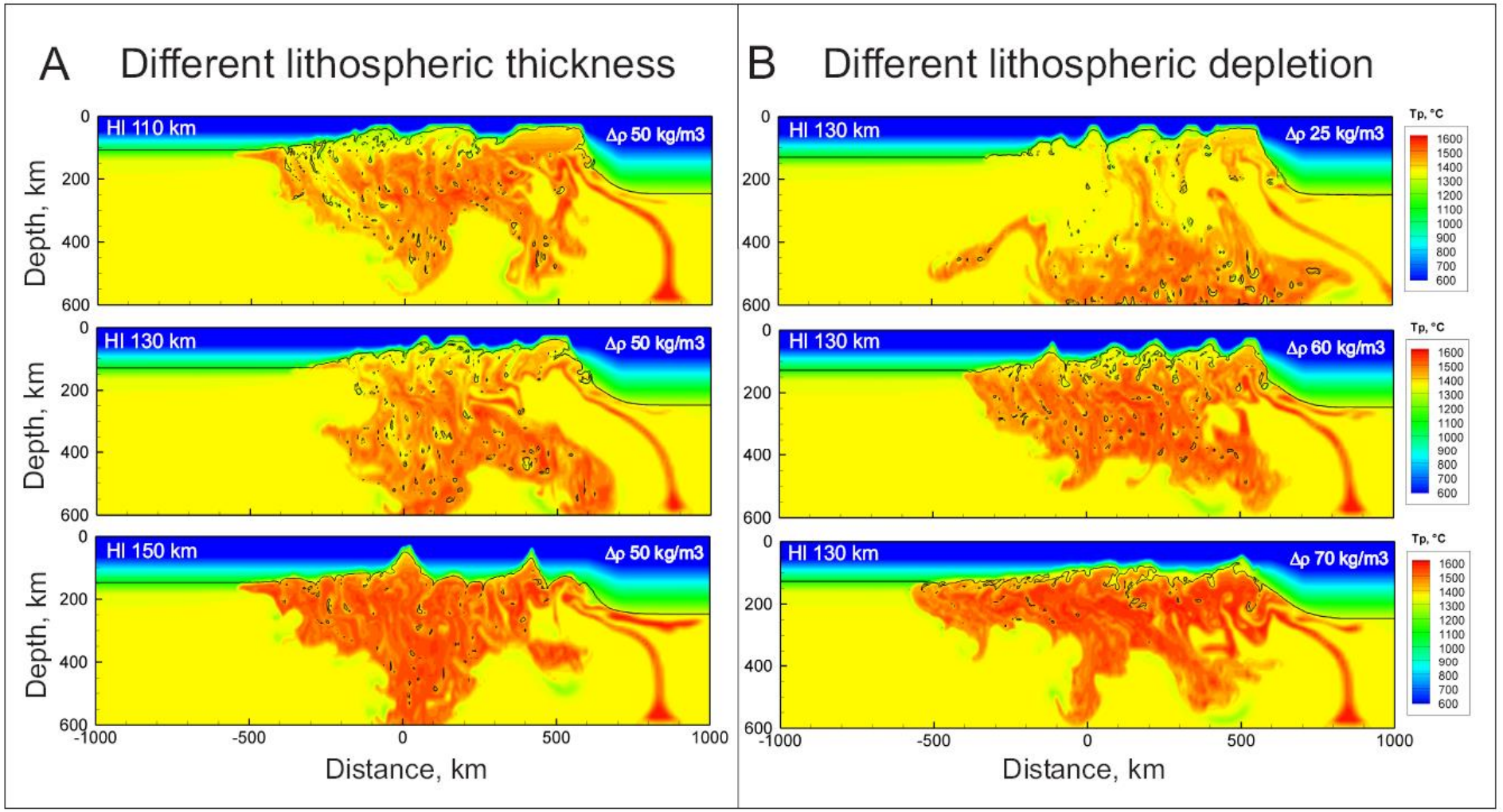

HI= thickness of the depleted lithosphere

model time 1.0 Myr

Sobolev et al., 2011, Nature

Effect of plume on the intensity of the lithospheric destruction

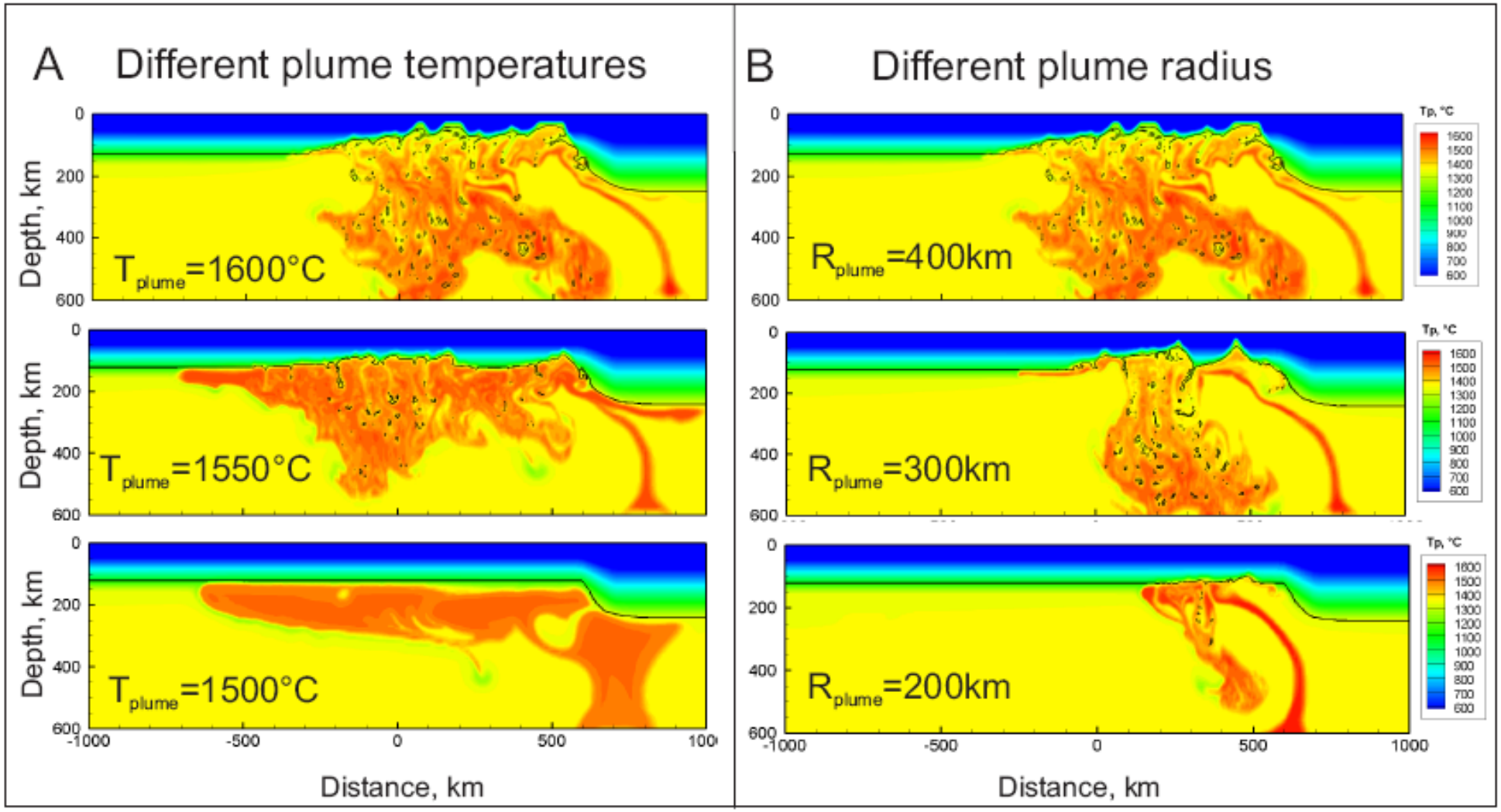

model time 1.0 Myr

Sobolev et al., 2011, Nature

Effect of plume on the surface topography and intensity of the lithospheric destruction

Different plume composition

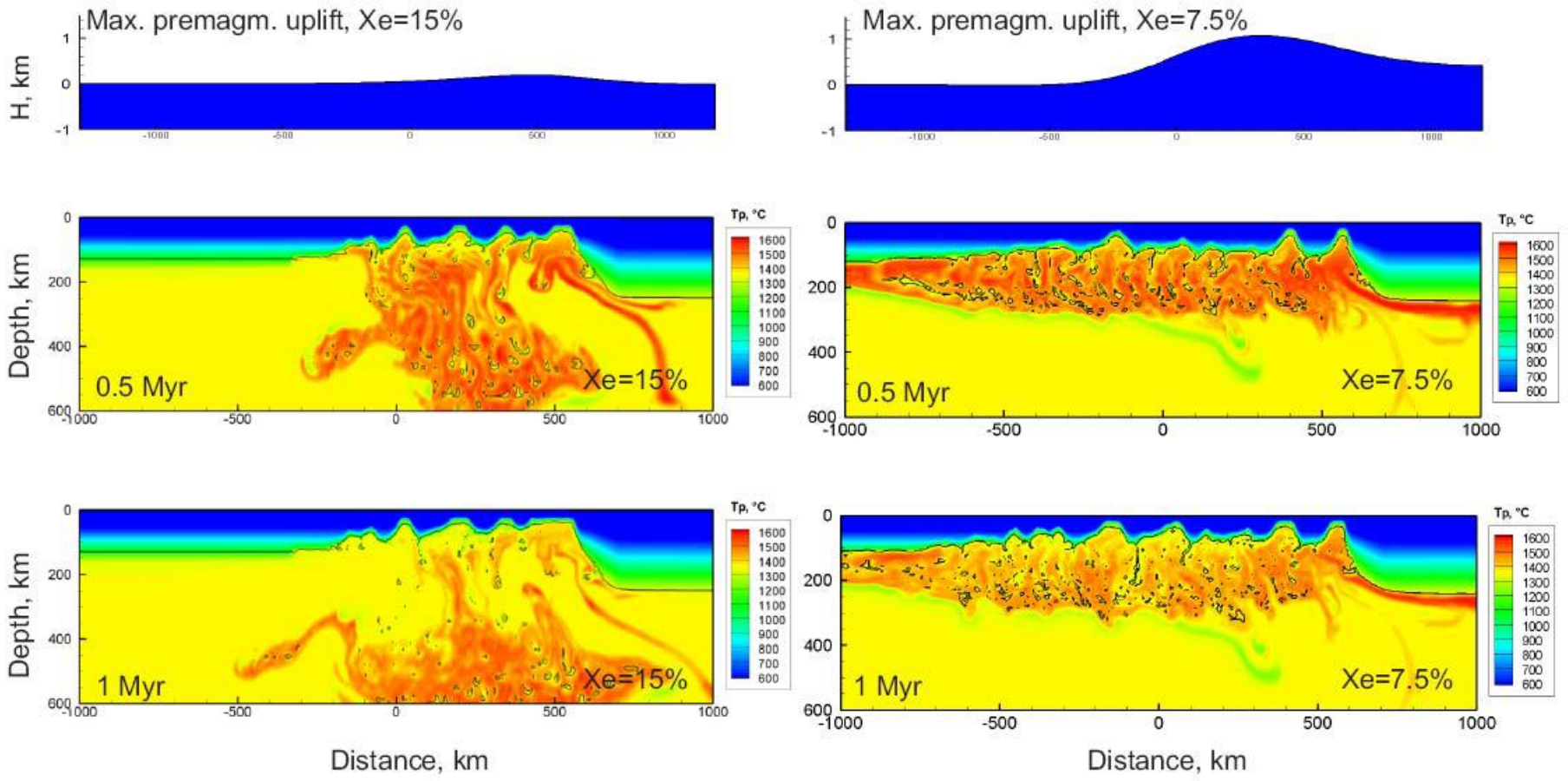

Sobolev et al., 2011, Nature

Results of plumes numerical models

- Thermochemical plume rich in recycled crust does not generate significant pre-magmatic uplift of the lithosphere.
- Such a plume is able to thin dramatically cratonic lithosphere without extension and to generate several mln km^3 of melt in few 100 thousand years.
- Massive CO_2 and HCl degassing from the plume could alone trigger the Permian-Triassic mass extinction and before the main volcanic phase.

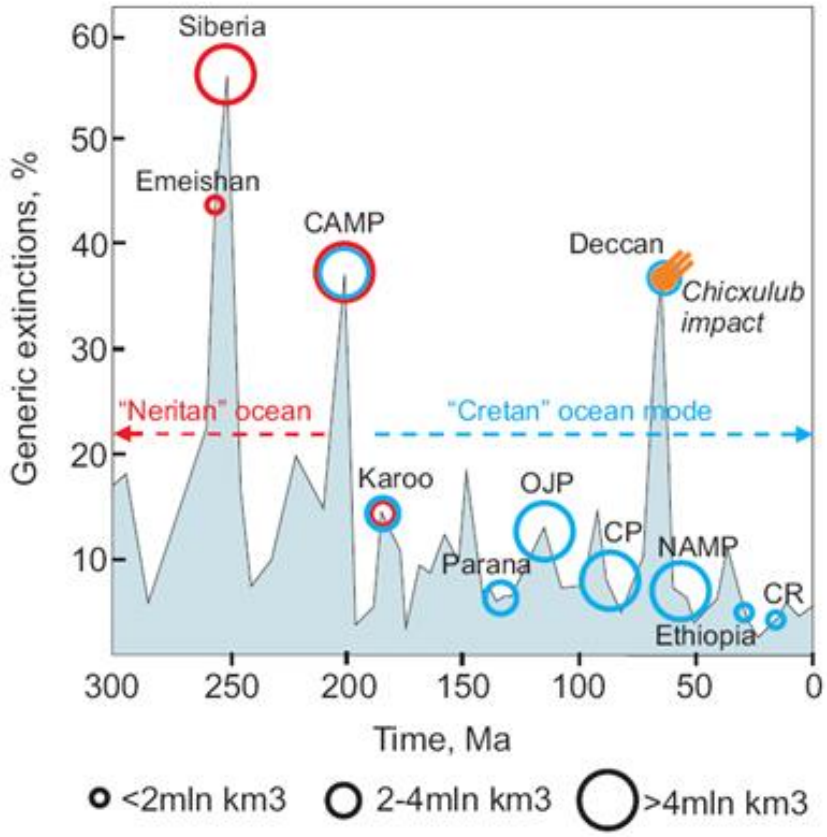

CAMP, Central Atlantic Magmatic Province; NAMP, Northern AtlanticMagmatic Provinces, OJP, Ontong Java; CP, Caribbean Plateaux; CR, Columbian River basalts.

Conclusions

Convection mode depends mostly on:

- The presence of cold high viscous lithospheric plates (plate-scale flow)
- The viscosity variations in the mantle
- The presence of transformation phases in the mantle

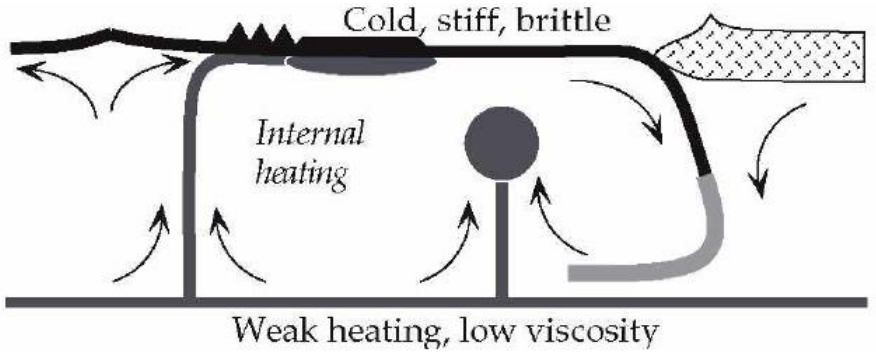

- The plates are an integral part of a convection system: stresses are transmitted through the viscous mantle as well as through the elastic plates.
- Evidence from seismic tomography and the gravity field supports the possibility that there is a large mass flow through the mantle transition zone, and that mantle convection occurs as a single layer rather than two.

- The hotspot swells constrain the buoyancy flux of plumes and indicate that plumes transport less than about 10% of the mantle heat budget (secondary mode of mantle convection).
- Plumes are produced in the lowermost mantle adjacent to the core within the so-called D'' layer, due to a difference in *T* (active upwelling), while mantle rising under mid-ocean occurs without *T* difference (passive upwelling).
- Plumes probably do not influence plate motions very much, though they may trigger some changes in favourable circumstances, such as major rifting.

References

Main Readings:

Books

- Allen and Allen, Basin Analysis, Chapter 5: Effects of Mantle Dynamics, 153-187.
- Davies, 1999, The Plume Mode (Chapter 11), Dynamic Earth Plates, Plumes and Mantle Convection, Cambridge and University Press.
- Davies, 1999, Convection (Chapter 8), Dynamic Earth Plates, Plumes and Mantle Convection, Cambridge and University Press.
- Frisch, Meschede, Blakey, 2011, Hot Spots (Chapter 6), Plate Tectonics.
- Jaupart and Mareshal, 2011, Heat Generation and Transport in the Earth, Chapter 9: Mantle Convection.
- Pasquale, Geothermics, Heat flow in the Lithosphere, Chapter 3: Thermal State, 53-77.
- Ito and van Keken, 2007, Hot Spots and Melting Anomalies, Treatise ofGeophysics, vol. 7, 371-435.

Articles

- Sobolev et al., 2011 Linking mantle plumes, large igneous provinces and environmental catastrophes. Nature 477.
- Schoonman et al., 2017, Radial viscous fingering of hot asthenosphere within the Icelandic plume beneath the North Atlantic Ocean, Earth and Planetary Science Letters 468, 51–61.

Further Readings:

Articles

- Baes et al., 2020, Plume-Induced Subduction Initiation: Single-Slab or Multi-Slab Subduction? *Geochem., Geophys., Geosyst., 21*.
- Burov and Cloetingh, 2009, Controls of mantle plumes and lithospheric folding on modes of intraplate continental tectonics: differences and similarities, Geophys. J. Int., 178, 1691–1722.
- Hoggard et al., 2020, Hotspots and mantle plumes revisited: Towards reconciling the mantle heat transfer discrepancy. EPSL, 542, 116317.
- Koptev et al., 2015, Dual continental rift systems generated by plume–lithosphere interaction, Nature Geoscience, vol. 8.
- Rogozhina et al., 2016, Melting at the base of the Greenland ice sheet explained by Iceland hotspot history, Nature Geoscience, vol. 9.
- McNutt and Caress, 2007, Crust and Lithospheric Structure – Hot Spots and Hot-Spot Swells, Treatise of Geophysics, vol. 1, 445-478.
- Sobolev et al, The Amount of Recycled Crust in Sources of Mantle-Derived Melts, *Science*, 2007, vol. 316, 412-417.
- Molnar, 2019. Lower Mantle Dynamics Perceived with 50 Years of Hindsight from Plate Tectonics. Geochemistry, Geophysics, Geosystem.
- Yu and Garnero, 2018, Ultralow Velocity Zone Locations: A Global Assessment, Geochemistry, Geophysics, Geosystems, 19.